Chaotic diffusion in galactic and planetary systems

P. M. Cincotta

UNLP/IALP–CONICET, La Plata, Argentina

In collaboration with: C. Beaugé, C. Giordano, F. Gómez, N. Maffione and J. Martí

Thanks to C. Simó for his valuable comments and discussions

Dynamics and chaos in astronomy and physics
Session Workshop IV (W4), September 17 - 24, 2016
School for advanced sciences of Luchon.

About chaotic diffusion

Global instabilities properties of near–integrable ND–Hamiltonian Systems $(N > 2)$ are far to be well understood.

- We know that local exponential divergence of nearby orbits (a positive LCE), does not imply chaotic diffusion (*stable chaos*, see for instance Milani et al. 1992 and further works.)

- Chaotic diffusion or chaotic mixing, roughly speaking, means large variations of the unperturbed integrals, actions (or orbital elements) of an integrable system under the effect of a (non-integrable) perturbation ϵV.

- In general, "fast diffusion" could be observed when a major overlap of resonances takes place.

- Overlap of resonances requires that the perturbation exceeds some critical value, ϵ_c.

About chaotic diffusion

Global instabilities properties of near–integrable ND–Hamiltonian Systems $(N > 2)$ are far to be well understood.

- We know that local exponential divergence of nearby orbits (a positive LCE), does not imply chaotic diffusion (*stable chaos*, see for instance Milani et al. 1992 and further works.)
- Chaotic diffusion or chaotic mixing, roughly speaking, means large variations of the unperturbed integrals, actions (or orbital elements) of an integrable system under the effect of a (non-integrable) perturbation ϵV.
- In general, "fast diffusion" could be observed when a major overlap of resonances takes place.
- Overlap of resonances requires that the perturbation exceeds some critical value, ϵ_c.

About chaotic diffusion

Global instabilities properties of near–integrable ND–Hamiltonian Systems ($N > 2$) are far to be well understood.

- We know that local exponential divergence of nearby orbits (a positive LCE), does not imply chaotic diffusion (*stable chaos*, see for instance Milani et al. 1992 and further works.)
- Chaotic diffusion or chaotic mixing, roughly speaking, means large variations of the unperturbed integrals, actions (or orbital elements) of an integrable system under the effect of a (non-integrable) perturbation ϵV.
- In general, "fast diffusion" could be observed when a major overlap of resonances takes place.
- Overlap of resonances requires that the perturbation exceeds some critical value, ϵ_c.

About chaotic diffusion

Global instabilities properties of near–integrable ND–Hamiltonian Systems $(N > 2)$ are far to be well understood.

- We know that local exponential divergence of nearby orbits (a positive LCE), does not imply chaotic diffusion (*stable chaos*, see for instance Milani et al. 1992 and further works.)
- Chaotic diffusion or chaotic mixing, roughly speaking, means large variations of the unperturbed integrals, actions (or orbital elements) of an integrable system under the effect of a (non-integrable) perturbation ϵV.
- In general, "fast diffusion" could be observed when a major overlap of resonances takes place.
- Overlap of resonances requires that the perturbation exceeds some critical value, ϵ_c.

About chaotic diffusion

Global instabilities properties of near–integrable ND–Hamiltonian Systems $(N > 2)$ are far to be well understood.

- We know that local exponential divergence of nearby orbits (a positive LCE), does not imply chaotic diffusion (*stable chaos*, see for instance Milani et al. 1992 and further works.)

- Chaotic diffusion or chaotic mixing, roughly speaking, means large variations of the unperturbed integrals, actions (or orbital elements) of an integrable system under the effect of a (non-integrable) perturbation ϵV.

- In general, "fast diffusion" could be observed when a major overlap of resonances takes place.

- Overlap of resonances requires that the perturbation exceeds some critical value, ϵ_c.

About chaotic diffusion

Global instabilities properties of near–integrable ND–Hamiltonian Systems $(N > 2)$ are far to be well understood.

- We know that local exponential divergence of nearby orbits (a positive LCE), does not imply chaotic diffusion (*stable chaos*, see for instance Milani et al. 1992 and further works.)
- Chaotic diffusion or chaotic mixing, roughly speaking, means large variations of the unperturbed integrals, actions (or orbital elements) of an integrable system under the effect of a (non-integrable) perturbation ϵV.
- In general, "fast diffusion" could be observed when a major overlap of resonances takes place.
- Overlap of resonances requires that the perturbation exceeds some critical value, ϵ_c.

- The heuristic/geometric criterion of overlap of resonances is due to Chirikov (1979) and earlier works of him.
- In the literature, it is common to find the statement that a system is in Chirikov's regime, when most of the invariant tori are destroyed by overlap of resonances and large chaotic domains are present, and thus the diffusion is assumed to be "fast" (normal diffusion).
- And it is in Nekhoroshev's regime, when chaos is completely confined to the narrow layers around resonances.
- Thus KAM theory is required: the size of the perturbation should be *small enough*, $\epsilon \ll \epsilon_c$, and, from Nekhoroshev theorem, the time–scale of any instability is exponentially large.

- The heuristic/geometric criterion of overlap of resonances is due to Chirikov (1979) and earlier works of him.
- In the literature, it is common to find the statement that a system is in Chirikov's regime, when most of the invariant tori are destroyed by overlap of resonances and large chaotic domains are present, and thus the diffusion is assumed to be "fast" (normal diffusion).
- And it is in Nekhoroshev's regime, when chaos is completely confined to the narrow layers around resonances.
- Thus KAM theory is required: the size of the perturbation should be *small enough*, $\epsilon \ll \epsilon_c$, and, from Nekhoroshev theorem, the time–scale of any instability is exponentially large.

- The heuristic/geometric criterion of overlap of resonances is due to Chirikov (1979) and earlier works of him.
- In the literature, it is common to find the statement that a system is in Chirikov's regime, when most of the invariant tori are destroyed by overlap of resonances and large chaotic domains are present, and thus the diffusion is assumed to be "fast" (normal diffusion).
- And it is in Nekhoroshev's regime, when chaos is completely confined to the narrow layers around resonances.
- Thus KAM theory is required: the size of the perturbation should be *small enough*, $\epsilon \ll \epsilon_c$, and, from Nekhoroshev theorem, the time–scale of any instability is exponentially large.

- The heuristic/geometric criterion of overlap of resonances is due to Chirikov (1979) and earlier works of him.
- In the literature, it is common to find the statement that a system is in Chirikov's regime, when most of the invariant tori are destroyed by overlap of resonances and large chaotic domains are present, and thus the diffusion is assumed to be "fast" (normal diffusion).
- And it is in Nekhoroshev's regime, when chaos is completely confined to the narrow layers around resonances.
- Thus KAM theory is required: the size of the perturbation should be *small enough*, $\epsilon \ll \epsilon_c$, and, from Nekhoroshev theorem, the time–scale of any instability is exponentially large.

- KAM theory and Nekhoroshev estimates are rigorous, but they only provide upper bounds for stability conditions and for the speed of the rather slow diffusion along the narrow chaotic layers $\sim$ Arnold diffusion.
- Chirikov's approach though heuristic, provides a constructive way to compute a diffusion coefficient (under the assumption of normal diffusion) in *both* scenarios, *fast* and *slow diffusion*.
- Physically speaking, *fast diffusion* should mean that the unperturbed actions/integrals/orbital elements present a significant variation over a physical time-scale.
- It is usual to find in the astronomical/astrophysical/physical literature, several estimations of the diffusion coefficient for different ($\sim$ non-ergodic) dynamical systems.

Let us review a few diffusion examples in two simple models: a $2\frac{1}{2}$ degrees of freedom Hamiltonian system and a 4D simplectic map.

- KAM theory and Nekhoroshev estimates are rigorous, but they only provide upper bounds for stability conditions and for the speed of the rather slow diffusion along the narrow chaotic layers $\sim$ Arnold diffusion.

- Chirikov's approach though heuristic, provides a constructive way to compute a diffusion coefficient (under the assumption of normal diffusion) in *both* scenarios, *fast* and *slow diffusion*.

- Physically speaking, *fast diffusion* should mean that the unperturbed actions/integrals/orbital elements present a significant variation over a physical time-scale.

- It is usual to find in the astronomical/astrophysical/physical literature, several estimations of the diffusion coefficient for different ($\sim$ non-ergodic) dynamical systems.

Let us review a few diffusion examples in two simple models: a $2\frac{1}{2}$ degrees of freedom Hamiltonian system and a 4D simplectic map.

- KAM theory and Nekhoroshev estimates are rigorous, but they only provide upper bounds for stability conditions and for the speed of the rather slow diffusion along the narrow chaotic layers $\sim$ Arnold diffusion.
- Chirikov's approach though heuristic, provides a constructive way to compute a diffusion coefficient (under the assumption of normal diffusion) in *both* scenarios, *fast* and *slow diffusion*.
- Physically speaking, *fast diffusion* should mean that the unperturbed actions/integrals/orbital elements present a significant variation over a physical time-scale.
- It is usual to find in the astronomical/astrophysical/physical literature, several estimations of the diffusion coefficient for different ($\sim$ non-ergodic) dynamical systems.

Let us review a few diffusion examples in two simple models: a $2\frac{1}{2}$ degrees of freedom Hamiltonian system and a 4D simplectic map.

- KAM theory and Nekhoroshev estimates are rigorous, but they only provide upper bounds for stability conditions and for the speed of the rather slow diffusion along the narrow chaotic layers $\sim$ Arnold diffusion.

- Chirikov's approach though heuristic, provides a constructive way to compute a diffusion coefficient (under the assumption of normal diffusion) in *both* scenarios, *fast* and *slow diffusion*.

- Physically speaking, *fast diffusion* should mean that the unperturbed actions/integrals/orbital elements present a significant variation over a physical time-scale.

- It is usual to find in the astronomical/astrophysical/physical literature, several estimations of the diffusion coefficient for different ($\sim$ non-ergodic) dynamical systems.

Let us review a few diffusion examples in two simple models: a $2\frac{1}{2}$ degrees of freedom Hamiltonian system and a 4D simplectic map.

- KAM theory and Nekhoroshev estimates are rigorous, but they only provide upper bounds for stability conditions and for the speed of the rather slow diffusion along the narrow chaotic layers $\sim$ Arnold diffusion.

- Chirikov's approach though heuristic, provides a constructive way to compute a diffusion coefficient (under the assumption of normal diffusion) in *both* scenarios, *fast* and *slow diffusion*.

- Physically speaking, *fast diffusion* should mean that the unperturbed actions/integrals/orbital elements present a significant variation over a physical time-scale.

- It is usual to find in the astronomical/astrophysical/physical literature, several estimations of the diffusion coefficient for different ($\sim$ non-ergodic) dynamical systems.

Let us review a few diffusion examples in two simple models: a $2\frac{1}{2}$ degrees of freedom Hamiltonian system and a 4D simplectic map.

- KAM theory and Nekhoroshev estimates are rigorous, but they only provide upper bounds for stability conditions and for the speed of the rather slow diffusion along the narrow chaotic layers $\sim$ Arnold diffusion.

- Chirikov's approach though heuristic, provides a constructive way to compute a diffusion coefficient (under the assumption of normal diffusion) in *both* scenarios, *fast* and *slow diffusion*.

- Physically speaking, *fast diffusion* should mean that the unperturbed actions/integrals/orbital elements present a significant variation over a physical time-scale.

- It is usual to find in the astronomical/astrophysical/physical literature, several estimations of the diffusion coefficient for different ($\sim$ non-ergodic) dynamical systems.

Let us review a few diffusion examples in two simple models: a $2\frac{1}{2}$ degrees of freedom Hamiltonian system and a 4D simplectic map.

The classical Arnold's model

$$H(I_1, I_2, \theta_1, \theta_2, t) = \frac{1}{2}(I_1^2+I_2^2)+\epsilon(\cos\theta_1 - 1)[1+\mu(\sin\theta_2 + \cos t)],$$

$$I_1, I_2 \in \mathbb{R}, \quad \theta_1, \theta_2, t \in \mathbb{S}^1, \qquad 0 < \epsilon\mu \ll \epsilon \ll 1.$$

– For $\epsilon = 0$: quasiperiodic motion, $\omega_1 = I_1$, $\omega_2 = I_2$.

– For $\epsilon \neq 0$, $\mu = 0$, two integrals:

$$H_1(I_1, \theta_1) = \frac{1}{2}I_1^2 + \epsilon(\cos\theta_1 - 1) = h_1, \qquad I_2.$$

$$\omega_1 = \omega_p(h_1), \qquad \omega_2 = I_2.$$

- H_1 : pendulum model for the resonance $\omega_1 = 0$.
- $h_1 = 0$: *separatrix*, $(I_1, \theta_1) = (0, 0)$ the unstable point or WT.
- Resonance half–width in action–space: $(\Delta I_1)^r = 2\sqrt{\epsilon}$.

The classical Arnold's model

$$H(I_1, I_2, \theta_1, \theta_2, t) = \frac{1}{2}(I_1^2 + I_2^2) + \epsilon(\cos\theta_1 - 1)[1 + \mu(\sin\theta_2 + \cos t)],$$

$$I_1, I_2 \in \mathbb{R}, \quad \theta_1, \theta_2, t \in \mathbb{S}^1, \qquad 0 < \epsilon\mu \ll \epsilon \ll 1.$$

– For $\epsilon = 0$: quasiperiodic motion, $\omega_1 = I_1$, $\omega_2 = I_2$.

– For $\epsilon \neq 0$, $\mu = 0$, two integrals:

$$H_1(I_1, \theta_1) = \frac{1}{2}I_1^2 + \epsilon(\cos\theta_1 - 1) = h_1, \qquad I_2.$$

$$\omega_1 = \omega_p(h_1), \qquad \omega_2 = I_2.$$

- H_1 : pendulum model for the resonance $\omega_1 = 0$.
- $h_1 = 0$: *separatrix*, $(I_1, \theta_1) = (0, 0)$ the unstable point or WT.
- Resonance half–width in action–space: $(\Delta I_1)^r = 2\sqrt{\epsilon}$.

The classical Arnold's model

$$H(I_1, I_2, \theta_1, \theta_2, t) = \frac{1}{2}(I_1^2 + I_2^2) + \epsilon(\cos\theta_1 - 1)[1 + \mu(\sin\theta_2 + \cos t)],$$

$$I_1, I_2 \in \mathbb{R}, \quad \theta_1, \theta_2, t \in \mathbb{S}^1, \qquad 0 < \epsilon\mu \ll \epsilon \ll 1.$$

– For $\epsilon = 0$: quasiperiodic motion, $\omega_1 = I_1$, $\omega_2 = I_2$.

– For $\epsilon \neq 0$, $\mu = 0$, two integrals:

$$H_1(I_1, \theta_1) = \frac{1}{2}I_1^2 + \epsilon(\cos\theta_1 - 1) = h_1, \qquad I_2.$$

$$\omega_1 = \omega_p(h_1), \qquad \omega_2 = I_2.$$

- H_1 : pendulum model for the resonance $\omega_1 = 0$.
- $h_1 = 0$: *separatrix*, $(I_1, \theta_1) = (0, 0)$ the unstable point or WT.
- Resonance half–width in action–space: $(\Delta I_1)^r = 2\sqrt{\epsilon}$.

The classical Arnold's model

$$H(I_1, I_2, \theta_1, \theta_2, t) = \frac{1}{2}(I_1^2 + I_2^2) + \epsilon(\cos\theta_1 - 1)[1 + \mu(\sin\theta_2 + \cos t)],$$

$$I_1, I_2 \in \mathbb{R}, \quad \theta_1, \theta_2, t \in \mathbb{S}^1, \qquad 0 < \epsilon\mu \ll \epsilon \ll 1.$$

– For $\epsilon = 0$: quasiperiodic motion, $\omega_1 = I_1$, $\omega_2 = I_2$.

– For $\epsilon \neq 0$, $\mu = 0$, two integrals:

$$H_1(I_1, \theta_1) = \frac{1}{2} I_1^2 + \epsilon(\cos\theta_1 - 1) = h_1, \qquad I_2.$$

$$\omega_1 = \omega_p(h_1), \qquad \omega_2 = I_2.$$

- H_1 : pendulum model for the resonance $\omega_1 = 0$.
- $h_1 = 0$: *separatrix*, $(I_1, \theta_1) = (0, 0)$ the unstable point or WT.
- Resonance half–width in action–space: $(\Delta I_1)^r = 2\sqrt{\epsilon}$.

The classical Arnold's model

$$H(I_1, I_2, \theta_1, \theta_2, t) = \frac{1}{2}(I_1^2 + I_2^2) + \epsilon(\cos\theta_1 - 1)[1 + \mu(\sin\theta_2 + \cos t)],$$

$$I_1, I_2 \in \mathbb{R}, \quad \theta_1, \theta_2, t \in \mathbb{S}^1, \qquad 0 < \epsilon\mu \ll \epsilon \ll 1.$$

– For $\epsilon = 0$: quasiperiodic motion, $\omega_1 = I_1$, $\omega_2 = I_2$.

– For $\epsilon \neq 0$, $\mu = 0$, two integrals:

$$H_1(I_1, \theta_1) = \frac{1}{2}I_1^2 + \epsilon(\cos\theta_1 - 1) = h_1, \qquad I_2.$$

$$\omega_1 = \omega_p(h_1), \qquad \omega_2 = I_2.$$

- H_1 : pendulum model for the resonance $\omega_1 = 0$.
- $h_1 = 0$: *separatrix*, $(I_1, \theta_1) = (0, 0)$ the unstable point or WT.
- Resonance half–width in action–space: $(\Delta I_1)^r = 2\sqrt{\epsilon}$.

The classical Arnold's model

$$H(I_1, I_2, \theta_1, \theta_2, t) = \frac{1}{2}(I_1^2 + I_2^2) + \epsilon(\cos\theta_1 - 1)[1 + \mu(\sin\theta_2 + \cos t)],$$

$$I_1, I_2 \in \mathbb{R}, \quad \theta_1, \theta_2, t \in \mathbb{S}^1, \qquad 0 < \epsilon\mu \ll \epsilon \ll 1.$$

– For $\epsilon = 0$: quasiperiodic motion, $\omega_1 = I_1$, $\omega_2 = I_2$.

– For $\epsilon \neq 0$, $\mu = 0$, two integrals:

$$H_1(I_1, \theta_1) = \frac{1}{2}I_1^2 + \epsilon(\cos\theta_1 - 1) = h_1, \qquad I_2.$$

$$\omega_1 = \omega_p(h_1), \qquad \omega_2 = I_2.$$

- H_1 : pendulum model for the resonance $\omega_1 = 0$.
- $h_1 = 0$: *separatrix*, $(I_1, \theta_1) = (0, 0)$ the unstable point or WT.
- Resonance half–width in action–space: $(\Delta I_1)^r = 2\sqrt{\epsilon}$.

The classical Arnold's model

$$H(I_1, I_2, \theta_1, \theta_2, t) = \frac{1}{2}(I_1^2+I_2^2)+\epsilon(\cos\theta_1 - 1)[1 + \mu(\sin\theta_2 + \cos t)],$$

$$I_1, I_2 \in \mathbb{R}, \quad \theta_1, \theta_2, t \in \mathbb{S}^1, \qquad 0 < \epsilon\mu \ll \epsilon \ll 1.$$

– For $\epsilon = 0$: quasiperiodic motion, $\omega_1 = I_1$, $\omega_2 = I_2$.

– For $\epsilon \neq 0$, $\mu = 0$, two integrals:

$$H_1(I_1, \theta_1) = \frac{1}{2}I_1^2 + \epsilon(\cos\theta_1 - 1) = h_1, \qquad I_2.$$

$$\omega_1 = \omega_p(h_1), \qquad \omega_2 = I_2.$$

- H_1 : pendulum model for the resonance $\omega_1 = 0$.
- $h_1 = 0$: *separatrix*, $(I_1, \theta_1) = (0, 0)$ the unstable point or WT.
- Resonance half–width in action–space: $(\Delta I_1)^r = 2\sqrt{\epsilon}$.

The classical Arnold's model

$$H(I_1, I_2, \theta_1, \theta_2, t) = \frac{1}{2}(I_1^2 + I_2^2) + \epsilon(\cos\theta_1 - 1)[1 + \mu(\sin\theta_2 + \cos t)],$$

$$I_1, I_2 \in \mathbb{R}, \quad \theta_1, \theta_2, t \in \mathbb{S}^1, \qquad 0 < \epsilon\mu \ll \epsilon \ll 1.$$

– For $\epsilon = 0$: quasiperiodic motion, $\omega_1 = I_1$, $\omega_2 = I_2$.

– For $\epsilon \neq 0$, $\mu = 0$, two integrals:

$$H_1(I_1, \theta_1) = \frac{1}{2}I_1^2 + \epsilon(\cos\theta_1 - 1) = h_1, \qquad I_2.$$

$$\omega_1 = \omega_p(h_1), \qquad \omega_2 = I_2.$$

- H_1 : pendulum model for the resonance $\omega_1 = 0$.
- $h_1 = 0$: *separatrix*, $(I_1, \theta_1) = (0, 0)$ the unstable point or WT.
- Resonance half–width in action–space: $(\Delta I_1)^r = 2\sqrt{\epsilon}$.

The classical Arnold's model

$$H(I_1, I_2, \theta_1, \theta_2, t) = \frac{1}{2}(I_1^2 + I_2^2) + \epsilon(\cos\theta_1 - 1)[1 + \mu(\sin\theta_2 + \cos t)],$$

$$I_1, I_2 \in \mathbb{R}, \quad \theta_1, \theta_2, t \in \mathbb{S}^1, \qquad 0 < \epsilon\mu \ll \epsilon \ll 1.$$

– For $\epsilon = 0$: quasiperiodic motion, $\omega_1 = I_1$, $\omega_2 = I_2$.

– For $\epsilon \neq 0$, $\mu = 0$, two integrals:

$$H_1(I_1, \theta_1) = \frac{1}{2}I_1^2 + \epsilon(\cos\theta_1 - 1) = h_1, \qquad I_2.$$

$$\omega_1 = \omega_p(h_1), \qquad \omega_2 = I_2.$$

- H_1 : pendulum model for the resonance $\omega_1 = 0$.
- $h_1 = 0$: *separatrix*, $(I_1, \theta_1) = (0, 0)$ the unstable point or WT.
- Resonance half–width in action–space: $(\Delta I_1)^r = 2\sqrt{\epsilon}$.

The classical Arnold's model

$$H(I_1, I_2, \theta_1, \theta_2, t) = \frac{1}{2}(I_1^2 + I_2^2) + \epsilon(\cos\theta_1 - 1)[1 + \mu(\sin\theta_2 + \cos t)],$$

$$I_1, I_2 \in \mathbb{R}, \quad \theta_1, \theta_2, t \in \mathbb{S}^1, \qquad 0 < \epsilon\mu \ll \epsilon \ll 1.$$

– For $\epsilon = 0$: quasiperiodic motion, $\omega_1 = I_1$, $\omega_2 = I_2$.

– For $\epsilon \neq 0$, $\mu = 0$, two integrals:

$$H_1(I_1, \theta_1) = \frac{1}{2}I_1^2 + \epsilon(\cos\theta_1 - 1) = h_1, \qquad I_2.$$

$$\omega_1 = \omega_p(h_1), \qquad \omega_2 = I_2.$$

- H_1 : pendulum model for the resonance $\omega_1 = 0$.
- $h_1 = 0$: *separatrix*, $(I_1, \theta_1) = (0, 0)$ the unstable point or WT.
- Resonance half–width in action–space: $(\Delta I_1)^r = 2\sqrt{\epsilon}$.

The classical Arnold's model

$$H(I_1, I_2, \theta_1, \theta_2, t) = \frac{1}{2}(I_1^2 + I_2^2) + \epsilon(\cos\theta_1 - 1)[1 + \mu(\sin\theta_2 + \cos t)],$$

$$I_1, I_2 \in \mathbb{R}, \quad \theta_1, \theta_2, t \in \mathbb{S}^1, \qquad 0 < \epsilon\mu \ll \epsilon \ll 1.$$

– For $\epsilon = 0$: quasiperiodic motion, $\omega_1 = I_1$, $\omega_2 = I_2$.

– For $\epsilon \neq 0$, $\mu = 0$, two integrals:

$$H_1(I_1, \theta_1) = \frac{1}{2}I_1^2 + \epsilon(\cos\theta_1 - 1) = h_1, \qquad I_2.$$

$$\omega_1 = \omega_p(h_1), \qquad \omega_2 = I_2.$$

- H_1 : pendulum model for the resonance $\omega_1 = 0$.
- $h_1 = 0$: *separatrix*, $(I_1, \theta_1) = (0, 0)$ the unstable point or WT.
- Resonance half–width in action–space: $(\Delta I_1)^r = 2\sqrt{\epsilon}$.

The classical Arnold's model

$$H(I_1, I_2, \theta_1, \theta_2, t) = \frac{1}{2}(I_1^2 + I_2^2) + \epsilon(\cos\theta_1 - 1)[1 + \mu(\sin\theta_2 + \cos t)],$$

$$I_1, I_2 \in \mathbb{R}, \quad \theta_1, \theta_2, t \in \mathbb{S}^1, \qquad 0 < \epsilon\mu \ll \epsilon \ll 1.$$

– For $\epsilon = 0$: quasiperiodic motion, $\omega_1 = I_1$, $\omega_2 = I_2$.

– For $\epsilon \neq 0$, $\mu = 0$, two integrals:

$$H_1(I_1, \theta_1) = \frac{1}{2}I_1^2 + \epsilon(\cos\theta_1 - 1) = h_1, \qquad I_2.$$

$$\omega_1 = \omega_p(h_1), \qquad \omega_2 = I_2.$$

- H_1 : pendulum model for the resonance $\omega_1 = 0$.
- $h_1 = 0$: *separatrix*, $(I_1, \theta_1) = (0, 0)$ the unstable point or WT.
- Resonance half–width in action–space: $(\Delta I_1)^r = 2\sqrt{\epsilon}$.

– For $\epsilon \neq 0, \mu \neq 0$, primary resonances at

$$\mathcal{O}(\epsilon): \;\; \omega_1 = 0, \qquad \mathcal{O}(\epsilon\mu): \;\; \omega_2 = 0, \quad \omega_1 = \pm\omega_2, \quad \omega_1 = \pm 1.$$

Full set of resonances: $k_1\omega_1 + k_2\omega_2 + k_3 = 0, \quad k_j \in \mathbb{Z},\; j = 1, 2, 3.$

In *energy–action* space: $k_1\omega_p(h_1) + k_2 I_2 + k_3 = 0,$

$$\omega_p(h_1, \epsilon) = \begin{cases} \frac{\pi\sqrt{\epsilon}}{2K(k_{h_1})} \leq \sqrt{\epsilon} & -2\epsilon \leq h_1 < 0 \\ \\ \frac{\pi\omega_r(h_1,\epsilon)}{2K\left(k_{h_1}^{-1}\right)} & h_1 > 0; \end{cases}$$

- $k_{h_1}^2 = (h_1 + 2\epsilon)/2\epsilon, \quad \omega_r(h_1, \epsilon) = \sqrt{\epsilon} k_{h_1},$
- $K(\kappa)$ is the complete elliptical integral of the first kind,
- $\omega_p(h_1, \epsilon) \to 0$ when $h_1 \to 0$ as $1/\ln(|h_1|)$.

– For $\epsilon \neq 0, \mu \neq 0$, primary resonances at

$$\mathcal{O}(\epsilon): \ \ \omega_1 = 0, \qquad \mathcal{O}(\epsilon\mu): \ \ \omega_2 = 0, \quad \omega_1 = \pm\omega_2, \quad \omega_1 = \pm 1.$$

Full set of resonances: $k_1\omega_1 + k_2\omega_2 + k_3 = 0, \quad k_j \in \mathbb{Z}, \ j = 1, 2, 3.$

In *energy–action* space: $k_1\omega_p(h_1) + k_2 I_2 + k_3 = 0,$

$$\omega_p(h_1, \epsilon) = \begin{cases} \frac{\pi\sqrt{\epsilon}}{2K\left(k_{h_1}\right)} \leq \sqrt{\epsilon} & -2\epsilon \leq h_1 < 0 \\ \\ \frac{\pi\omega_r(h_1,\epsilon)}{2K\left(k_{h_1}^{-1}\right)} & h_1 > 0; \end{cases}$$

- $k_{h_1}^2 = (h_1 + 2\epsilon)/2\epsilon, \quad \omega_r(h_1, \epsilon) = \sqrt{\epsilon}k_{h_1},$
- $K(\kappa)$ is the complete elliptical integral of the first kind,
- $\omega_p(h_1, \epsilon) \to 0$ when $h_1 \to 0$ as $1/\ln(|h_1|)$.

– For $\epsilon \neq 0, \mu \neq 0$, primary resonances at

$$\mathcal{O}(\epsilon): \;\; \omega_1 = 0, \qquad \mathcal{O}(\epsilon\mu): \;\; \omega_2 = 0, \quad \omega_1 = \pm\omega_2, \quad \omega_1 = \pm 1.$$

Full set of resonances: $k_1\omega_1 + k_2\omega_2 + k_3 = 0, \quad k_j \in \mathbb{Z}, \; j = 1, 2, 3.$

In *energy–action* space: $k_1\omega_p(h_1) + k_2 I_2 + k_3 = 0,$

$$\omega_p(h_1, \epsilon) = \begin{cases} \frac{\pi\sqrt{\epsilon}}{2K\left(k_{h_1}\right)} \leq \sqrt{\epsilon} & -2\epsilon \leq h_1 < 0 \\ \\ \frac{\pi\omega_r(h_1,\epsilon)}{2K\left(k_{h_1}^{-1}\right)} & h_1 > 0; \end{cases}$$

- $k_{h_1}^2 = (h_1 + 2\epsilon)/2\epsilon, \quad \omega_r(h_1, \epsilon) = \sqrt{\epsilon}k_{h_1},$
- $K(\kappa)$ is the complete elliptical integral of the first kind,
- $\omega_p(h_1, \epsilon) \to 0$ when $h_1 \to 0$ as $1/\ln(|h_1|)$.

– For $\epsilon \neq 0, \mu \neq 0$, primary resonances at

$$\mathcal{O}(\epsilon): \ \omega_1 = 0, \qquad \mathcal{O}(\epsilon\mu): \ \omega_2 = 0, \quad \omega_1 = \pm\omega_2, \quad \omega_1 = \pm 1.$$

Full set of resonances: $k_1\omega_1 + k_2\omega_2 + k_3 = 0, \quad k_j \in \mathbb{Z}, \ j = 1, 2, 3.$

In *energy–action* space: $k_1\omega_p(h_1) + k_2 I_2 + k_3 = 0,$

$$\omega_p(h_1, \epsilon) = \begin{cases} \frac{\pi\sqrt{\epsilon}}{2K(k_{h_1})} \leq \sqrt{\epsilon} & -2\epsilon \leq h_1 < 0 \\ \\ \frac{\pi\omega_r(h_1,\epsilon)}{2K\left(k_{h_1}^{-1}\right)} & h_1 > 0; \end{cases}$$

- $k_{h_1}^2 = (h_1 + 2\epsilon)/2\epsilon, \quad \omega_r(h_1, \epsilon) = \sqrt{\epsilon}k_{h_1},$
- $K(\kappa)$ is the complete elliptical integral of the first kind,
- $\omega_p(h_1, \epsilon) \to 0$ when $h_1 \to 0$ as $1/\ln(|h_1|)$.

– For $\epsilon \neq 0, \mu \neq 0$, primary resonances at

$$\mathcal{O}(\epsilon): \;\; \omega_1 = 0, \qquad \mathcal{O}(\epsilon\mu): \;\; \omega_2 = 0, \quad \omega_1 = \pm\omega_2, \quad \omega_1 = \pm 1.$$

Full set of resonances: $k_1\omega_1 + k_2\omega_2 + k_3 = 0, \quad k_j \in \mathbb{Z},\; j = 1, 2, 3.$

In *energy–action* space: $k_1\omega_p(h_1) + k_2 I_2 + k_3 = 0,$

$$\omega_p(h_1, \epsilon) = \begin{cases} \frac{\pi\sqrt{\epsilon}}{2K\left(k_{h_1}\right)} \leq \sqrt{\epsilon} & -2\epsilon \leq h_1 < 0 \\ \\ \frac{\pi\omega_r(h_1,\epsilon)}{2K\left(k_{h_1}^{-1}\right)} & h_1 > 0; \end{cases}$$

- $k_{h_1}^2 = (h_1 + 2\epsilon)/2\epsilon, \quad \omega_r(h_1, \epsilon) = \sqrt{\epsilon} k_{h_1},$
- $K(\kappa)$ is the complete elliptical integral of the first kind,
- $\omega_p(h_1, \epsilon) \to 0$ when $h_1 \to 0$ as $1/\ln(|h_1|)$.

– For $\epsilon \neq 0, \mu \neq 0$, primary resonances at

$$\mathcal{O}(\epsilon): \;\; \omega_1 = 0, \qquad \mathcal{O}(\epsilon\mu): \;\; \omega_2 = 0, \quad \omega_1 = \pm\omega_2, \quad \omega_1 = \pm 1.$$

Full set of resonances: $k_1\omega_1 + k_2\omega_2 + k_3 = 0, \quad k_j \in \mathbb{Z}, \; j = 1, 2, 3.$

In *energy–action* space: $k_1\omega_p(h_1) + k_2 I_2 + k_3 = 0,$

$$\omega_p(h_1, \epsilon) = \begin{cases} \frac{\pi\sqrt{\epsilon}}{2K\left(k_{h_1}\right)} \leq \sqrt{\epsilon} & -2\epsilon \leq h_1 < 0 \\ \\ \frac{\pi\omega_r(h_1,\epsilon)}{2K\left(k_{h_1}^{-1}\right)} & h_1 > 0; \end{cases}$$

- $k_{h_1}^2 = (h_1 + 2\epsilon)/2\epsilon, \quad \omega_r(h_1, \epsilon) = \sqrt{\epsilon}k_{h_1},$
- $K(\kappa)$ is the complete elliptical integral of the first kind,
- $\omega_p(h_1, \epsilon) \to 0$ when $h_1 \to 0$ as $1/\ln(|h_1|)$.

– For $\epsilon \neq 0, \mu \neq 0$, primary resonances at

$$\mathcal{O}(\epsilon): \;\; \omega_1 = 0, \qquad \mathcal{O}(\epsilon\mu): \;\; \omega_2 = 0, \quad \omega_1 = \pm\omega_2, \quad \omega_1 = \pm 1.$$

Full set of resonances: $k_1\omega_1 + k_2\omega_2 + k_3 = 0, \quad k_j \in \mathbb{Z},\; j = 1, 2, 3.$

In *energy–action* space: $k_1\omega_p(h_1) + k_2 I_2 + k_3 = 0,$

$$\omega_p(h_1, \epsilon) = \begin{cases} \frac{\pi\sqrt{\epsilon}}{2K\left(k_{h_1}\right)} \leq \sqrt{\epsilon} & -2\epsilon \leq h_1 < 0 \\ \\ \frac{\pi\omega_r(h_1,\epsilon)}{2K\left(k_{h_1}^{-1}\right)} & h_1 > 0; \end{cases}$$

- $k_{h_1}^2 = (h_1 + 2\epsilon)/2\epsilon, \quad \omega_r(h_1, \epsilon) = \sqrt{\epsilon} k_{h_1},$
- $K(\kappa)$ is the complete elliptical integral of the first kind,
- $\omega_p(h_1, \epsilon) \to 0$ when $h_1 \to 0$ as $1/\ln(|h_1|)$.

– For $\epsilon \neq 0, \mu \neq 0$, primary resonances at

$$\mathcal{O}(\epsilon): \ \ \omega_1 = 0, \qquad \mathcal{O}(\epsilon\mu): \ \ \omega_2 = 0, \quad \omega_1 = \pm\omega_2, \quad \omega_1 = \pm 1.$$

Full set of resonances: $k_1\omega_1 + k_2\omega_2 + k_3 = 0, \quad k_j \in \mathbb{Z}, \ j = 1, 2, 3.$

In *energy–action* space: $k_1\omega_p(h_1) + k_2 I_2 + k_3 = 0,$

$$\omega_p(h_1, \epsilon) = \begin{cases} \frac{\pi\sqrt{\epsilon}}{2K\left(k_{h_1}\right)} \leq \sqrt{\epsilon} & -2\epsilon \leq h_1 < 0 \\ \\ \frac{\pi\omega_r(h_1,\epsilon)}{2K\left(k_{h_1}^{-1}\right)} & h_1 > 0; \end{cases}$$

- $k_{h_1}^2 = (h_1 + 2\epsilon)/2\epsilon, \quad \omega_r(h_1, \epsilon) = \sqrt{\epsilon}k_{h_1},$
- $K(\kappa)$ is the complete elliptical integral of the first kind,
- $\omega_p(h_1, \epsilon) \to 0$ when $h_1 \to 0$ as $1/\ln(|h_1|)$.

$$H_1(I_1, \theta_1) = \frac{1}{2} I_1^2 + \epsilon(\cos\theta_1 - 1) = h_1,$$

$$\theta_1 = \pi, \quad I_1 = \sqrt{2h_1 + 4\epsilon}, \quad k_1 \omega_p(h_1) + k_2 I_2 + k_3 = 0, \quad k_i \in \mathbb{Z} :$$

$$H_1(I_1, \theta_1) = \frac{1}{2} I_1^2 + \epsilon(\cos\theta_1 - 1) = h_1,$$

$$\theta_1 = \pi, \quad I_1 = \sqrt{2h_1 + 4\epsilon}, \quad k_1 \omega_p(h_1) + k_2 I_2 + k_3 = 0, \quad k_i \in \mathbb{Z} :$$

$$H_1(I_1, \theta_1) = \frac{1}{2} I_1^2 + \epsilon(\cos\theta_1 - 1) = h_1,$$

$$\theta_1 = \pi, \quad I_1 = \sqrt{2h_1 + 4\epsilon}, \quad k_1 \omega_p(h_1) + k_2 I_2 + k_3 = 0, \quad k_i \in \mathbb{Z}:$$

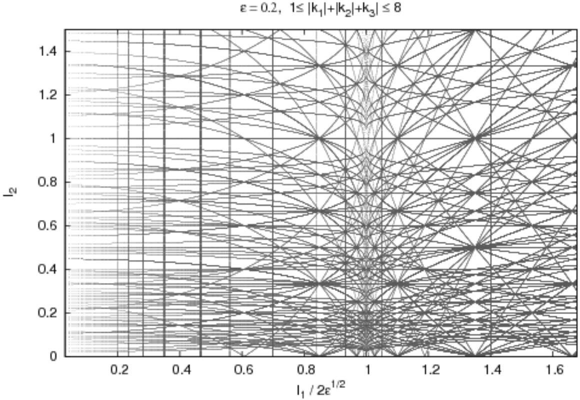

For $\mu = 0$:

While for $\mu \neq 0$:

For $\mu = 0$:

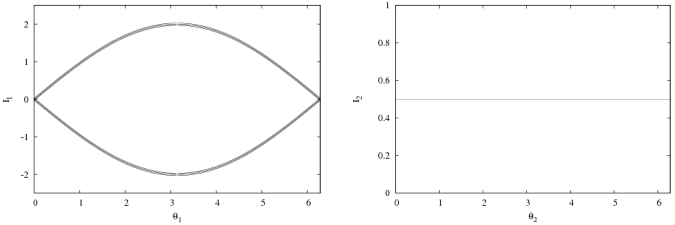

While for $\mu \neq 0$:

For $\mu = 0$:

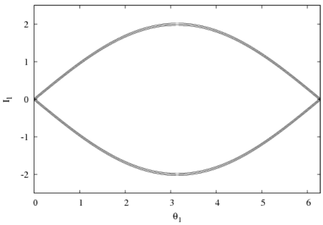

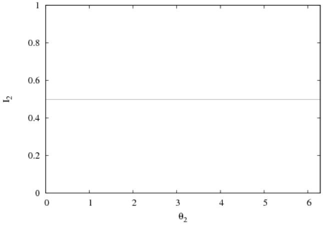

While for $\mu \neq 0$:

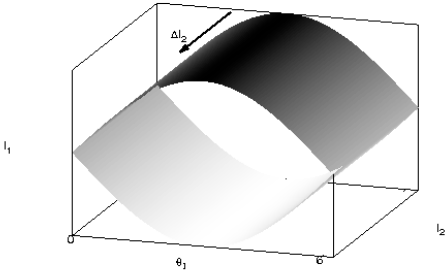

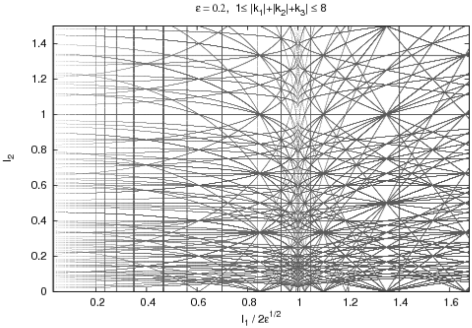

ε = 0.2, 1≤ |k1|+|k2|+k3| ≤ 8
1.4
1.2
1
0.8
0.6
0.4
0.2
0
I2
0.2
0.4
0.6
0.8
1
1.2
1.4
1.6
I1 / 2ε^1/2

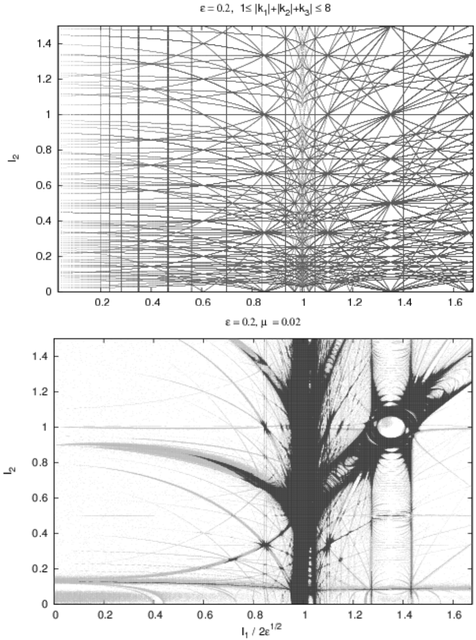

Figure: Megno contour plot for $\theta_1 = \pi, \theta_2 = t = 0$ and 10^6 i.c. on the (I_1, I_2) plane.

- For given values of $I_1(0), I_2(0)$ along the chaotic layer of the resonance $\omega_1 = 0$
- Ensembles of 1.000 i.c., size 10^{-7}
- Parameters not too small, $\epsilon = 0.25, \mu = 0.025$, far from Nekhoroshev regime
- For the adopted values of the parameters, the mean period of motion inside this chaotic layer is $\lesssim 10$
- Motion times $5 \times 10^6/10^7$.
- Double section: $|\theta_1 - \pi| + |\theta_2| < 0.01$ to see the diffusion in the 2D dynamical map,
- section: $|\theta_2| < 10^{-5}$ for the 3D visualization of the diffusion.

- For given values of $I_1(0), I_2(0)$ along the chaotic layer of the resonance $\omega_1 = 0$
- Ensembles of 1.000 i.c., size 10^{-7}
- Parameters not too small, $\epsilon = 0.25, \mu = 0.025$, far from Nekhoroshev regime
- For the adopted values of the parameters, the mean period of motion inside this chaotic layer is $\lesssim 10$
- Motion times $5 \times 10^6/10^7$.
- Double section: $|\theta_1 - \pi| + |\theta_2| < 0.01$ to see the diffusion in the 2D dynamical map,
- section: $|\theta_2| < 10^{-5}$ for the 3D visualization of the diffusion.

- For given values of $I_1(0), I_2(0)$ along the chaotic layer of the resonance $\omega_1 = 0$
- Ensembles of 1.000 i.c., size 10^{-7}
- Parameters not too small, $\epsilon = 0.25, \mu = 0.025$, far from Nekhoroshev regime
- For the adopted values of the parameters, the mean period of motion inside this chaotic layer is $\lesssim 10$
- Motion times $5 \times 10^6/10^7$.
- Double section: $|\theta_1 - \pi| + |\theta_2| < 0.01$ to see the diffusion in the 2D dynamical map,
- section: $|\theta_2| < 10^{-5}$ for the 3D visualization of the diffusion.

- For given values of $I_1(0), I_2(0)$ along the chaotic layer of the resonance $\omega_1 = 0$
- Ensembles of 1.000 i.c., size 10^{-7}
- Parameters not too small, $\epsilon = 0.25, \mu = 0.025$, far from Nekhoroshev regime
- For the adopted values of the parameters, the mean period of motion inside this chaotic layer is $\lesssim 10$
- Motion times $5 \times 10^6/10^7$.
- Double section: $|\theta_1 - \pi| + |\theta_2| < 0.01$ to see the diffusion in the 2D dynamical map,
- section: $|\theta_2| < 10^{-5}$ for the 3D visualization of the diffusion.

- For given values of $I_1(0), I_2(0)$ along the chaotic layer of the resonance $\omega_1 = 0$
- Ensembles of 1.000 i.c., size 10^{-7}
- Parameters not too small, $\epsilon = 0.25, \mu = 0.025$, far from Nekhoroshev regime
- For the adopted values of the parameters, the mean period of motion inside this chaotic layer is $\lesssim 10$
- Motion times $5 \times 10^6/10^7$.
- Double section: $|\theta_1 - \pi| + |\theta_2| < 0.01$ to see the diffusion in the 2D dynamical map,
- section: $|\theta_2| < 10^{-5}$ for the 3D visualization of the diffusion.

- For given values of $I_1(0), I_2(0)$ along the chaotic layer of the resonance $\omega_1 = 0$
- Ensembles of 1.000 i.c., size 10^{-7}
- Parameters not too small, $\epsilon = 0.25, \mu = 0.025$, far from Nekhoroshev regime
- For the adopted values of the parameters, the mean period of motion inside this chaotic layer is $\lesssim 10$
- Motion times $5 \times 10^6/10^7$.
- Double section: $|\theta_1 - \pi| + |\theta_2| < 0.01$ to see the diffusion in the 2D dynamical map,
- section: $|\theta_2| < 10^{-5}$ for the 3D visualization of the diffusion.

- For given values of $I_1(0), I_2(0)$ along the chaotic layer of the resonance $\omega_1 = 0$
- Ensembles of 1.000 i.c., size 10^{-7}
- Parameters not too small, $\epsilon = 0.25, \mu = 0.025$, far from Nekhoroshev regime
- For the adopted values of the parameters, the mean period of motion inside this chaotic layer is $\lesssim 10$
- Motion times $5 \times 10^6/10^7$.
- Double section: $|\theta_1 - \pi| + |\theta_2| < 0.01$ to see the diffusion in the 2D dynamical map,
- section: $|\theta_2| < 10^{-5}$ for the 3D visualization of the diffusion.

$\varepsilon = 0.25, \mu = 0.025, t_f = 5\,10^6, |\theta_2| < 10^{-5}$

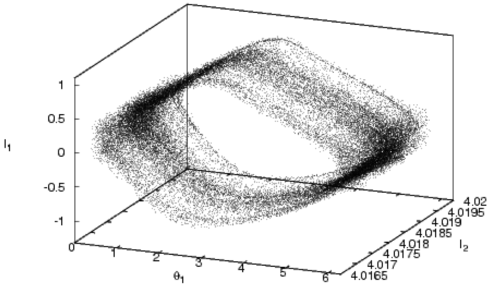

$\varepsilon = 0.25, \mu = 0.025, t_f = 5\,10^6, |\theta_2| < 10^{-5}$

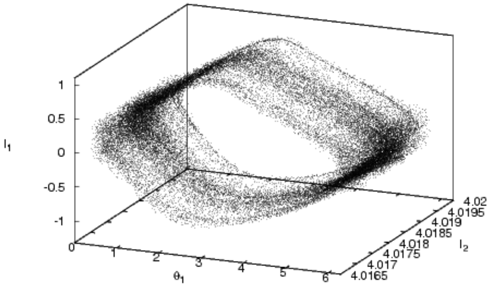

$\varepsilon = 0.25, \mu = 0.025, t_f = 5\,10^6, |\theta_1 - \pi| + |\theta_2| < 0.01$

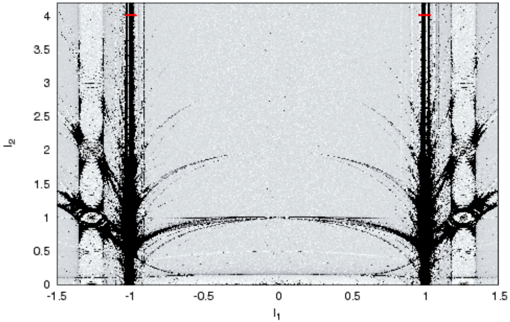

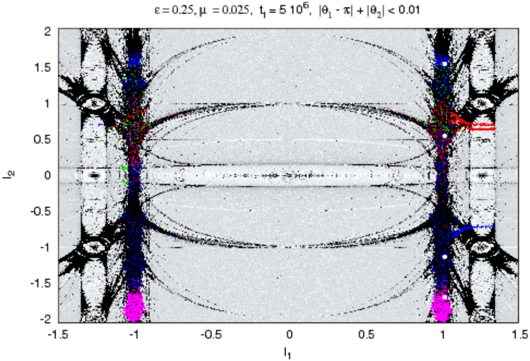
ε = 0.25, μ = 0.025, t_1 = 5 10^6, $|\theta_1 - \pi| + |\theta_2| < 0.01$
2
1.5
1
0.5
0
-0.5
-1
-1.5
-2
I_2
-1.5
-1
-0.5
0
0.5
1
1.5
I_1

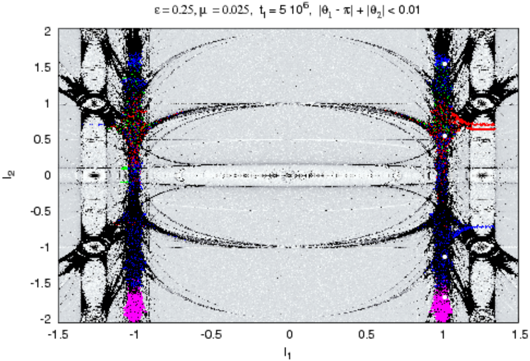

ε = 0.25, μ = 0.025, t_f = 5 10^6, |θ_1 - π| + |θ_2| < 0.01
I_2
I_1

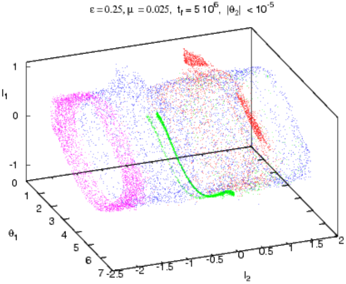

ε = 0.25, μ = 0.025, t_f = 5 10^6, |θ_2| < 10^-5
I_1
θ_1
I_2

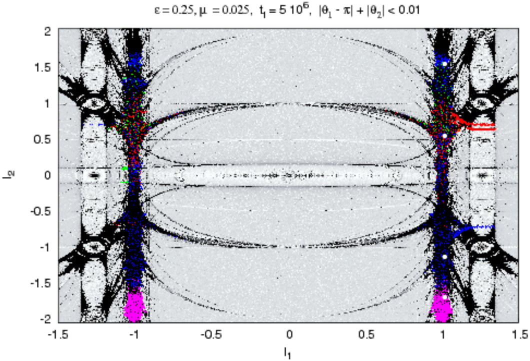
ε = 0.25, μ = 0.025, $t_f = 5\ 10^6$, $|\theta_1 - \pi| + |\theta_2| < 0.01$
I_2
I_1

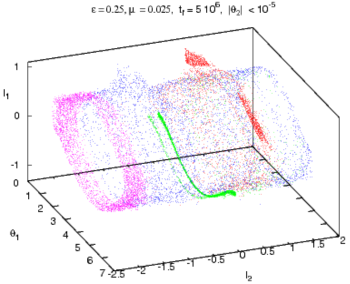
ε = 0.25, μ = 0.025, $t_f = 5\ 10^6$, $|\theta_2| < 10^{-5}$
I_1
θ_1
I_2

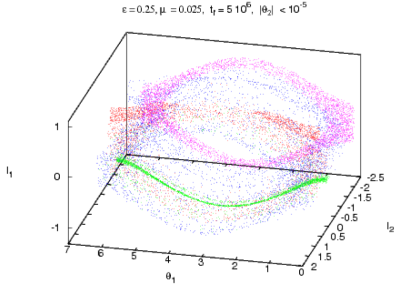
ε = 0.25, μ = 0.025, $t_f = 5\ 10^6$, $|\theta_2| < 10^{-5}$
I_1
θ_1
I_2

Chirikov's estimates for $\mu \ll \epsilon \ll 1$:

– Width of the chaotic layer of the resonance $\omega_1 = 0$:

$$w_s \sim \begin{cases} \frac{\mu}{\epsilon^{3/2}} \exp\left(\frac{-\pi}{2\sqrt{\epsilon}}\right) & \omega_2 > 1 \\ \\ \frac{\mu\omega_2}{\epsilon^{3/2}} \exp\left(\frac{-\pi\omega_2}{2\sqrt{\epsilon}}\right) & 0 < \omega_2 < 1. \end{cases}$$

– Diffusion coefficient (assuming normal diffusion):

$$D(\omega_2) \sim \begin{cases} \frac{\omega_2^2\mu^2}{T_a} \exp\left(\frac{-\pi\omega_2}{\sqrt{\epsilon}}\right), & \omega_2 > 1 \\ \\ \frac{\mu^2}{T_a} \exp\left(\frac{-\pi}{\sqrt{\epsilon}}\right) & 0 < \omega_2 < 1; \end{cases}$$

$$T_a \approx \frac{1}{\sqrt{\epsilon}} \ln\left(\frac{32e}{w_s}\right) \sim \frac{\pi}{2\epsilon} + \frac{c(\omega_2) + \ln(\epsilon^{3/2}/\mu)}{\sqrt{\epsilon}}, \qquad |c(\omega_2)| \sim 1$$

Chirikov's estimates for $\mu \ll \epsilon \ll 1$:

– Width of the chaotic layer of the resonance $\omega_1 = 0$:

$$w_s \sim \begin{cases} \frac{\mu}{\epsilon^{3/2}} \exp\left(\frac{-\pi}{2\sqrt{\epsilon}}\right) & \omega_2 > 1 \\ \\ \frac{\mu\omega_2}{\epsilon^{3/2}} \exp\left(\frac{-\pi\omega_2}{2\sqrt{\epsilon}}\right) & 0 < \omega_2 < 1. \end{cases}$$

– Diffusion coefficient (assuming normal diffusion):

$$D(\omega_2) \sim \begin{cases} \frac{\omega_2^2\mu^2}{T_a} \exp\left(\frac{-\pi\omega_2}{\sqrt{\epsilon}}\right), & \omega_2 > 1 \\ \\ \frac{\mu^2}{T_a} \exp\left(\frac{-\pi}{\sqrt{\epsilon}}\right) & 0 < \omega_2 < 1; \end{cases}$$

$$T_a \approx \frac{1}{\sqrt{\epsilon}} \ln\left(\frac{32e}{w_s}\right) \sim \frac{\pi}{2\epsilon} + \frac{c(\omega_2) + \ln(\epsilon^{3/2}/\mu)}{\sqrt{\epsilon}}, \qquad |c(\omega_2)| \sim 1$$

Chirikov's estimates for $\mu \ll \epsilon \ll 1$:

– Width of the chaotic layer of the resonance $\omega_1 = 0$:

$$w_s \sim \begin{cases} \frac{\mu}{\epsilon^{3/2}} \exp\left(\frac{-\pi}{2\sqrt{\epsilon}}\right) & \omega_2 > 1 \\ \\ \frac{\mu\omega_2}{\epsilon^{3/2}} \exp\left(\frac{-\pi\omega_2}{2\sqrt{\epsilon}}\right) & 0 < \omega_2 < 1. \end{cases}$$

– Diffusion coefficient (assuming normal diffusion):

$$D(\omega_2) \sim \begin{cases} \frac{\omega_2^2\mu^2}{T_a} \exp\left(\frac{-\pi\omega_2}{\sqrt{\epsilon}}\right), & \omega_2 > 1 \\ \\ \frac{\mu^2}{T_a} \exp\left(\frac{-\pi}{\sqrt{\epsilon}}\right) & 0 < \omega_2 < 1; \end{cases}$$

$$T_a \approx \frac{1}{\sqrt{\epsilon}} \ln\left(\frac{32e}{w_s}\right) \sim \frac{\pi}{2\epsilon} + \frac{c(\omega_2) + \ln(\epsilon^{3/2}/\mu)}{\sqrt{\epsilon}}, \qquad |c(\omega_2)| \sim 1$$

Chirikov's estimates for $\mu \ll \epsilon \ll 1$:

– Width of the chaotic layer of the resonance $\omega_1 = 0$:

$$w_s \sim \begin{cases} \frac{\mu}{\epsilon^{3/2}} \exp\left(\frac{-\pi}{2\sqrt{\epsilon}}\right) & \omega_2 > 1 \\ \\ \frac{\mu\omega_2}{\epsilon^{3/2}} \exp\left(\frac{-\pi\omega_2}{2\sqrt{\epsilon}}\right) & 0 < \omega_2 < 1. \end{cases}$$

– Diffusion coefficient (assuming normal diffusion):

$$D(\omega_2) \sim \begin{cases} \frac{\omega_2^2\mu^2}{T_a} \exp\left(\frac{-\pi\omega_2}{\sqrt{\epsilon}}\right), & \omega_2 > 1 \\ \\ \frac{\mu^2}{T_a} \exp\left(\frac{-\pi}{\sqrt{\epsilon}}\right) & 0 < \omega_2 < 1; \end{cases}$$

$$T_a \approx \frac{1}{\sqrt{\epsilon}} \ln\left(\frac{32e}{w_s}\right) \sim \frac{\pi}{2\epsilon} + \frac{c(\omega_2) + \ln(\epsilon^{3/2}/\mu)}{\sqrt{\epsilon}}, \qquad |c(\omega_2)| \sim 1$$

Chirikov's estimates for $\mu \ll \epsilon \ll 1$:

– Width of the chaotic layer of the resonance $\omega_1 = 0$:

$$w_s \sim \begin{cases} \frac{\mu}{\epsilon^{3/2}} \exp\left(\frac{-\pi}{2\sqrt{\epsilon}}\right) & \omega_2 > 1 \\ \\ \frac{\mu\omega_2}{\epsilon^{3/2}} \exp\left(\frac{-\pi\omega_2}{2\sqrt{\epsilon}}\right) & 0 < \omega_2 < 1. \end{cases}$$

– Diffusion coefficient (assuming normal diffusion):

$$D(\omega_2) \sim \begin{cases} \frac{\omega_2^2\mu^2}{T_a} \exp\left(\frac{-\pi\omega_2}{\sqrt{\epsilon}}\right), & \omega_2 > 1 \\ \\ \frac{\mu^2}{T_a} \exp\left(\frac{-\pi}{\sqrt{\epsilon}}\right) & 0 < \omega_2 < 1; \end{cases}$$

$$T_a \approx \frac{1}{\sqrt{\epsilon}} \ln\left(\frac{32e}{w_s}\right) \sim \frac{\pi}{2\epsilon} + \frac{c(\omega_2) + \ln(\epsilon^{3/2}/\mu)}{\sqrt{\epsilon}}, \qquad |c(\omega_2)| \sim 1$$

Chirikov's estimates for $\mu \ll \epsilon \ll 1$:

– Width of the chaotic layer of the resonance $\omega_1 = 0$:

$$w_s \sim \begin{cases} \frac{\mu}{\epsilon^{3/2}} \exp\left(\frac{-\pi}{2\sqrt{\epsilon}}\right) & \omega_2 > 1 \\ \\ \frac{\mu\omega_2}{\epsilon^{3/2}} \exp\left(\frac{-\pi\omega_2}{2\sqrt{\epsilon}}\right) & 0 < \omega_2 < 1. \end{cases}$$

– Diffusion coefficient (assuming normal diffusion):

$$D(\omega_2) \sim \begin{cases} \frac{\omega_2^2\mu^2}{T_a} \exp\left(\frac{-\pi\omega_2}{\sqrt{\epsilon}}\right), & \omega_2 > 1 \\ \\ \frac{\mu^2}{T_a} \exp\left(\frac{-\pi}{\sqrt{\epsilon}}\right) & 0 < \omega_2 < 1; \end{cases}$$

$$T_a \approx \frac{1}{\sqrt{\epsilon}} \ln\left(\frac{32e}{w_s}\right) \sim \frac{\pi}{2\epsilon} + \frac{c(\omega_2) + \ln(\epsilon^{3/2}/\mu)}{\sqrt{\epsilon}}, \qquad |c(\omega_2)| \sim 1$$

Models of discrete time: 4D generalized standard map

$$
\begin{aligned}
y_1' &= y_1 + \epsilon_1^2 f_1(x_1) + \epsilon_1\gamma_+ f_3(x_1+x_2) + \epsilon_1\gamma_- f_3(x_1-x_2), \\
y_2' &= y_2 + \epsilon_2^2 f_2(x_2) + \epsilon_2\gamma_+ f_3(x_1+x_2) - \epsilon_2\gamma_- f_3(x_1-x_2), \\
x_1' &= x_1 + y_1', \\
x_2' &= x_2 + y_2',
\end{aligned}
$$

$$
f_k(u) = \frac{\pm \sin u}{1 - \mu_k \cos u}, \qquad 0 \le \mu_k < 1,
$$

$x_i, y_i \in [0 : 2\pi),\ \gamma_s < \epsilon_j < 1.$

f_k is such that for $-$ sign, $(y_i, x_i) = (0,0)$ is the stable fixed point, while for the $+$ sign, $(0,0)$ is the unstable one.

For simplicity, assume that $\epsilon_1 = \epsilon_2 = \epsilon$, $\gamma_+ = \gamma_- = \gamma$ and $\mu_1 = \mu_2 = \mu_3 = \mu$.

Models of discrete time: 4D generalized standard map

$$
\begin{aligned}
y_1' &= y_1 + \epsilon_1^2 f_1(x_1) + \epsilon_1\gamma_+ f_3(x_1+x_2) + \epsilon_1\gamma_- f_3(x_1-x_2),\\
y_2' &= y_2 + \epsilon_2^2 f_2(x_2) + \epsilon_2\gamma_+ f_3(x_1+x_2) - \epsilon_2\gamma_- f_3(x_1-x_2),\\
x_1' &= x_1 + y_1',\\
x_2' &= x_2 + y_2',
\end{aligned}
$$

$$f_k(u) = \frac{\pm \sin u}{1-\mu_k \cos u}, \qquad 0 \le \mu_k < 1,$$

$x_i, y_i \in [0:2\pi),\ \gamma_s < \epsilon_j < 1.$

f_k is such that for $-$ sign, $(y_i, x_i) = (0,0)$ is the stable fixed point, while for the $+$ sign, $(0,0)$ is the unstable one.

For simplicity, assume that $\epsilon_1 = \epsilon_2 = \epsilon$, $\gamma_+ = \gamma_- = \gamma$ and $\mu_1 = \mu_2 = \mu_3 = \mu$.

Models of discrete time: 4D generalized standard map

$$
\begin{aligned}
y_1' &= y_1 + \epsilon_1^2 f_1(x_1) + \epsilon_1\gamma_+ \, f_3(x_1+x_2) + \epsilon_1\gamma_- \, f_3(x_1-x_2), \\
y_2' &= y_2 + \epsilon_2^2 \, f_2(x_2) + \epsilon_2\gamma_+ \, f_3(x_1+x_2) - \epsilon_2\gamma_- \, f_3(x_1-x_2), \\
x_1' &= x_1 + y_1', \\
x_2' &= x_2 + y_2',
\end{aligned}
$$

$$
f_k(u) = \frac{\pm \sin u}{1-\mu_k \cos u}, \qquad 0 \le \mu_k < 1,
$$

$x_i, y_i \in [0:2\pi)$, $\gamma_s < \epsilon_j < 1$.

f_k is such that for $-$ sign, $(y_i, x_i) = (0,0)$ is the stable fixed point, while for the $+$ sign, $(0,0)$ is the unstable one.

For simplicity, assume that $\epsilon_1 = \epsilon_2 = \epsilon$, $\gamma_+ = \gamma_- = \gamma$ and $\mu_1 = \mu_2 = \mu_3 = \mu$.

Models of discrete time: 4D generalized standard map

$$\begin{aligned}
y_1' &= y_1 + \epsilon_1^2 f_1(x_1) + \epsilon_1\gamma_+ f_3(x_1+x_2) + \epsilon_1\gamma_- f_3(x_1-x_2),\\
y_2' &= y_2 + \epsilon_2^2 f_2(x_2) + \epsilon_2\gamma_+ f_3(x_1+x_2) - \epsilon_2\gamma_- f_3(x_1-x_2),\\
x_1' &= x_1 + y_1',\\
x_2' &= x_2 + y_2',
\end{aligned}$$

$$f_k(u) = \frac{\pm\sin u}{1-\mu_k\cos u}, \qquad 0 \le \mu_k < 1,$$

$x_i, y_i \in [0:2\pi)$, $\gamma_s < \epsilon_j < 1$.

f_k is such that for $-$ sign, $(y_i, x_i) = (0,0)$ is the stable fixed point, while for the $+$ sign, $(0,0)$ is the unstable one.

For simplicity, assume that $\epsilon_1 = \epsilon_2 = \epsilon$, $\gamma_+ = \gamma_- = \gamma$ and $\mu_1 = \mu_2 = \mu_3 = \mu$.

Models of discrete time: 4D generalized standard map

$$
\begin{aligned}
y_1' &= y_1 + \epsilon_1^2 f_1(x_1) + \epsilon_1\gamma_+ f_3(x_1+x_2) + \epsilon_1\gamma_- f_3(x_1-x_2), \\
y_2' &= y_2 + \epsilon_2^2 f_2(x_2) + \epsilon_2\gamma_+ f_3(x_1+x_2) - \epsilon_2\gamma_- f_3(x_1-x_2), \\
x_1' &= x_1 + y_1', \\
x_2' &= x_2 + y_2',
\end{aligned}
$$

$$
f_k(u) = \frac{\pm\sin u}{1-\mu_k\cos u}, \qquad 0 \le \mu_k < 1,
$$

$x_i, y_i \in [0:2\pi),\ \gamma_s < \epsilon_j < 1.$

f_k is such that for $-$ sign, $(y_i, x_i) = (0,0)$ is the stable fixed point, while for the $+$ sign, $(0,0)$ is the unstable one.

For simplicity, assume that $\epsilon_1 = \epsilon_2 = \epsilon$, $\gamma_+ = \gamma_- = \gamma$ and $\mu_1 = \mu_2 = \mu_3 = \mu$.

The potential function for $f \equiv -V'$ is

$$V(u) = \pm\frac{1}{\mu}\ln\Big\{1 - \mu\,\cos u\Big\}, \qquad \mu \neq 0.$$

Expanding $V(u)$ in powers of μ and using the $\delta_{2\pi}$: 2π–periodic δ, any of the four terms in the potential

$$U(x_1, \epsilon^2) + U(x_2, \epsilon^2) + U(x_1 + x_2, \epsilon\gamma) + U(x_1 - x_2, \epsilon\gamma)$$

of the corresponding Hamiltonian has the form ($\varepsilon \equiv \epsilon^2, \epsilon\gamma$):

$$\begin{aligned} U(u,\varepsilon) &= \frac{\varepsilon}{4\pi^2}\Bigg\{\left(1+\frac{\mu^2}{4}\right)\sum_{n=-\infty}^{\infty}\cos(u+nt) + \\ &+ \frac{\mu}{4}\sum_{n=-\infty}^{\infty}\cos(2u+nt) + \frac{\mu^2}{12}\sum_{n=-\infty}^{\infty}\cos(3u+nt) + \ldots\Bigg\}, \end{aligned}$$

with $u = x_1, x_2, x_1 \pm x_2$, $\;2\pi\dot{u} = y_1, y_2, y_1 \pm y_2$.

The potential function for $f \equiv -V'$ is

$$V(u) = \pm\frac{1}{\mu}\ln\Big\{1 - \mu\,\cos u\Big\}, \qquad \mu \neq 0.$$

Expanding $V(u)$ in powers of μ and using the $\delta_{2\pi}$: 2π–periodic δ, any of the four terms in the potential

$$U(x_1,\epsilon^2) + U(x_2,\epsilon^2) + U(x_1+x_2,\epsilon\gamma) + U(x_1-x_2,\epsilon\gamma)$$

of the corresponding Hamiltonian has the form ($\varepsilon \equiv \epsilon^2, \epsilon\gamma$):

$$\begin{aligned} U(u,\varepsilon) &= \frac{\varepsilon}{4\pi^2}\Bigg\{\left(1+\frac{\mu^2}{4}\right)\sum_{n=-\infty}^{\infty}\cos(u+nt) + \\ &+ \frac{\mu}{4}\sum_{n=-\infty}^{\infty}\cos(2u+nt) + \frac{\mu^2}{12}\sum_{n=-\infty}^{\infty}\cos(3u+nt) + \ldots\Bigg\}, \end{aligned}$$

with $u = x_1, x_2, x_1 \pm x_2$, $\quad 2\pi\dot{u} = y_1, y_2, y_1 \pm y_2$.

The potential function for $f \equiv -V'$ is

$$V(u) = \pm\frac{1}{\mu}\ln\left\{1 - \mu\,\cos u\right\}, \qquad \mu \neq 0.$$

Expanding $V(u)$ in powers of μ and using the $\delta_{2\pi}$: 2π–periodic δ, any of the four terms in the potential

$$U(x_1, \epsilon^2) + U(x_2, \epsilon^2) + U(x_1 + x_2, \epsilon\gamma) + U(x_1 - x_2, \epsilon\gamma)$$

of the corresponding Hamiltonian has the form ($\varepsilon \equiv \epsilon^2, \epsilon\gamma$):

$$\begin{aligned} U(u,\varepsilon) &= \frac{\varepsilon}{4\pi^2}\left\{\left(1+\frac{\mu^2}{4}\right)\sum_{n=-\infty}^{\infty}\cos(u\,+nt) + \right. \\ &+ \left. \frac{\mu}{4}\sum_{n=-\infty}^{\infty}\cos(2u\,+nt) + \frac{\mu^2}{12}\sum_{n=-\infty}^{\infty}\cos(3u\,+nt) + \ldots\right\}, \end{aligned}$$

with $u = x_1, x_2, x_1 \pm x_2, \quad 2\pi\dot{u} = y_1, y_2, y_1 \pm y_2$.

Denoting

$$\hat{y_1} = \frac{y_1}{2\pi}, \quad \hat{y_2} = \frac{y_2}{2\pi},$$

"first order" resonances up to $\mathcal{O}(\varepsilon\mu^2)$:

$$\mathcal{O}(\epsilon^2): \quad \hat{y_1}, \hat{y_2} = 0, 1;$$

$$\mathcal{O}(\epsilon^2\mu): \quad \hat{y_1}, \hat{y_2} = 0, \frac{1}{2}, 1;$$

$$\mathcal{O}(\epsilon^2\mu^2): \quad \hat{y_1}, \hat{y_2} = 0, \frac{1}{3}, \frac{2}{3}, 1;$$

$$\mathcal{O}(\epsilon\gamma): \quad \hat{y_1} \pm \hat{y_2} = 0, 1;$$

$$\mathcal{O}(\epsilon\gamma\mu): \quad \hat{y_1} \pm \hat{y_2} = 0, \frac{1}{2}, 1;$$

$$\mathcal{O}(\epsilon\gamma\mu^2): \quad \hat{y_1} \pm \hat{y_2} = 0, \frac{1}{3}, \frac{2}{3}, 1.$$

Denoting

$$\hat{y_1} = \frac{y_1}{2\pi}, \quad \hat{y_2} = \frac{y_2}{2\pi},$$

"first order" resonances up to $\mathcal{O}(\varepsilon\mu^2)$:

$$\mathcal{O}(\epsilon^2): \quad \hat{y_1}, \hat{y_2} = 0, 1;$$

$$\mathcal{O}(\epsilon^2\mu): \quad \hat{y_1}, \hat{y_2} = 0, \frac{1}{2}, 1;$$

$$\mathcal{O}(\epsilon^2\mu^2): \quad \hat{y_1}, \hat{y_2} = 0, \frac{1}{3}, \frac{2}{3}, 1;$$

$$\mathcal{O}(\epsilon\gamma): \quad \hat{y_1} \pm \hat{y_2} = 0, 1;$$

$$\mathcal{O}(\epsilon\gamma\mu): \quad \hat{y_1} \pm \hat{y_2} = 0, \frac{1}{2}, 1;$$

$$\mathcal{O}(\epsilon\gamma\mu^2): \quad \hat{y_1} \pm \hat{y_2} = 0, \frac{1}{3}, \frac{2}{3}, 1.$$

Denoting

$$\hat{y_1} = \frac{y_1}{2\pi}, \quad \hat{y_2} = \frac{y_2}{2\pi},$$

"first order" resonances up to $\mathcal{O}(\varepsilon\mu^2)$:

$$\mathcal{O}(\epsilon^2) : \quad \hat{y_1}, \hat{y_2} = 0, 1;$$

$$\mathcal{O}(\epsilon^2\mu) : \quad \hat{y_1}, \hat{y_2} = 0, \frac{1}{2}, 1;$$

$$\mathcal{O}(\epsilon^2\mu^2) : \quad \hat{y_1}, \hat{y_2} = 0, \frac{1}{3}, \frac{2}{3}, 1;$$

$$\mathcal{O}(\epsilon\gamma) : \quad \hat{y_1} \pm \hat{y_2} = 0, 1;$$

$$\mathcal{O}(\epsilon\gamma\mu) : \quad \hat{y_1} \pm \hat{y_2} = 0, \frac{1}{2}, 1;$$

$$\mathcal{O}(\epsilon\gamma\mu^2) : \quad \hat{y_1} \pm \hat{y_2} = 0, \frac{1}{3}, \frac{2}{3}, 1.$$

Denoting

$$\hat{y_1} = \frac{y_1}{2\pi}, \quad \hat{y_2} = \frac{y_2}{2\pi},$$

"first order" resonances up to $\mathcal{O}(\varepsilon\mu^2)$:

$$\mathcal{O}(\epsilon^2): \quad \hat{y_1}, \hat{y_2} = 0, 1;$$

$$\mathcal{O}(\epsilon^2\mu): \quad \hat{y_1}, \hat{y_2} = 0, \frac{1}{2}, 1;$$

$$\mathcal{O}(\epsilon^2\mu^2): \quad \hat{y_1}, \hat{y_2} = 0, \frac{1}{3}, \frac{2}{3}, 1;$$

$$\mathcal{O}(\epsilon\gamma): \quad \hat{y_1} \pm \hat{y_2} = 0, 1;$$

$$\mathcal{O}(\epsilon\gamma\mu): \quad \hat{y_1} \pm \hat{y_2} = 0, \frac{1}{2}, 1;$$

$$\mathcal{O}(\epsilon\gamma\mu^2): \quad \hat{y_1} \pm \hat{y_2} = 0, \frac{1}{3}, \frac{2}{3}, 1.$$

Denoting

$$\hat{y_1} = \frac{y_1}{2\pi}, \quad \hat{y_2} = \frac{y_2}{2\pi},$$

"first order" resonances up to $\mathcal{O}(\varepsilon\mu^2)$:

$$\mathcal{O}(\epsilon^2): \quad \hat{y_1}, \hat{y_2} = 0, 1;$$

$$\mathcal{O}(\epsilon^2\mu): \quad \hat{y_1}, \hat{y_2} = 0, \frac{1}{2}, 1;$$

$$\mathcal{O}(\epsilon^2\mu^2): \quad \hat{y_1}, \hat{y_2} = 0, \frac{1}{3}, \frac{2}{3}, 1;$$

$$\mathcal{O}(\epsilon\gamma): \quad \hat{y_1} \pm \hat{y_2} = 0, 1;$$

$$\mathcal{O}(\epsilon\gamma\mu): \quad \hat{y_1} \pm \hat{y_2} = 0, \frac{1}{2}, 1;$$

$$\mathcal{O}(\epsilon\gamma\mu^2): \quad \hat{y_1} \pm \hat{y_2} = 0, \frac{1}{3}, \frac{2}{3}, 1.$$

Denoting

$$\hat{y_1} = \frac{y_1}{2\pi}, \quad \hat{y_2} = \frac{y_2}{2\pi},$$

"first order" resonances up to $\mathcal{O}(\varepsilon\mu^2)$:

$$\mathcal{O}(\epsilon^2): \quad \hat{y_1}, \hat{y_2} = 0, 1;$$

$$\mathcal{O}(\epsilon^2\mu): \quad \hat{y_1}, \hat{y_2} = 0, \frac{1}{2}, 1;$$

$$\mathcal{O}(\epsilon^2\mu^2): \quad \hat{y_1}, \hat{y_2} = 0, \frac{1}{3}, \frac{2}{3}, 1;$$

$$\mathcal{O}(\epsilon\gamma): \quad \hat{y_1} \pm \hat{y_2} = 0, 1;$$

$$\mathcal{O}(\epsilon\gamma\mu): \quad \hat{y_1} \pm \hat{y_2} = 0, \frac{1}{2}, 1;$$

$$\mathcal{O}(\epsilon\gamma\mu^2): \quad \hat{y_1} \pm \hat{y_2} = 0, \frac{1}{3}, \frac{2}{3}, 1.$$

Denoting

$$\hat{y_1} = \frac{y_1}{2\pi}, \quad \hat{y_2} = \frac{y_2}{2\pi},$$

"first order" resonances up to $\mathcal{O}(\varepsilon\mu^2)$:

$$\mathcal{O}(\epsilon^2): \quad \hat{y_1}, \hat{y_2} = 0, 1;$$

$$\mathcal{O}(\epsilon^2\mu): \quad \hat{y_1}, \hat{y_2} = 0, \frac{1}{2}, 1;$$

$$\mathcal{O}(\epsilon^2\mu^2): \quad \hat{y_1}, \hat{y_2} = 0, \frac{1}{3}, \frac{2}{3}, 1;$$

$$\mathcal{O}(\epsilon\gamma): \quad \hat{y_1} \pm \hat{y_2} = 0, 1;$$

$$\mathcal{O}(\epsilon\gamma\mu): \quad \hat{y_1} \pm \hat{y_2} = 0, \frac{1}{2}, 1;$$

$$\mathcal{O}(\epsilon\gamma\mu^2): \quad \hat{y_1} \pm \hat{y_2} = 0, \frac{1}{3}, \frac{2}{3}, 1.$$

Full set of resonances: $k_1\hat{y_1} + k_2\hat{y_2} + k_3 = 0, \quad k_j \in \mathbb{Z}$

Full set of resonances: $k_1\hat{y_1} + k_2\hat{y_2} + k_3 = 0, \quad k_j \in \mathbb{Z}$

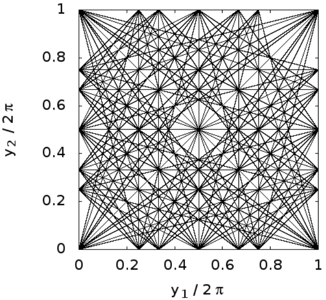

Full set of resonances: $k_1\hat{y_1} + k_2\hat{y_2} + k_3 = 0, \quad k_j \in \mathbb{Z}$

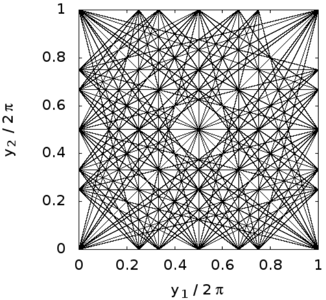

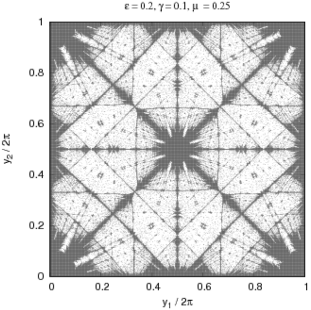

Full set of resonances: $k_1\hat{y_1} + k_2\hat{y_2} + k_3 = 0, \quad k_j \in \mathbb{Z}$

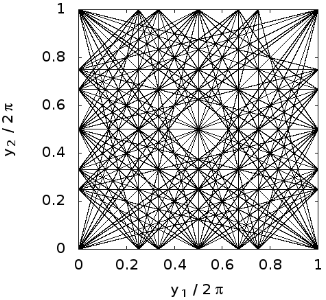

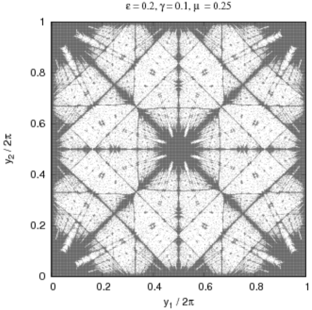

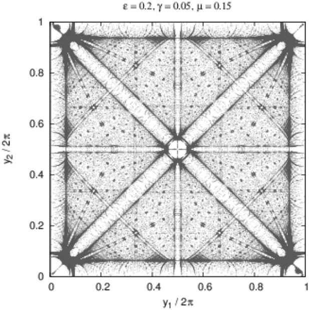

Full set of resonances: $k_1\hat{y_1} + k_2\hat{y_2} + k_3 = 0, \quad k_j \in \mathbb{Z}$

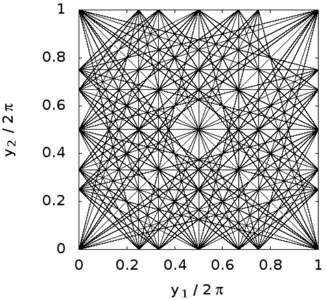

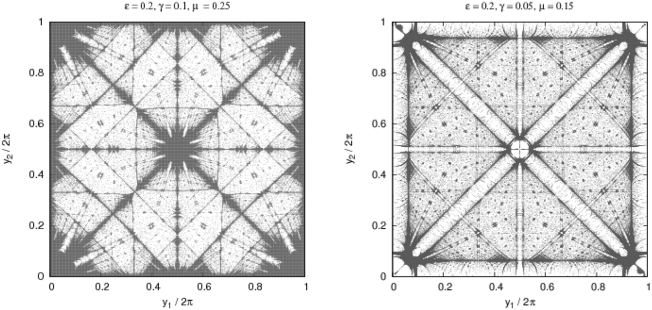

Figure: MEGNO contour plot for $x_1 = x_2 = 0$ (+ sign left, − sign right)

- Ensemble of 2000 i.cs. of size $10^{-7/-8}$ around $y_1(0), y_2(0)$,
- $y_1(0), y_2(0)$ on different main resonances,
- $\epsilon_s, \gamma_s, \mu_s$ not too small such that the system is far from Nekhoroshev regime,
- Motion times $N = 10^7/10^8$, large enough but not “infinite”, $N \ll 10^{11} - 10^{12}$.

- Ensemble of 2000 i.cs. of size $10^{-7/-8}$ around $y_1(0), y_2(0)$,
- $y_1(0), y_2(0)$ on different main resonances,
- $\epsilon_s, \gamma_s, \mu_s$ not too small such that the system is far from Nekhoroshev regime,
- Motion times $N = 10^7/10^8$, large enough but not "infinite", $N \ll 10^{11} - 10^{12}$.

- Ensemble of 2000 i.cs. of size $10^{-7/-8}$ around $y_1(0), y_2(0)$,
- $y_1(0), y_2(0)$ on different main resonances,
- $\epsilon_s, \gamma_s, \mu_s$ not too small such that the system is far from Nekhoroshev regime,
- Motion times $N = 10^7/10^8$, large enough but not "infinite", $N \ll 10^{11} - 10^{12}$.

- Ensemble of 2000 i.cs. of size $10^{-7/-8}$ around $y_1(0), y_2(0)$,
- $y_1(0), y_2(0)$ on different main resonances,
- $\epsilon_s, \gamma_s, \mu_s$ not too small such that the system is far from Nekhoroshev regime,
- Motion times $N = 10^7/10^8$, large enough but not "infinite", $N \ll 10^{11} - 10^{12}$.

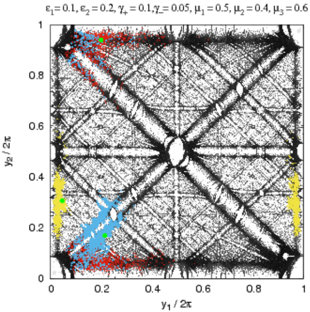
$\varepsilon_1 = 0.1, \varepsilon_2 = 0.2, \gamma_+ = 0.1, \gamma_- = 0.05, \mu_1 = 0.5, \mu_2 = 0.4, \mu_3 = 0.6$
$y_2 / 2\pi$
$y_1 / 2\pi$
0
0.2
0.4
0.6
0.8
1

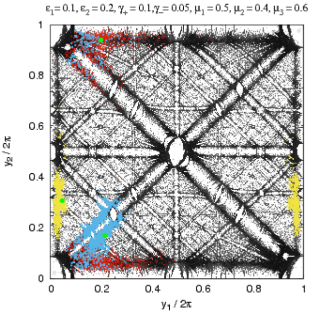
$\varepsilon_1 = 0.1, \varepsilon_2 = 0.2, \gamma_+ = 0.1, \gamma_- = 0.05, \mu_1 = 0.5, \mu_2 = 0.4, \mu_3 = 0.6$
$y_1 / 2\pi$
$y_2 / 2\pi$
0
0.2
0.4
0.6
0.8
1

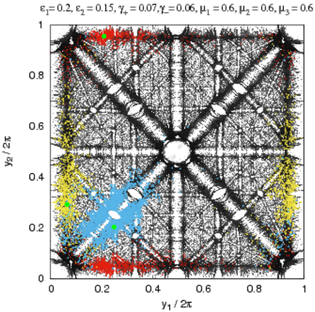
$\varepsilon_1 = 0.2, \varepsilon_2 = 0.15, \gamma_+ = 0.07, \gamma_- = 0.06, \mu_1 = 0.6, \mu_2 = 0.6, \mu_3 = 0.6$
$y_1 / 2\pi$
$y_2 / 2\pi$
0
0.2
0.4
0.6
0.8
1

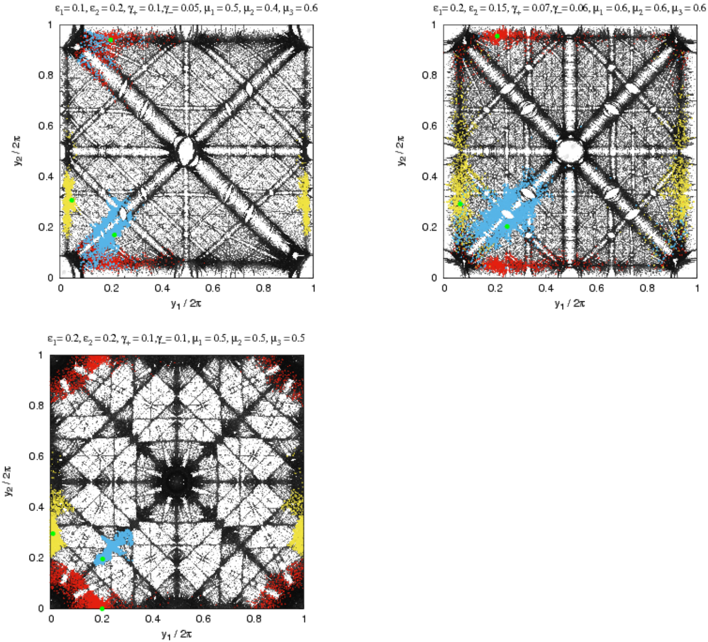
ε1= 0.1, ε2 = 0.2, γ+ = 0.1,γ− = 0.05, μ1 = 0.5, μ2 = 0.4, μ3 = 0.6
ε1= 0.2, ε2 = 0.15, γ+ = 0.07,γ− = 0.06, μ1 = 0.6, μ2 = 0.6, μ3 = 0.6
ε1= 0.2, ε2 = 0.2, γ+ = 0.1,γ− = 0.1, μ1 = 0.5, μ2 = 0.5, μ3 = 0.5
y2 / 2π
y1 / 2π
0
0.2
0.4
0.6
0.8
1

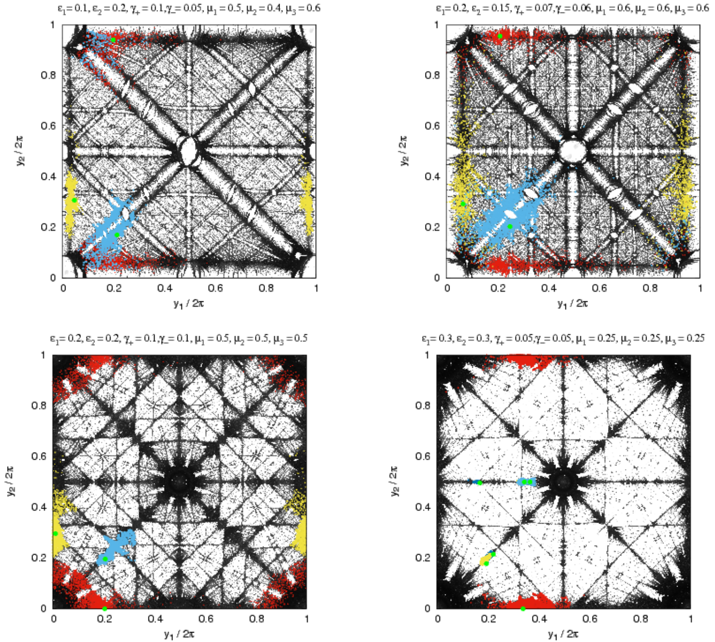

ε1= 0.1, ε2 = 0.2, γ+ = 0.1, γ_ = 0.05, μ1 = 0.5, μ2 = 0.4, μ3 = 0.6
ε1= 0.2, ε2 = 0.15, γ+ = 0.07, γ_ = 0.06, μ1 = 0.6, μ2 = 0.6, μ3 = 0.6
ε1= 0.2, ε2 = 0.2, γ+ = 0.1, γ_ = 0.1, μ1 = 0.5, μ2 = 0.5, μ3 = 0.5
ε1= 0.3, ε2 = 0.3, γ+ = 0.05, γ_ = 0.05, μ1 = 0.25, μ2 = 0.25, μ3 = 0.25
y1 / 2π
y2 / 2π
0
0.2
0.4
0.6
0.8
1

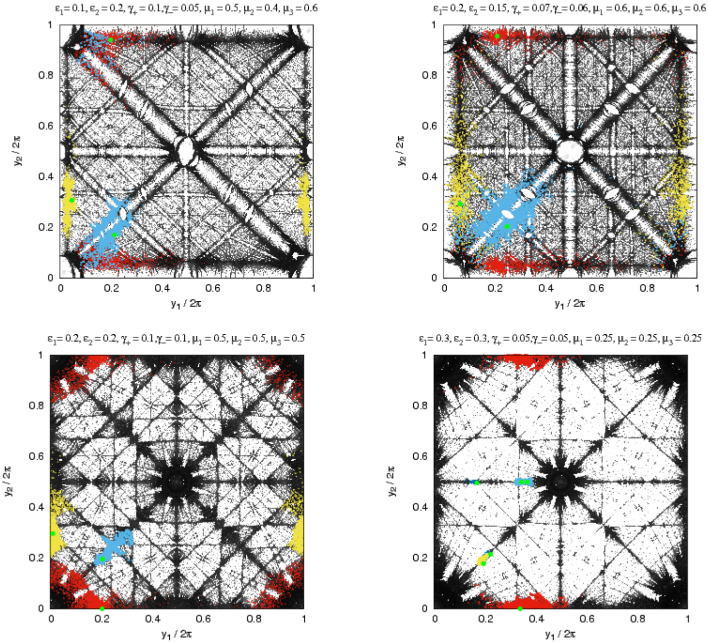

Figure: Diffusion after $t = 10^7/10^8$ iterates on the section $x_1 = x_2 = 0$.

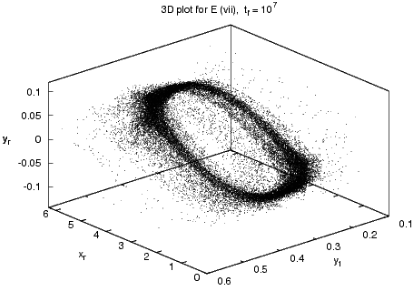
3D plot for E (vii), $t_f = 10^7$
0.1
0.05
y_r
0
-0.05
-0.1
6
5
4
3
2
1
0
x_r
0.6
0.5
0.4
0.3
y_1
0.2
0.1

3D plot for E (vii), $t_f = 10^7$

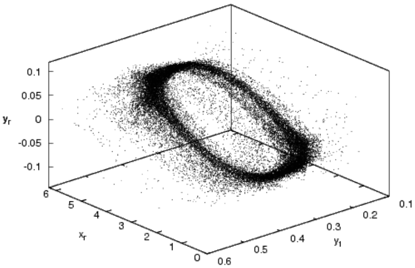

3D plot for E (iv), $t_l = 10^7$

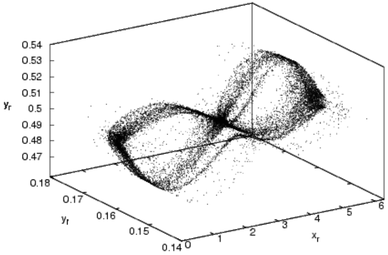

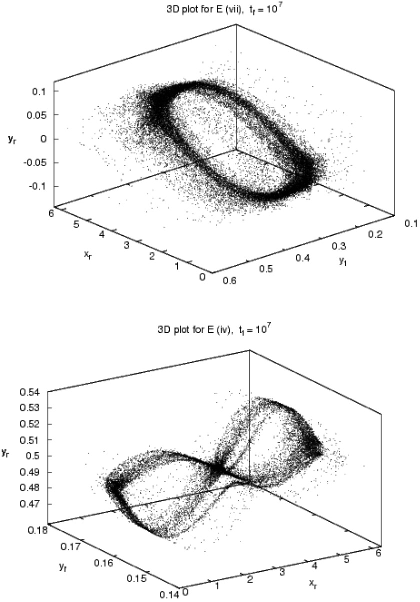

Figure: 3D visualization for an integer and semi-integer resonance.

About the derivation of the diffusion coefficient

- In all cases, the estimation of the diffusion coefficient rests on the assumption of *free diffusion*,
- this means that an ensemble of i.c. evolves as Brownian motion,
- so, successive values of phases involved in the time evolution of the actions should be uncorrelated.
- The diffusion is assumed to be homogeneous and isotropic.
- Under this approximation, $\langle(\Delta I)^2(t)\rangle \approx Dt$ over all chaotic domains, Normal diffusion.
- Thus, D only depends on the perturbation parameter, and it is just the constant rate at which the variance evolves with time.
- However, in general, $\langle(\Delta I)^2(t)\rangle \approx Ct^{\alpha}$, $\alpha < 1$, due to the correlations of the successive values of the phases.
- Theory including correlations of phases is still lacking.

About the derivation of the diffusion coefficient

- In all cases, the estimation of the diffusion coefficient rests on the assumption of *free diffusion*,
- this means that an ensemble of i.c. evolves as Brownian motion,
- so, successive values of phases involved in the time evolution of the actions should be uncorrelated.
- The diffusion is assumed to be homogeneous and isotropic.
- Under this approximation, $\langle(\Delta I)^2(t)\rangle \approx Dt$ over all chaotic domains, Normal diffusion.
- Thus, D only depends on the perturbation parameter, and it is just the constant rate at which the variance evolves with time.
- However, in general, $\langle(\Delta I)^2(t)\rangle \approx Ct^{\alpha}$, $\alpha < 1$, due to the correlations of the successive values of the phases.
- Theory including correlations of phases is still lacking.

About the derivation of the diffusion coefficient

- In all cases, the estimation of the diffusion coefficient rests on the assumption of *free diffusion*,
- this means that an ensemble of i.c. evolves as Brownian motion,
- so, successive values of phases involved in the time evolution of the actions should be uncorrelated.
- The diffusion is assumed to be homogeneous and isotropic.
- Under this approximation, $\langle (\Delta I)^2(t) \rangle \approx Dt$ over all chaotic domains, Normal diffusion.
- Thus, D only depends on the perturbation parameter, and it is just the constant rate at which the variance evolves with time.
- However, in general, $\langle (\Delta I)^2(t) \rangle \approx Ct^\alpha$, $\alpha < 1$, due to the correlations of the successive values of the phases.
- Theory including correlations of phases is still lacking.

About the derivation of the diffusion coefficient

- In all cases, the estimation of the diffusion coefficient rests on the assumption of *free diffusion*,
- this means that an ensemble of i.c. evolves as Brownian motion,
- so, successive values of phases involved in the time evolution of the actions should be uncorrelated.
- The diffusion is assumed to be homogeneous and isotropic.
- Under this approximation, $\langle (\Delta I)^2(t) \rangle \approx Dt$ over all chaotic domains, Normal diffusion.
- Thus, D only depends on the perturbation parameter, and it is just the constant rate at which the variance evolves with time.
- However, in general, $\langle (\Delta I)^2(t) \rangle \approx Ct^{\alpha}$, $\alpha < 1$, due to the correlations of the successive values of the phases.
- Theory including correlations of phases is still lacking.

About the derivation of the diffusion coefficient

- In all cases, the estimation of the diffusion coefficient rests on the assumption of *free diffusion*,
- this means that an ensemble of i.c. evolves as Brownian motion,
- so, successive values of phases involved in the time evolution of the actions should be uncorrelated.
- The diffusion is assumed to be homogeneous and isotropic.
- Under this approximation, $\langle(\Delta I)^2(t)\rangle \approx Dt$ over all chaotic domains, Normal diffusion.
- Thus, D only depends on the perturbation parameter, and it is just the constant rate at which the variance evolves with time.
- However, in general, $\langle(\Delta I)^2(t)\rangle \approx Ct^{\alpha}$, $\alpha < 1$, due to the correlations of the successive values of the phases.
- Theory including correlations of phases is still lacking.

About the derivation of the diffusion coefficient

- In all cases, the estimation of the diffusion coefficient rests on the assumption of *free diffusion*,
- this means that an ensemble of i.c. evolves as Brownian motion,
- so, successive values of phases involved in the time evolution of the actions should be uncorrelated.
- The diffusion is assumed to be homogeneous and isotropic.
- Under this approximation, $\langle (\Delta I)^2(t) \rangle \approx Dt$ over all chaotic domains, Normal diffusion.
- Thus, D only depends on the perturbation parameter, and it is just the constant rate at which the variance evolves with time.
- However, in general, $\langle (\Delta I)^2(t) \rangle \approx Ct^{\alpha}$, $\alpha < 1$, due to the correlations of the successive values of the phases.
- Theory including correlations of phases is still lacking.

About the derivation of the diffusion coefficient

- In all cases, the estimation of the diffusion coefficient rests on the assumption of *free diffusion*,
- this means that an ensemble of i.c. evolves as Brownian motion,
- so, successive values of phases involved in the time evolution of the actions should be uncorrelated.
- The diffusion is assumed to be homogeneous and isotropic.
- Under this approximation, $\langle(\Delta I)^2(t)\rangle \approx Dt$ over all chaotic domains, Normal diffusion.
- Thus, D only depends on the perturbation parameter, and it is just the constant rate at which the variance evolves with time.
- However, in general, $\langle(\Delta I)^2(t)\rangle \approx Ct^{\alpha}$, $\alpha < 1$, due to the correlations of the successive values of the phases.
- Theory including correlations of phases is still lacking.

About the derivation of the diffusion coefficient

- In all cases, the estimation of the diffusion coefficient rests on the assumption of *free diffusion*,
- this means that an ensemble of i.c. evolves as Brownian motion,
- so, successive values of phases involved in the time evolution of the actions should be uncorrelated.
- The diffusion is assumed to be homogeneous and isotropic.
- Under this approximation, $\langle (\Delta I)^2(t) \rangle \approx Dt$ over all chaotic domains, Normal diffusion.
- Thus, D only depends on the perturbation parameter, and it is just the constant rate at which the variance evolves with time.
- However, in general, $\langle (\Delta I)^2(t) \rangle \approx Ct^{\alpha}$, $\alpha < 1$, due to the correlations of the successive values of the phases.
- Theory including correlations of phases is still lacking.

About the derivation of the diffusion coefficient

- In all cases, the estimation of the diffusion coefficient rests on the assumption of *free diffusion*,
- this means that an ensemble of i.c. evolves as Brownian motion,
- so, successive values of phases involved in the time evolution of the actions should be uncorrelated.
- The diffusion is assumed to be homogeneous and isotropic.
- Under this approximation, $\langle(\Delta I)^2(t)\rangle \approx Dt$ over all chaotic domains, Normal diffusion.
- Thus, D only depends on the perturbation parameter, and it is just the constant rate at which the variance evolves with time.
- However, in general, $\langle(\Delta I)^2(t)\rangle \approx Ct^{\alpha}$, $\alpha < 1$, due to the correlations of the successive values of the phases.
- Theory including correlations of phases is still lacking.

The numerical computation of the variance of the actions

Being N_p the number of i.c. in a small neighborhood $d \ll 1$ of $y_1(0), y_2(0)$, and $I_r(0), I_f(0)$ the corresponding resonant and *fast* actions,

let $t_j = t_0 + j\delta t$, δt being for instance, the time step.

– Ensemble average:

$$\sigma_1^2(t_j) = \frac{1}{N_p} \sum_{j=1}^{N_p} (I_f(t_j) - I_f(0))^2.$$

σ_1^2 could be rather noisy and for small perturbations, its time evolution may hide any slow secular growth.
Alternatives:
Normal form construction to eliminate the deformation effect due to oscillations (Giorgilli, Efthymiopoulos, PMC, etc.)
or using a double section (Guzzo, Lega, Froeshlé, etc).

The numerical computation of the variance of the actions

Being N_p the number of i.c. in a small neighborhood $d \ll 1$ of $y_1(0), y_2(0)$, and $I_r(0), I_f(0)$ the corresponding resonant and *fast* actions,

let $t_j = t_0 + j\delta t$, δt being for instance, the time step.

– Ensemble average:

$$\sigma_1^2(t_j) = \frac{1}{N_p} \sum_{j=1}^{N_p} (I_f(t_j) - I_f(0))^2.$$

σ_1^2 could be rather noisy and for small perturbations, its time evolution may hide any slow secular growth.
Alternatives:
Normal form construction to eliminate the deformation effect due to oscillations (Giorgilli, Efthymiopoulos, PMC, etc.)
or using a double section (Guzzo, Lega, Froeshlé, etc).

The numerical computation of the variance of the actions

Being N_p the number of i.c. in a small neighborhood $d \ll 1$ of $y_1(0), y_2(0)$, and $I_r(0), I_f(0)$ the corresponding resonant and *fast* actions,

let $t_j = t_0 + j\delta t$, δt being for instance, the time step.

– Ensemble average:

$$\sigma_1^2(t_j) = \frac{1}{N_p} \sum_{j=1}^{N_p} (I_f(t_j) - I_f(0))^2.$$

σ_1^2 could be rather noisy and for small perturbations, its time evolution may hide any slow secular growth.
Alternatives:
Normal form construction to eliminate the deformation effect due to oscillations (Giorgilli, Efthymiopoulos, PMC, etc.)
or using a double section (Guzzo, Lega, Froeshlé, etc).

The numerical computation of the variance of the actions

Being N_p the number of i.c. in a small neighborhood $d \ll 1$ of $y_1(0), y_2(0)$, and $I_r(0), I_f(0)$ the corresponding resonant and *fast* actions,

let $t_j = t_0 + j\delta t$, δt being for instance, the time step.

– Ensemble average:

$$\sigma_1^2(t_j) = \frac{1}{N_p} \sum_{j=1}^{N_p} (I_f(t_j) - I_f(0))^2.$$

σ_1^2 could be rather noisy and for small perturbations, its time evolution may hide any slow secular growth.
Alternatives:
Normal form construction to eliminate the deformation effect due to oscillations (Giorgilli, Efthymiopoulos, PMC, etc.)
or using a double section (Guzzo, Lega, Froeshlé, etc).

The numerical computation of the variance of the actions

Being N_p the number of i.c. in a small neighborhood $d \ll 1$ of $y_1(0), y_2(0)$, and $I_r(0), I_f(0)$ the corresponding resonant and *fast* actions,

let $t_j = t_0 + j\delta t$, δt being for instance, the time step.

– Ensemble average:

$$\sigma_1^2(t_j) = \frac{1}{N_p}\sum_{j=1}^{N_p}(I_f(t_j) - I_f(0))^2.$$

σ_1^2 could be rather noisy and for small perturbations, its time evolution may hide any slow secular growth.

Alternatives:

Normal form construction to eliminate the deformation effect due to oscillations (Giorgilli, Efthymiopoulos, PMC, etc.)

or using a double section (Guzzo, Lega, Froeshlé, etc).

The numerical computation of the variance of the actions

Being N_p the number of i.c. in a small neighborhood $d \ll 1$ of $y_1(0), y_2(0)$, and $I_r(0), I_f(0)$ the corresponding resonant and *fast* actions,

let $t_j = t_0 + j\delta t$, δt being for instance, the time step.

– Ensemble average:

$$\sigma_1^2(t_j) = \frac{1}{N_p} \sum_{j=1}^{N_p} (I_f(t_j) - I_f(0))^2.$$

σ_1^2 could be rather noisy and for small perturbations, its time evolution may hide any slow secular growth.

Alternatives:

Normal form construction to eliminate the deformation effect due to oscillations (Giorgilli, Efthymiopoulos, PMC, etc.)

or using a double section (Guzzo, Lega, Froeshlé, etc).

The numerical computation of the variance of the actions

Being N_p the number of i.c. in a small neighborhood $d \ll 1$ of $y_1(0), y_2(0)$, and $I_r(0), I_f(0)$ the corresponding resonant and *fast* actions,

let $t_j = t_0 + j\delta t$, δt being for instance, the time step.

– Ensemble average:

$$\sigma_1^2(t_j) = \frac{1}{N_p} \sum_{j=1}^{N_p} (I_f(t_j) - I_f(0))^2.$$

σ_1^2 could be rather noisy and for small perturbations, its time evolution may hide any slow secular growth.
Alternatives:
Normal form construction to eliminate the deformation effect due to oscillations (Giorgilli, Efthymiopoulos, PMC, etc.)
or using a double section (Guzzo, Lega, Froeshlé, etc).

The numerical computation of the variance of the actions

Being N_p the number of i.c. in a small neighborhood $d \ll 1$ of $y_1(0), y_2(0)$, and $I_r(0), I_f(0)$ the corresponding resonant and *fast* actions,

let $t_j = t_0 + j\delta t$, δt being for instance, the time step.

– Ensemble average:

$$\sigma_1^2(t_j) = \frac{1}{N_p} \sum_{j=1}^{N_p} (I_f(t_j) - I_f(0))^2.$$

σ_1^2 could be rather noisy and for small perturbations, its time evolution may hide any slow secular growth.
Alternatives:
Normal form construction to eliminate the deformation effect due to oscillations (Giorgilli, Efthymiopoulos, PMC, etc.)
or using a double section (Guzzo, Lega, Froeshlé, etc).

– Average over a given section

For instance $|\theta_1| + |\theta_2| < \varepsilon \ll 1$ after a time interval $\Delta t \gg \delta t$.

For the map: $\delta t = 1, \Delta t = 10^4$, total motion time $10^7/10^8$,

while for the Arnolds'model: $\delta t = 2 \times 10^{-4}, \Delta t = 5 \times 10^4$, total motion time $5 \times 10^6/10^7$.

$$\sigma_2^2(t_l) = \frac{1}{N_s(t_l)} \sum_{m=1}^{N_s(t_l)} (I_f(t_m) - I_f(0))^2,$$

where $N_s(t_l)$ is the number of points on the section in the interval $((l-1)\Delta t, l\Delta t)$,

$$|((l-1)\Delta t, l\Delta t)| = \Delta t.$$

– Average over a given section

For instance $|\theta_1| + |\theta_2| < \varepsilon \ll 1$ after a time interval $\Delta t \gg \delta t$.

For the map: $\delta t = 1, \Delta t = 10^4$, total motion time $10^7/10^8$,

while for the Arnolds'model: $\delta t = 2 \times 10^{-4}, \Delta t = 5 \times 10^4$, total motion time $5 \times 10^6/10^7$.

$$\sigma_2^2(t_l) = \frac{1}{N_s(t_l)} \sum_{m=1}^{N_s(t_l)} (I_f(t_m) - I_f(0))^2,$$

where $N_s(t_l)$ is the number of points on the section in the interval $((l-1)\Delta t, l\Delta t)$,

$$|((l-1)\Delta t, l\Delta t)| = \Delta t.$$

– Average over a given section

For instance $|\theta_1| + |\theta_2| < \varepsilon \ll 1$ after a time interval $\Delta t \gg \delta t$.

For the map: $\delta t = 1, \Delta t = 10^4$, total motion time $10^7/10^8$,

while for the Arnolds'model: $\delta t = 2 \times 10^{-4}, \Delta t = 5 \times 10^4$, total motion time $5 \times 10^6/10^7$.

$$\sigma_2^2(t_l) = \frac{1}{N_s(t_l)} \sum_{m=1}^{N_s(t_l)} (I_f(t_m) - I_f(0))^2,$$

where $N_s(t_l)$ is the number of points on the section in the interval $((l-1)\Delta t, l\Delta t)$,

$$|((l-1)\Delta t, l\Delta t)| = \Delta t.$$

– Average over a given section

For instance $|\theta_1| + |\theta_2| < \varepsilon \ll 1$ after a time interval $\Delta t \gg \delta t$.

For the map: $\delta t = 1, \Delta t = 10^4$, total motion time $10^7/10^8$,

while for the Arnolds'model: $\delta t = 2 \times 10^{-4}, \Delta t = 5 \times 10^4$, total motion time $5 \times 10^6/10^7$.

$$\sigma_2^2(t_l) = \frac{1}{N_s(t_l)} \sum_{m=1}^{N_s(t_l)} (I_f(t_m) - I_f(0))^2,$$

where $N_s(t_l)$ is the number of points on the section in the interval $((l-1)\Delta t, l\Delta t)$,

$$|((l-1)\Delta t, l\Delta t)| = \Delta t.$$

– Average over a given section

For instance $|\theta_1| + |\theta_2| < \varepsilon \ll 1$ after a time interval $\Delta t \gg \delta t$.

For the map: $\delta t = 1, \Delta t = 10^4$, total motion time $10^7/10^8$,

while for the Arnolds'model: $\delta t = 2 \times 10^{-4}, \Delta t = 5 \times 10^4$, total motion time $5 \times 10^6/10^7$.

$$\sigma_2^2(t_l) = \frac{1}{N_s(t_l)} \sum_{m=1}^{N_s(t_l)} (I_f(t_m) - I_f(0))^2,$$

where $N_s(t_l)$ is the number of points on the section in the interval $((l-1)\Delta t, l\Delta t)$,

$$|((l-1)\Delta t, l\Delta t)| = \Delta t.$$

– Average over a given section

For instance $|\theta_1| + |\theta_2| < \varepsilon \ll 1$ after a time interval $\Delta t \gg \delta t$.

For the map: $\delta t = 1, \Delta t = 10^4$, total motion time $10^7/10^8$,

while for the Arnolds'model: $\delta t = 2 \times 10^{-4}, \Delta t = 5 \times 10^4$, total motion time $5 \times 10^6/10^7$.

$$\sigma_2^2(t_l) = \frac{1}{N_s(t_l)} \sum_{m=1}^{N_s(t_l)} (I_f(t_m) - I_f(0))^2,$$

where $N_s(t_l)$ is the number of points on the section in the interval $((l-1)\Delta t, l\Delta t)$,

$$|((l-1)\Delta t, l\Delta t)| = \Delta t.$$

– Average over a given section

For instance $|\theta_1| + |\theta_2| < \varepsilon \ll 1$ after a time interval $\Delta t \gg \delta t$.

For the map: $\delta t = 1, \Delta t = 10^4$, total motion time $10^7/10^8$,

while for the Arnolds'model: $\delta t = 2 \times 10^{-4}, \Delta t = 5 \times 10^4$, total motion time $5 \times 10^6/10^7$.

$$\sigma_2^2(t_l) = \frac{1}{N_s(t_l)} \sum_{m=1}^{N_s(t_l)} (I_f(t_m) - I_f(0))^2,$$

where $N_s(t_l)$ is the number of points on the section in the interval $((l-1)\Delta t, l\Delta t)$,

$$|((l-1)\Delta t, l\Delta t)| = \Delta t.$$

– Cumulative average over a given section

$$\sigma_3^2(t_l) = \frac{1}{N_s(< t_l)} \sum_{m=1}^{N_s(<t_l)} (I_f(t_m) - I_f(0))^2,$$

where $N_s(< t_l)$ is the number of points on the section in the interval $(t_0, l\Delta t)$,

$$|(t_0, l\Delta t)| = l\Delta t.$$

Experimentally, $N_s(t_l) \approx N_0 \gg 1$, so

$$N_s(< t_l) = \sum_{m=1}^{l} N_s(t_m) \approx l N_0, \quad \to \quad \sigma_3^2(t_l) \approx \frac{1}{l} \sum_{m=1}^{l} \sigma_2^2(t_m).$$

If $\sigma_2^2(t) \approx C t^{\alpha}$,

$$\sigma_3^2(t) \approx \frac{C}{\alpha+1} t^{\alpha} \approx \frac{\sigma_2^2(t)}{\alpha+1}.$$

– Cumulative average over a given section

$$\sigma_3^2(t_l) = \frac{1}{N_s(< t_l)} \sum_{m=1}^{N_s(<t_l)} (I_f(t_m) - I_f(0))^2,$$

where $N_s(< t_l)$ is the number of points on the section in the interval $(t_0, l\Delta t)$,

$$|(t_0, l\Delta t)| = l\Delta t.$$

Experimentally, $N_s(t_l) \approx N_0 \gg 1$, so

$$N_s(< t_l) = \sum_{m=1}^{l} N_s(t_m) \approx l N_0, \quad \rightarrow \quad \sigma_3^2(t_l) \approx \frac{1}{l} \sum_{m=1}^{l} \sigma_2^2(t_m).$$

If $\sigma_2^2(t) \approx C t^\alpha$,

$$\sigma_3^2(t) \approx \frac{C}{\alpha + 1} t^\alpha \approx \frac{\sigma_2^2(t)}{\alpha + 1}.$$

– Cumulative average over a given section

$$\sigma_3^2(t_l) = \frac{1}{N_s(< t_l)} \sum_{m=1}^{N_s(<t_l)} (I_f(t_m) - I_f(0))^2,$$

where $N_s(< t_l)$ is the number of points on the section in the interval $(t_0, l\Delta t)$,

$$|(t_0, l\Delta t)| = l\Delta t.$$

Experimentally, $N_s(t_l) \approx N_0 \gg 1$, so

$$N_s(< t_l) = \sum_{m=1}^{l} N_s(t_m) \approx l N_0, \quad \to \quad \sigma_3^2(t_l) \approx \frac{1}{l} \sum_{m=1}^{l} \sigma_2^2(t_m).$$

If $\sigma_2^2(t) \approx C t^\alpha$,

$$\sigma_3^2(t) \approx \frac{C}{\alpha+1} t^\alpha \approx \frac{\sigma_2^2(t)}{\alpha+1}.$$

– Cumulative average over a given section

$$\sigma_3^2(t_l) = \frac{1}{N_s(< t_l)} \sum_{m=1}^{N_s(<t_l)} (I_f(t_m) - I_f(0))^2,$$

where $N_s(< t_l)$ is the number of points on the section in the interval $(t_0, l\Delta t)$,

$$|(t_0, l\Delta t)| = l\Delta t.$$

Experimentally, $N_s(t_l) \approx N_0 \gg 1$, so

$$N_s(< t_l) = \sum_{m=1}^{l} N_s(t_m) \approx l N_0, \quad \rightarrow \quad \sigma_3^2(t_l) \approx \frac{1}{l} \sum_{m=1}^{l} \sigma_2^2(t_m).$$

If $\sigma_2^2(t) \approx Ct^\alpha$,

$$\sigma_3^2(t) \approx \frac{C}{\alpha+1} t^\alpha \approx \frac{\sigma_2^2(t)}{\alpha+1}.$$

– Cumulative average over a given section

$$\sigma_3^2(t_l) = \frac{1}{N_s(< t_l)} \sum_{m=1}^{N_s(<t_l)} (I_f(t_m) - I_f(0))^2,$$

where $N_s(< t_l)$ is the number of points on the section in the interval $(t_0, l\Delta t)$,

$$|(t_0, l\Delta t)| = l\Delta t.$$

Experimentally, $N_s(t_l) \approx N_0 \gg 1$, so

$$N_s(< t_l) = \sum_{m=1}^{l} N_s(t_m) \approx l N_0, \quad \rightarrow \quad \sigma_3^2(t_l) \approx \frac{1}{l} \sum_{m=1}^{l} \sigma_2^2(t_m).$$

If $\sigma_2^2(t) \approx C t^\alpha$,

$$\sigma_3^2(t) \approx \frac{C}{\alpha + 1} t^\alpha \approx \frac{\sigma_2^2(t)}{\alpha + 1}.$$

– Cumulative average over a given section

$$\sigma_3^2(t_l) = \frac{1}{N_s(< t_l)} \sum_{m=1}^{N_s(<t_l)} (I_f(t_m) - I_f(0))^2,$$

where $N_s(< t_l)$ is the number of points on the section in the interval $(t_0, l\Delta t)$,

$$|(t_0, l\Delta t)| = l\Delta t.$$

Experimentally, $N_s(t_l) \approx N_0 \gg 1$, so

$$N_s(< t_l) = \sum_{m=1}^{l} N_s(t_m) \approx l N_0, \quad \rightarrow \quad \sigma_3^2(t_l) \approx \frac{1}{l} \sum_{m=1}^{l} \sigma_2^2(t_m).$$

If $\sigma_2^2(t) \approx C t^\alpha$,

$$\sigma_3^2(t) \approx \frac{C}{\alpha+1} t^\alpha \approx \frac{\sigma_2^2(t)}{\alpha+1}.$$

– Cumulative average over a given section

$$\sigma_3^2(t_l) = \frac{1}{N_s(< t_l)} \sum_{m=1}^{N_s(<t_l)} (I_f(t_m) - I_f(0))^2,$$

where $N_s(< t_l)$ is the number of points on the section in the interval $(t_0, l\Delta t)$,

$$|(t_0, l\Delta t)| = l\Delta t.$$

Experimentally, $N_s(t_l) \approx N_0 \gg 1$, so

$$N_s(< t_l) = \sum_{m=1}^{l} N_s(t_m) \approx l N_0, \quad \rightarrow \quad \sigma_3^2(t_l) \approx \frac{1}{l} \sum_{m=1}^{l} \sigma_2^2(t_m).$$

If $\sigma_2^2(t) \approx C t^\alpha$,

$$\sigma_3^2(t) \approx \frac{C}{\alpha+1} t^\alpha \approx \frac{\sigma_2^2(t)}{\alpha+1}.$$

– Cumulative average over a given section

$$\sigma_3^2(t_l) = \frac{1}{N_s(< t_l)} \sum_{m=1}^{N_s(<t_l)} (I_f(t_m) - I_f(0))^2,$$

where $N_s(< t_l)$ is the number of points on the section in the interval $(t_0, l\Delta t)$,

$$|(t_0, l\Delta t)| = l\Delta t.$$

Experimentally, $N_s(t_l) \approx N_0 \gg 1$, so

$$N_s(< t_l) = \sum_{m=1}^{l} N_s(t_m) \approx l N_0, \quad \rightarrow \quad \sigma_3^2(t_l) \approx \frac{1}{l} \sum_{m=1}^{l} \sigma_2^2(t_m).$$

If $\sigma_2^2(t) \approx C t^\alpha$,

$$\sigma_3^2(t) \approx \frac{C}{\alpha + 1} t^\alpha \approx \frac{\sigma_2^2(t)}{\alpha + 1}.$$

For the 4D-map

- I.Cs. on different main resonances
- Section along the *fast* plane, $|\theta_1(t)| + |\theta_2(t)| \leq \varepsilon \ll 1$
- The three variances, $\sigma_1^2(t), \sigma_2^2(t), \sigma_3^2(t)$ are computed
- As an illustration, three examples (as in all cases) for parameters $\epsilon_s, \gamma_s, \mu_s$ not too small such that the system is far from Nekhoroshev regime
- Considering motion times $10^7/10^8$, large enough
- A power law, $\sigma^2 = C\, t^\alpha (+d)$ (if necessary) is fitted in several numerical experiments.

For the 4D-map

- I.Cs. on different main resonances
- Section along the *fast* plane, $|\theta_1(t)| + |\theta_2(t)| \leq \varepsilon \ll 1$
- The three variances, $\sigma_1^2(t), \sigma_2^2(t), \sigma_3^2(t)$ are computed
- As an illustration, three examples (as in all cases) for parameters $\epsilon_s, \gamma_s, \mu_s$ not too small such that the system is far from Nekhoroshev regime
- Considering motion times $10^7/10^8$, large enough
- A power law, $\sigma^2 = C\, t^{\alpha}(+d)$ (if necessary) is fitted in several numerical experiments.

For the 4D-map

- I.Cs. on different main resonances
- Section along the *fast* plane, $|\theta_1(t)| + |\theta_2(t)| \leq \varepsilon \ll 1$
- The three variances, $\sigma_1^2(t), \sigma_2^2(t), \sigma_3^2(t)$ are computed
- As an illustration, three examples (as in all cases) for parameters $\epsilon_s, \gamma_s, \mu_s$ not too small such that the system is far from Nekhoroshev regime
- Considering motion times $10^7/10^8$, large enough
- A power law, $\sigma^2 = C\, t^\alpha (+d)$ (if necessary) is fitted in several numerical experiments.

For the 4D-map

- I.Cs. on different main resonances
- Section along the *fast* plane, $|\theta_1(t)| + |\theta_2(t)| \leq \varepsilon \ll 1$
- The three variances, $\sigma_1^2(t), \sigma_2^2(t), \sigma_3^2(t)$ are computed
- As an illustration, three examples (as in all cases) for parameters $\epsilon_s, \gamma_s, \mu_s$ not too small such that the system is far from Nekhoroshev regime
- Considering motion times $10^7/10^8$, large enough
- A power law, $\sigma^2 = C\, t^{\alpha}(+d)$ (if necessary) is fitted in several numerical experiments.

For the 4D-map

- I.Cs. on different main resonances
- Section along the *fast* plane, $|\theta_1(t)| + |\theta_2(t)| \leq \varepsilon \ll 1$
- The three variances, $\sigma_1^2(t), \sigma_2^2(t), \sigma_3^2(t)$ are computed
- As an illustration, three examples (as in all cases) for parameters $\epsilon_s, \gamma_s, \mu_s$ not too small such that the system is far from Nekhoroshev regime
- Considering motion times $10^7/10^8$, large enough
- A power law, $\sigma^2 = C\, t^\alpha (+d)$ (if necessary) is fitted in several numerical experiments.

For the 4D-map

- I.Cs. on different main resonances
- Section along the *fast* plane, $|\theta_1(t)| + |\theta_2(t)| \leq \varepsilon \ll 1$
- The three variances, $\sigma_1^2(t), \sigma_2^2(t), \sigma_3^2(t)$ are computed
- As an illustration, three examples (as in all cases) for parameters $\epsilon_s, \gamma_s, \mu_s$ not too small such that the system is far from Nekhoroshev regime
- Considering motion times $10^7/10^8$, large enough
- A power law, $\sigma^2 = C\, t^{\alpha}(+d)$ (if necessary) is fitted in several numerical experiments.

For the 4D-map

- I.Cs. on different main resonances
- Section along the *fast* plane, $|\theta_1(t)| + |\theta_2(t)| \leq \varepsilon \ll 1$
- The three variances, $\sigma_1^2(t), \sigma_2^2(t), \sigma_3^2(t)$ are computed
- As an illustration, three examples (as in all cases) for parameters $\epsilon_s, \gamma_s, \mu_s$ not too small such that the system is far from Nekhoroshev regime
- Considering motion times $10^7/10^8$, large enough
- A power law, $\sigma^2 = C\, t^\alpha (+d)$ (if necessary) is fitted in several numerical experiments.

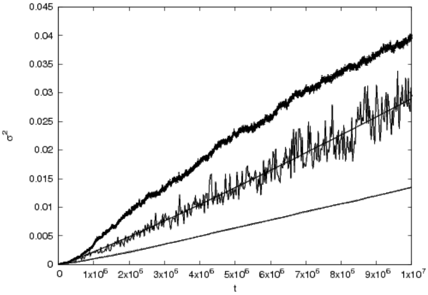
0.045
0.04
0.035
0.03
0.025
0.02
0.015
0.01
0.005
0
σ^2
0
1x10^6
2x10^6
3x10^6
4x10^6
5x10^6
6x10^6
7x10^6
8x10^6
9x10^6
1x10^7
t

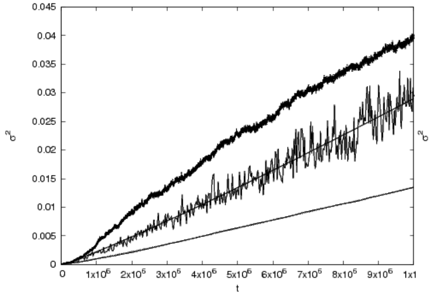
σ²
t
0.045
0.04
0.035
0.03
0.025
0.02
0.015
0.01
0.005
0
1x10⁶
2x10⁶
3x10⁶
4x10⁶
5x10⁶
6x10⁶
7x10⁶
8x10⁶
9x10⁶
1x1

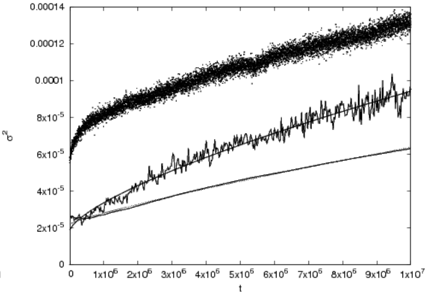
σ²
t
0.00014
0.00012
0.0001
8x10⁻⁵
6x10⁻⁵
4x10⁻⁵
2x10⁻⁵
0
1x10⁶
2x10⁶
3x10⁶
4x10⁶
5x10⁶
6x10⁶
7x10⁶
8x10⁶
9x10⁶
1x10⁷

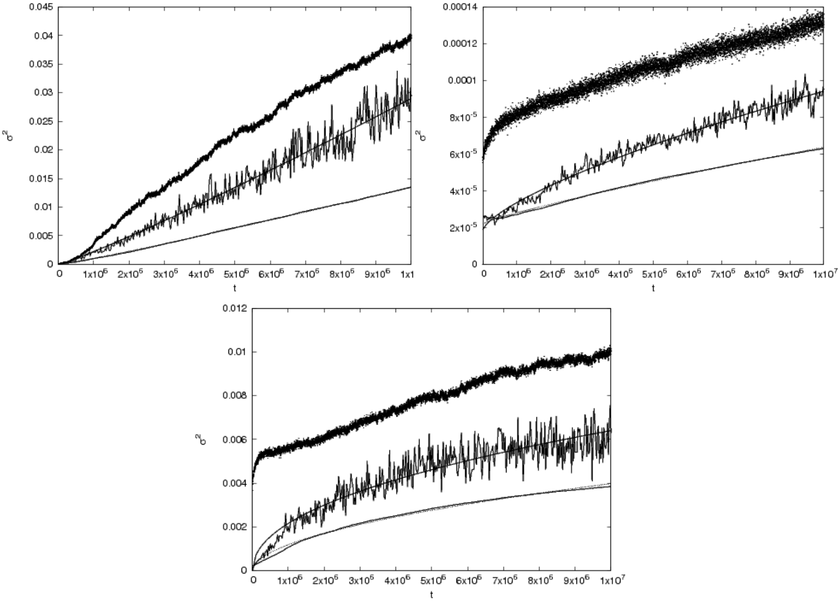

0.045
0.04
0.035
0.03
0.025
0.02
0.015
0.01
0.005
0
σ2
0
1x10^6
2x10^6
3x10^6
4x10^6
5x10^6
6x10^6
7x10^6
8x10^6
9x10^6
1x1
t
0.00014
0.00012
0.0001
8x10^-5
6x10^-5
4x10^-5
2x10^-5
0
σ2
0
1x10^6
2x10^6
3x10^6
4x10^6
5x10^6
6x10^6
7x10^6
8x10^6
9x10^6
1x10^7
t
0.012
0.01
0.008
0.006
0.004
0.002
0
σ2
0
1x10^6
2x10^6
3x10^6
4x10^6
5x10^6
6x10^6
7x10^6
8x10^6
9x10^6
1x10^7
t

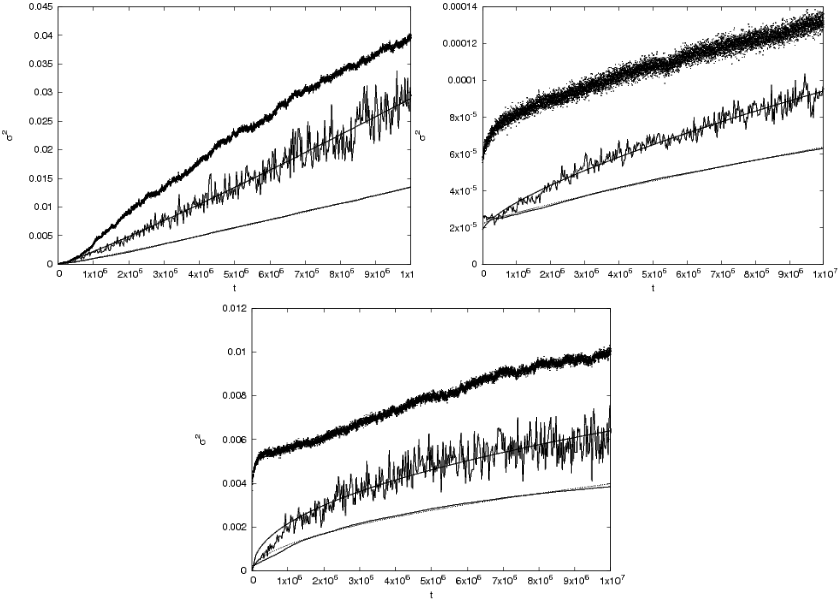

Figure: $\sigma_1^2, \sigma_2^2, \sigma_3^2$ as a function of time. Here $\alpha \approx 1; 0.8; 0.5$, respectively.

Exp.	i.c.	res.	C	α
A	(i)	$y_1 = 0$	1.12e-07	0.64
A	(ii)	$y_2 = 0$	1.60e-08	0.79
A	(iii)	$1:1$	3.40e-09	0.95*
B	(i)	$y_1 = 0$	3.97e-07	0.35
B	(ii)	$y_2 = 0$	1.67e-10	0.79
B	(iii)	$1:1$	2.36e-10	0.65
C	(i)	$y_1 = 0$	2.44e-08	0.85
C	(ii)	$y_2 = 0$	2.61e-10	1.10*
C	(iii)	$1:1$	1.0e-06	0.60
D	(i)	$y_1 = 0$	2.09e-07	0.61
D	(ii)	$y_2 = 0$	8.16e-07	0.53
D	(iii)	$1:1$	5.14e-09	0.81
E	(ii)	$y_2 = 0$	1.74e-07	0.36
E	(v)	$y_2 = 1/2$	5.41e-11	0.84
E	(vi)	$y_2 = 1/2$	4.44e-12	1.00*
E	(vii)	$y_2 = 0$	7.95e-09	0.71
E	(viii)	$1:1$	1.90e-10	0.89

What about Arnold's' model?

What about Arnold's' model?

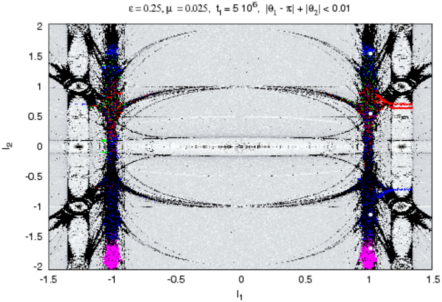

What about Arnold's' model?

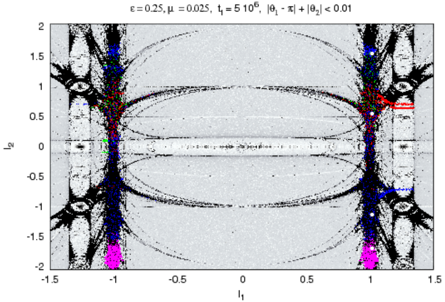

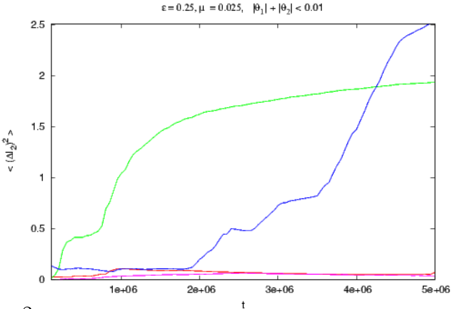

Figure: σ_3^2 as a function of time for the four ensembles.

Varying μ

Varying μ

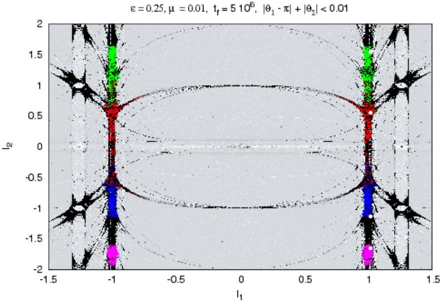
ε = 0.25, μ = 0.01, t_f = 5 10^6, |θ_1 - π| + |θ_2| < 0.01
I_2
I_1
2
1.5
1
0.5
0
-0.5
-1
-1.5
-2
-1.5
-1
-0.5
0
0.5
1
1.5

Varying μ

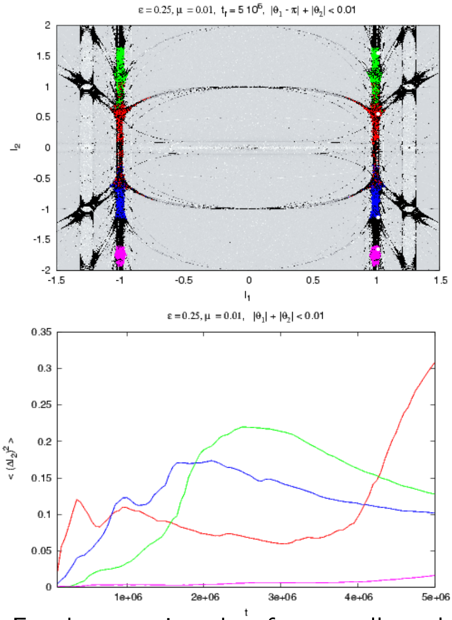

Figure: For the same i.cs. but for a smaller value of μ.

- From all these experiments, $\sigma^2(t)$ is far from being linear, thus it has no sense to try to derive a diffusion coefficient by a linear fit. It is necessary to understand how to cope with phase correlations in order to estimate any reliable value of D.
- Even in low dimensional Hamiltonian systems (or simplectic maps), this *anomalous* diffusion was observed.
- For instance: N. Miguel, C. Simó and A. Vieiro: On the effect of islands in the diffusive properties of the standard map, for large parameter values (2015).
- Cantor sets, stickiness, etc, seriously affect the diffusion.
- In general $D(\varepsilon, \boldsymbol{x})$.
- Diffusion is inhomogeneous and quite anisotropic.
- Anyway, diffusion experiments would help us to guess about stability/instability within chaotic domains over finite (or physical) times.

- From all these experiments, $\sigma^2(t)$ is far from being linear, thus it has no sense to try to derive a diffusion coefficient by a linear fit. It is necessary to understand how to cope with phase correlations in order to estimate any reliable value of D.
- Even in low dimensional Hamiltonian systems (or simplectic maps), this *anomalous* diffusion was observed.
- For instance: N. Miguel, C. Simó and A. Vieiro: On the effect of islands in the diffusive properties of the standard map, for large parameter values (2015).
- Cantor sets, stickiness, etc, seriously affect the diffusion.
- In general $D(\varepsilon, x)$.
- Diffusion is inhomogeneous and quite anisotropic.
- Anyway, diffusion experiments would help us to guess about stability/instability within chaotic domains over finite (or physical) times.

- From all these experiments, $\sigma^2(t)$ is far from being linear, thus it has no sense to try to derive a diffusion coefficient by a linear fit. It is necessary to understand how to cope with phase correlations in order to estimate any reliable value of D.
- Even in low dimensional Hamiltonian systems (or simplectic maps), this *anomalous* diffusion was observed.
- For instance: N. Miguel, C. Simó and A. Vieiro: On the effect of islands in the diffusive properties of the standard map, for large parameter values (2015).
- Cantor sets, stickiness, etc, seriously affect the diffusion.
- In general $D(\varepsilon, x)$.
- Diffusion is inhomogeneous and quite anisotropic.
- Anyway, diffusion experiments would help us to guess about stability/instability within chaotic domains over finite (or physical) times.

- From all these experiments, $\sigma^2(t)$ is far from being linear, thus it has no sense to try to derive a diffusion coefficient by a linear fit. It is necessary to understand how to cope with phase correlations in order to estimate any reliable value of D.
- Even in low dimensional Hamiltonian systems (or simplectic maps), this *anomalous* diffusion was observed.
- For instance: N. Miguel, C. Simó and A. Vieiro: On the effect of islands in the diffusive properties of the standard map, for large parameter values (2015).
- Cantor sets, stickiness, etc, seriously affect the diffusion.
- In general $D(\varepsilon, x)$.
- Diffusion is inhomogeneous and quite anisotropic.
- Anyway, diffusion experiments would help us to guess about stability/instability within chaotic domains over finite (or physical) times.

- From all these experiments, $\sigma^2(t)$ is far from being linear, thus it has no sense to try to derive a diffusion coefficient by a linear fit. It is necessary to understand how to cope with phase correlations in order to estimate any reliable value of D.
- Even in low dimensional Hamiltonian systems (or simplectic maps), this *anomalous* diffusion was observed.
- For instance: N. Miguel, C. Simó and A. Vieiro: On the effect of islands in the diffusive properties of the standard map, for large parameter values (2015).
- Cantor sets, stickiness, etc, seriously affect the diffusion.
- In general $D(\varepsilon, x)$.
- Diffusion is inhomogeneous and quite anisotropic.
- Anyway, diffusion experiments would help us to guess about stability/instability within chaotic domains over finite (or physical) times.

- From all these experiments, $\sigma^2(t)$ is far from being linear, thus it has no sense to try to derive a diffusion coefficient by a linear fit. It is necessary to understand how to cope with phase correlations in order to estimate any reliable value of D.
- Even in low dimensional Hamiltonian systems (or simplectic maps), this *anomalous* diffusion was observed.
- For instance: N. Miguel, C. Simó and A. Vieiro: On the effect of islands in the diffusive properties of the standard map, for large parameter values (2015).
- Cantor sets, stickiness, etc, seriously affect the diffusion.
- In general $D(\varepsilon, \boldsymbol{x})$.
- Diffusion is inhomogeneous and quite anisotropic.
- Anyway, diffusion experiments would help us to guess about stability/instability within chaotic domains over finite (or physical) times.

- From all these experiments, $\sigma^2(t)$ is far from being linear, thus it has no sense to try to derive a diffusion coefficient by a linear fit. It is necessary to understand how to cope with phase correlations in order to estimate any reliable value of D.

- Even in low dimensional Hamiltonian systems (or simplectic maps), this *anomalous* diffusion was observed.

- For instance: N. Miguel, C. Simó and A. Vieiro: On the effect of islands in the diffusive properties of the standard map, for large parameter values (2015).

- Cantor sets, stickiness, etc, seriously affect the diffusion.

- In general $D(\varepsilon, \boldsymbol{x})$.

- Diffusion is inhomogeneous and quite anisotropic.

- Anyway, diffusion experiments would help us to guess about stability/instability within chaotic domains over finite (or physical) times.

- From all these experiments, $\sigma^2(t)$ is far from being linear, thus it has no sense to try to derive a diffusion coefficient by a linear fit. It is necessary to understand how to cope with phase correlations in order to estimate any reliable value of D.
- Even in low dimensional Hamiltonian systems (or simplectic maps), this *anomalous* diffusion was observed.
- For instance: N. Miguel, C. Simó and A. Vieiro: On the effect of islands in the diffusive properties of the standard map, for large parameter values (2015).
- Cantor sets, stickiness, etc, seriously affect the diffusion.
- In general $D(\varepsilon, \boldsymbol{x})$.
- Diffusion is inhomogeneous and quite anisotropic.
- Anyway, diffusion experiments would help us to guess about stability/instability within chaotic domains over finite (or physical) times.

Diffusion in the Gliese-876 planetary system

Parameter	Planet c (1)	Planet b (2)	Planet e (3)
P (days)	30.0881	61.1166	124.26
$m\,(\mathrm{M}_{jup})$	0.7142	2.2756	0.0459
a (AU)	0.129590	0.208317	0.3343
e	0.25591	0.0324	0.055
$\varpi\,(^\circ)$	0.0	0.0	180.0
$M\,(^\circ)$	240.0	120.0	60.0

Table: Masses and orbital elements for the three planets of GJ-876 involved in the Laplace resonance. The values of the angular variables (ϖ and M) were chosen to minimize the variations of the orbital elements over time, and lead to small-amplitude librations of the resonant angles. The (a_3, e_3) values correspond to those obtained by the four-planet coplanar fit.

Diffusion in the Gliese-876 planetary system

Parameter	Planet c (1)	Planet b (2)	Planet e (3)
P (days)	30.0881	61.1166	124.26
$m\,(\mathrm{M}_{jup})$	0.7142	2.2756	0.0459
a (AU)	0.129590	0.208317	0.3343
e	0.25591	0.0324	0.055
$\varpi\,(^\circ)$	0.0	0.0	180.0
$M\,(^\circ)$	240.0	120.0	60.0

Table: Masses and orbital elements for the three planets of GJ-876 involved in the Laplace resonance. The values of the angular variables (ϖ and M) were chosen to minimize the variations of the orbital elements over time, and lead to small-amplitude librations of the resonant angles. The (a_3, e_3) values correspond to those obtained by the four-planet coplanar fit.

In the vicinity of a Laplace-type resonance, we can define the 2:1 two-body MMR resonant angles

$$\sigma_1 = 2\lambda_2 - \lambda_1 - \varpi_1$$
$$\sigma_2 = 2\lambda_3 - \lambda_2 - \varpi_2$$

Thus the three-body/orbit resonant Laplace angle is:

$$\phi_{lap} = \lambda_1 - 3\lambda_2 + 2\lambda_3.$$

After an averaging process with respect to the short-period terms, the resulting resonant Hamiltonian reduces to a system of four degrees-of-freedom.

In the vicinity of a Laplace-type resonance, we can define the 2:1 two-body MMR resonant angles

$$\sigma_1 = 2\lambda_2 - \lambda_1 - \varpi_1$$
$$\sigma_2 = 2\lambda_3 - \lambda_2 - \varpi_2$$

Thus the three-body/orbit resonant Laplace angle is:

$$\phi_{lap} = \lambda_1 - 3\lambda_2 + 2\lambda_3.$$

After an averaging process with respect to the short-period terms, the resulting resonant Hamiltonian reduces to a system of four degrees-of-freedom.

In the vicinity of a Laplace-type resonance, we can define the 2:1 two-body MMR resonant angles

$$\sigma_1 = 2\lambda_2 - \lambda_1 - \varpi_1$$
$$\sigma_2 = 2\lambda_3 - \lambda_2 - \varpi_2$$

Thus the three-body/orbit resonant Laplace angle is:

$$\phi_{lap} = \lambda_1 - 3\lambda_2 + 2\lambda_3.$$

After an averaging process with respect to the short-period terms, the resulting resonant Hamiltonian reduces to a system of four degrees-of-freedom.

In the vicinity of a Laplace-type resonance, we can define the 2:1 two-body MMR resonant angles

$$\sigma_1 = 2\lambda_2 - \lambda_1 - \varpi_1$$
$$\sigma_2 = 2\lambda_3 - \lambda_2 - \varpi_2$$

Thus the three-body/orbit resonant Laplace angle is:

$$\phi_{lap} = \lambda_1 - 3\lambda_2 + 2\lambda_3.$$

After an averaging process with respect to the short-period terms, the resulting resonant Hamiltonian reduces to a system of four degrees-of-freedom.

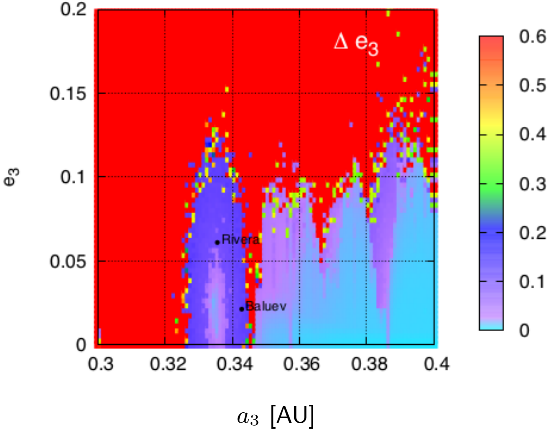

Figure: Δe_3 dynamical map in the vicinity of the $2/1$ MMR between m_3 and m_2 (corresponding to $a_3 \approx 0.335$ AU). The remainder variables take the values given in the table.

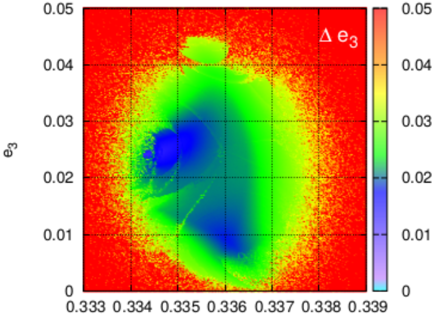
Δ e3
e3
0.05
0.04
0.03
0.02
0.01
0
0.333 0.334 0.335 0.336 0.337 0.338 0.339

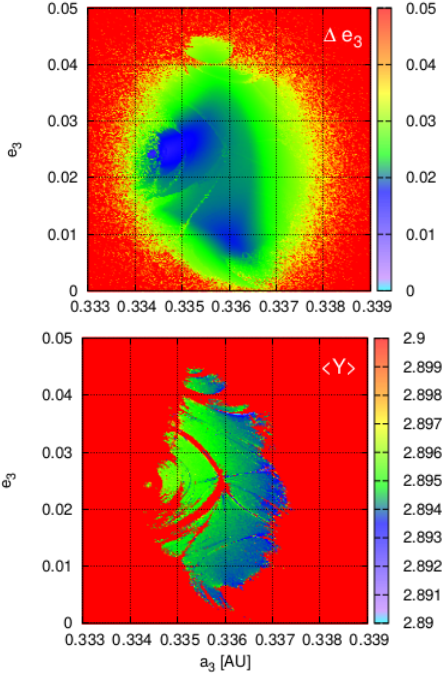

0.05
0.04
0.03
0.02
0.01
0
e_3
$\Delta\ e_3$
0.333 0.334 0.335 0.336 0.337 0.338 0.339
0.05
0.04
0.03
0.02
0.01
0
$\langle Y \rangle$
2.9
2.899
2.898
2.897
2.896
2.895
2.894
2.893
2.892
2.891
2.89
a_3 [AU]

The (chaotic) dynamics of this resonance could be completely understood in the framework of Nesvorný & Morbidelli (1999) three–body mean resonance model for the SS, as it is shown in Martí, PMC & Beaugé (2016).

Thus, let us see if diffusion experiments provide more information about stability/instability regions inside the Laplace resonance.

- Ensembles: 256 i. c. around several values $(a_3(0), e_3(0))$.
- Size: 10^{-3} in Δe_3 and 2×10^{-4} in Δa_3.
- Total time of 2×10^5 years, twice longer than the time-span used for the original map.
- Multisection:
- $\Sigma_{i=1}^{3}(|M_i - M_i^0| + |\varpi_i - \varpi_i^0|) < \epsilon_{ang}$,
- $\Sigma_{i=1}^{2}|e_i - e_i^0| < \epsilon_e$,
- $\Sigma_{i=1}^{2}|a_i - a_i^0| < \epsilon_a$,
- $\epsilon_{ang} = 6^\circ$, $\epsilon_a = 0.005\mathrm{AU}$ and $\epsilon_e = 0.005$.
- 9 ensembles: 1S, 2S, ... , 9S.

The (chaotic) dynamics of this resonance could be completely understood in the framework of Nesvorný & Morbidelli (1999) three–body mean resonance model for the SS, as it is shown in Martí, PMC & Beaugé (2016).

Thus, let us see if diffusion experiments provide more information about stability/instability regions inside the Laplace resonance.

- Ensembles: 256 i. c. around several values $(a_3(0), e_3(0))$.
- Size: 10^{-3} in Δe_3 and 2×10^{-4} in Δa_3.
- Total time of 2×10^5 years, twice longer than the time-span used for the original map.
- Multisection:
- $\Sigma_{i=1}^{3}(|M_i - M_i^0| + |\varpi_i - \varpi_i^0|) < \epsilon_{ang}$,
- $\Sigma_{i=1}^{2}|e_i - e_i^0| < \epsilon_e$,
- $\Sigma_{i=1}^{2}|a_i - a_i^0| < \epsilon_a$,
- $\epsilon_{ang} = 6^\circ$, $\epsilon_a = 0.005\mathrm{AU}$ and $\epsilon_e = 0.005$.
- 9 ensembles: 1S, 2S, ... , 9S.

The (chaotic) dynamics of this resonance could be completely understood in the framework of Nesvorný & Morbidelli (1999) three–body mean resonance model for the SS, as it is shown in Martí, PMC & Beaugé (2016).
Thus, let us see if diffusion experiments provide more information about stability/instability regions inside the Laplace resonance.

- Ensembles: 256 i. c. around several values $(a_3(0), e_3(0))$.
- Size: 10^{-3} in Δe_3 and 2×10^{-4} in Δa_3.
- Total time of 2×10^5 years, twice longer than the time-span used for the original map.
- Multisection:
- $\Sigma_{i=1}^{3}(|M_i - M_i^0| + |\varpi_i - \varpi_i^0|) < \epsilon_{ang}$,
- $\Sigma_{i=1}^{2}|e_i - e_i^0| < \epsilon_e$,
- $\Sigma_{i=1}^{2}|a_i - a_i^0| < \epsilon_a$,
- $\epsilon_{ang} = 6^\circ$, $\epsilon_a = 0.005\mathrm{AU}$ and $\epsilon_e = 0.005$.
- 9 ensembles: 1S, 2S, ... , 9S.

The (chaotic) dynamics of this resonance could be completely understood in the framework of Nesvorný & Morbidelli (1999) three–body mean resonance model for the SS, as it is shown in Martí, PMC & Beaugé (2016).
Thus, let us see if diffusion experiments provide more information about stability/instability regions inside the Laplace resonance.

- Ensembles: 256 i. c. around several values $(a_3(0), e_3(0))$.
- Size: 10^{-3} in Δe_3 and 2×10^{-4} in Δa_3.
- Total time of 2×10^5 years, twice longer than the time-span used for the original map.
- Multisection:
- $\Sigma_{i=1}^{3}(|M_i - M_i^0| + |\varpi_i - \varpi_i^0|) < \epsilon_{ang}$,
- $\Sigma_{i=1}^{2}|e_i - e_i^0| < \epsilon_e$,
- $\Sigma_{i=1}^{2}|a_i - a_i^0| < \epsilon_a$,
- $\epsilon_{ang} = 6^\circ$, $\epsilon_a = 0.005\mathrm{AU}$ and $\epsilon_e = 0.005$.
- 9 ensembles: 1S, 2S, ... , 9S.

The (chaotic) dynamics of this resonance could be completely understood in the framework of Nesvorný & Morbidelli (1999) three–body mean resonance model for the SS, as it is shown in Martí, PMC & Beaugé (2016).
Thus, let us see if diffusion experiments provide more information about stability/instability regions inside the Laplace resonance.

- Ensembles: 256 i. c. around several values $(a_3(0), e_3(0))$.
- Size: 10^{-3} in Δe_3 and 2×10^{-4} in Δa_3.
- Total time of 2×10^5 years, twice longer than the time-span used for the original map.
- Multisection:
- $\Sigma_{i=1}^{3}(|M_i - M_i^0| + |\varpi_i - \varpi_i^0|) < \epsilon_{ang}$,
- $\Sigma_{i=1}^{2}|e_i - e_i^0| < \epsilon_e$,
- $\Sigma_{i=1}^{2}|a_i - a_i^0| < \epsilon_a$,
- $\epsilon_{ang} = 6^\circ$, $\epsilon_a = 0.005\mathrm{AU}$ and $\epsilon_e = 0.005$.
- 9 ensembles: 1S, 2S, ... , 9S.

The (chaotic) dynamics of this resonance could be completely understood in the framework of Nesvorný & Morbidelli (1999) three–body mean resonance model for the SS, as it is shown in Martí, PMC & Beaugé (2016).
Thus, let us see if diffusion experiments provide more information about stability/instability regions inside the Laplace resonance.

- Ensembles: 256 i. c. around several values $(a_3(0), e_3(0))$.
- Size: 10^{-3} in Δe_3 and 2×10^{-4} in Δa_3.
- Total time of 2×10^5 years, twice longer than the time-span used for the original map.
- Multisection:
- $\Sigma_{i=1}^3(|M_i - M_i^0| + |\varpi_i - \varpi_i^0|) < \epsilon_{ang}$,
- $\Sigma_{i=1}^2|e_i - e_i^0| < \epsilon_e$,
- $\Sigma_{i=1}^2|a_i - a_i^0| < \epsilon_a$,
- $\epsilon_{ang} = 6^\circ$, $\epsilon_a = 0.005\mathrm{AU}$ and $\epsilon_e = 0.005$.
- 9 ensembles: 1S, 2S, ... , 9S.

The (chaotic) dynamics of this resonance could be completely understood in the framework of Nesvorný & Morbidelli (1999) three–body mean resonance model for the SS, as it is shown in Martí, PMC & Beaugé (2016).
Thus, let us see if diffusion experiments provide more information about stability/instability regions inside the Laplace resonance.

- Ensembles: 256 i. c. around several values $(a_3(0), e_3(0))$.
- Size: 10^{-3} in Δe_3 and 2×10^{-4} in Δa_3.
- Total time of 2×10^5 years, twice longer than the time-span used for the original map.
- Multisection:
- $\Sigma_{i=1}^{3}(|M_i - M_i^0| + |\varpi_i - \varpi_i^0|) < \epsilon_{ang}$,
- $\Sigma_{i=1}^{2}|e_i - e_i^0| < \epsilon_e$,
- $\Sigma_{i=1}^{2}|a_i - a_i^0| < \epsilon_a$,
- $\epsilon_{ang} = 6^\circ$, $\epsilon_a = 0.005\mathrm{AU}$ and $\epsilon_e = 0.005$.
- 9 ensembles: 1S, 2S, ... , 9S.

The (chaotic) dynamics of this resonance could be completely understood in the framework of Nesvorný & Morbidelli (1999) three–body mean resonance model for the SS, as it is shown in Martí, PMC & Beaugé (2016).
Thus, let us see if diffusion experiments provide more information about stability/instability regions inside the Laplace resonance.

- Ensembles: 256 i. c. around several values $(a_3(0), e_3(0))$.
- Size: 10^{-3} in Δe_3 and 2×10^{-4} in Δa_3.
- Total time of 2×10^5 years, twice longer than the time-span used for the original map.
- Multisection:
- $\Sigma_{i=1}^{3}(|M_i - M_i^0| + |\varpi_i - \varpi_i^0|) < \epsilon_{ang}$,
- $\Sigma_{i=1}^{2}|e_i - e_i^0| < \epsilon_e$,
- $\Sigma_{i=1}^{2}|a_i - a_i^0| < \epsilon_a$,
- $\epsilon_{ang} = 6^\circ$, $\epsilon_a = 0.005\mathrm{AU}$ and $\epsilon_e = 0.005$.
- 9 ensembles: 1S, 2S, ... , 9S.

The (chaotic) dynamics of this resonance could be completely understood in the framework of Nesvorný & Morbidelli (1999) three–body mean resonance model for the SS, as it is shown in Martí, PMC & Beaugé (2016).
Thus, let us see if diffusion experiments provide more information about stability/instability regions inside the Laplace resonance.

- Ensembles: 256 i. c. around several values $(a_3(0), e_3(0))$.
- Size: 10^{-3} in Δe_3 and 2×10^{-4} in Δa_3.
- Total time of 2×10^5 years, twice longer than the time-span used for the original map.
- Multisection:
- $\Sigma_{i=1}^{3}(|M_i - M_i^0| + |\varpi_i - \varpi_i^0|) < \epsilon_{ang}$,
- $\Sigma_{i=1}^{2}|e_i - e_i^0| < \epsilon_e$,
- $\Sigma_{i=1}^{2}|a_i - a_i^0| < \epsilon_a$,
- $\epsilon_{ang} = 6^\circ$, $\epsilon_a = 0.005\mathrm{AU}$ and $\epsilon_e = 0.005$.
- 9 ensembles: 1S, 2S, ... , 9S.

The (chaotic) dynamics of this resonance could be completely understood in the framework of Nesvorný & Morbidelli (1999) three–body mean resonance model for the SS, as it is shown in Martí, PMC & Beaugé (2016).
Thus, let us see if diffusion experiments provide more information about stability/instability regions inside the Laplace resonance.

- Ensembles: 256 i. c. around several values $(a_3(0), e_3(0))$.
- Size: 10^{-3} in Δe_3 and 2×10^{-4} in Δa_3.
- Total time of 2×10^5 years, twice longer than the time-span used for the original map.
- Multisection:
- $\Sigma_{i=1}^{3}(|M_i - M_i^0| + |\varpi_i - \varpi_i^0|) < \epsilon_{ang}$,
- $\Sigma_{i=1}^{2}|e_i - e_i^0| < \epsilon_e$,
- $\Sigma_{i=1}^{2}|a_i - a_i^0| < \epsilon_a$,
- $\epsilon_{ang} = 6^\circ$, $\epsilon_a = 0.005\mathrm{AU}$ and $\epsilon_e = 0.005$.
- 9 ensembles: 1S, 2S, ... , 9S.

The (chaotic) dynamics of this resonance could be completely understood in the framework of Nesvorný & Morbidelli (1999) three–body mean resonance model for the SS, as it is shown in Martí, PMC & Beaugé (2016).
Thus, let us see if diffusion experiments provide more information about stability/instability regions inside the Laplace resonance.

- Ensembles: 256 i. c. around several values $(a_3(0), e_3(0))$.
- Size: 10^{-3} in Δe_3 and 2×10^{-4} in Δa_3.
- Total time of 2×10^5 years, twice longer than the time-span used for the original map.
- Multisection:
- $\Sigma_{i=1}^{3}(|M_i - M_i^0| + |\varpi_i - \varpi_i^0|) < \epsilon_{ang}$,
- $\Sigma_{i=1}^{2}|e_i - e_i^0| < \epsilon_e$,
- $\Sigma_{i=1}^{2}|a_i - a_i^0| < \epsilon_a$,
- $\epsilon_{ang} = 6^\circ$, $\epsilon_a = 0.005\mathrm{AU}$ and $\epsilon_e = 0.005$.
- 9 ensembles: 1S, 2S, ... , 9S.

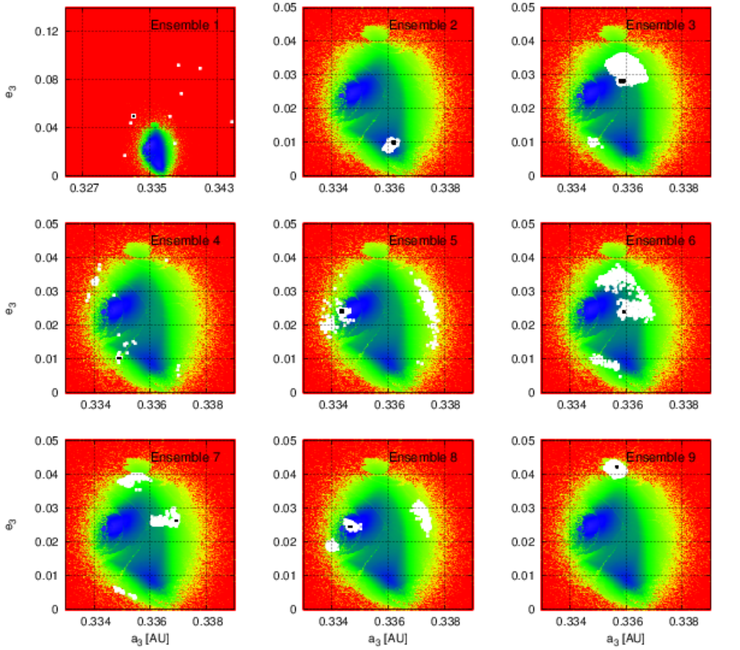
Ensemble 1
Ensemble 2
Ensemble 3
Ensemble 4
Ensemble 5
Ensemble 6
Ensemble 7
Ensemble 8
Ensemble 9
e3
a3 [AU]
0.12
0.08
0.04
0
0.327
0.335
0.343
0.05
0.04
0.03
0.02
0.01
0.334
0.336
0.338

Ensemble	α
S 1	0.942715
S 2	0.585784
S 3	0.494802
S 4	0.923109
S 5	0.648737
S 6	0.448689
S 7	0.686534
S 8	0.592316
S 9	0.462431

Table: Exponents α calculated by a least-squares fit for the data obtained by the variances from each of the nine ensembles: $\sigma_e^2(t) = Ct^\alpha$.

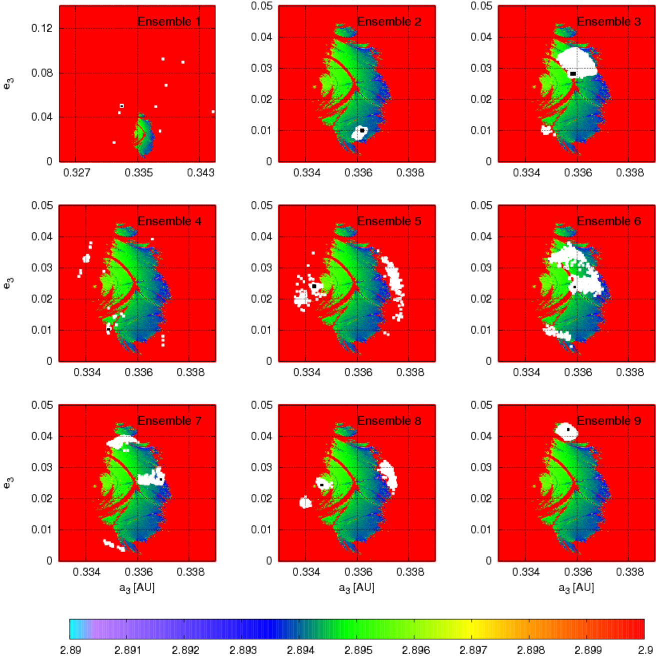

Ensemble 1
Ensemble 2
Ensemble 3
Ensemble 4
Ensemble 5
Ensemble 6
Ensemble 7
Ensemble 8
Ensemble 9
e_3
a_3 [AU]
0.12
0.08
0.04
0
0.327
0.335
0.343
0.05
0.04
0.03
0.02
0.01
0.334
0.336
0.338
2.89
2.891
2.892
2.893
2.894
2.895
2.896
2.897
2.898
2.899
2.9

LCE for a larger time-span

LCE for a larger time-span

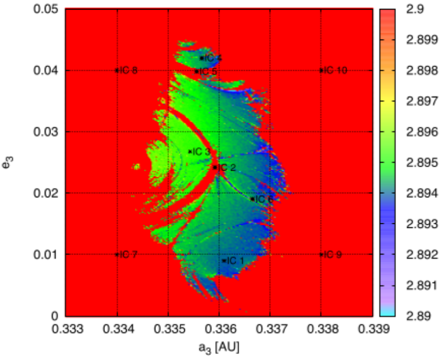

LCE for a larger time-span

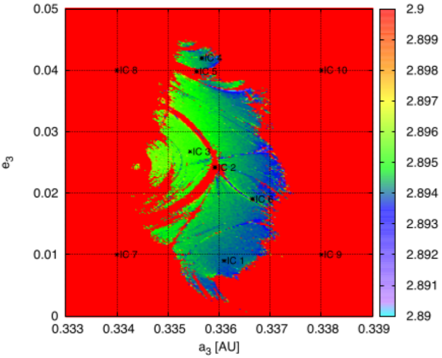

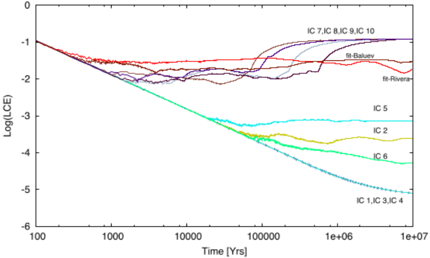

- There are two main regions in the surroundings of the Laplace resonance:
- The inner resonant region is characterized by large Lyapunov times and very slow diffusion.
- The multi-resonant configuration of the system seems to be responsible for its long-term stability.
- The outer resonant region is dominated by a extremely chaotic dynamics, having LCE's somewhat higher than in the inner region and exhibiting a fast diffusion.
- Although these results correspond to a specific planetary system, it seems reasonable that the main characteristics of any system representing similar multi-resonant configurations could share all these main features.

- There are two main regions in the surroundings of the Laplace resonance:
- The inner resonant region is characterized by large Lyapunov times and very slow diffusion.
- The multi-resonant configuration of the system seems to be responsible for its long-term stability.
- The outer resonant region is dominated by a extremely chaotic dynamics, having LCE's somewhat higher than in the inner region and exhibiting a fast diffusion.
- Although these results correspond to a specific planetary system, it seems reasonable that the main characteristics of any system representing similar multi-resonant configurations could share all these main features.

- There are two main regions in the surroundings of the Laplace resonance:
- The inner resonant region is characterized by large Lyapunov times and very slow diffusion.
- The multi-resonant configuration of the system seems to be responsible for its long-term stability.
- The outer resonant region is dominated by a extremely chaotic dynamics, having LCE's somewhat higher than in the inner region and exhibiting a fast diffusion.
- Although these results correspond to a specific planetary system, it seems reasonable that the main characteristics of any system representing similar multi-resonant configurations could share all these main features.

- There are two main regions in the surroundings of the Laplace resonance:
- The inner resonant region is characterized by large Lyapunov times and very slow diffusion.
- The multi-resonant configuration of the system seems to be responsible for its long-term stability.
- The outer resonant region is dominated by a extremely chaotic dynamics, having LCE's somewhat higher than in the inner region and exhibiting a fast diffusion.
- Although these results correspond to a specific planetary system, it seems reasonable that the main characteristics of any system representing similar multi-resonant configurations could share all these main features.

- There are two main regions in the surroundings of the Laplace resonance:
- The inner resonant region is characterized by large Lyapunov times and very slow diffusion.
- The multi-resonant configuration of the system seems to be responsible for its long-term stability.
- The outer resonant region is dominated by a extremely chaotic dynamics, having LCE's somewhat higher than in the inner region and exhibiting a fast diffusion.
- Although these results correspond to a specific planetary system, it seems reasonable that the main characteristics of any system representing similar multi-resonant configurations could share all these main features.

On the relevance of chaos for halo stars in the solar neighborhood (Maffione et al. 2014–2016)

The galactic potential (DM Halo)

$$\Phi_{\rm tri} = -\frac{A}{r_p}\ln\left(1+\frac{r_p}{r_s}\right) \qquad A, r_s = \text{const.},$$

$$r_p = \frac{(r_s+r)r_e}{r_s+r_e}, \qquad r_e = \sqrt{\left(\frac{x}{a}\right)^2+\left(\frac{y}{b}\right)^2+\left(\frac{z}{c}\right)^2}.$$

All parameters of this model were fitted using DM particles located within 6 to 12 kpc (Aquarius Project).

The potential changes from ellipsoidal to near spherical at r_s :

- $r \ll r_s$, $r_p \simeq r_e$;
- $r \gg r_s$, $r_p \simeq r$.

Up to the 10% level, this approximation can reproduce the true gravitational potential within $r \lesssim 100$ kpc.

On the relevance of chaos for halo stars in the solar neighborhood (Maffione et al. 2014–2016)

The galactic potential (DM Halo)

$$\Phi_{\rm tri} = -\frac{A}{r_p}\ln\left(1+\frac{r_p}{r_s}\right) \qquad A, r_s = \text{const.},$$

$$r_p = \frac{(r_s + r)r_e}{r_s + r_e}, \qquad r_e = \sqrt{\left(\frac{x}{a}\right)^2 + \left(\frac{y}{b}\right)^2 + \left(\frac{z}{c}\right)^2}.$$

All parameters of this model were fitted using DM particles located within 6 to 12 kpc (Aquarius Project).

The potential changes from ellipsoidal to near spherical at r_s :

- $r \ll r_s$, $r_p \simeq r_e$;
- $r \gg r_s$, $r_p \simeq r$.

Up to the 10% level, this approximation can reproduce the true gravitational potential within $r \lesssim 100$ kpc.

On the relevance of chaos for halo stars in the solar neighborhood (Maffione et al. 2014–2016)

The galactic potential (DM Halo)

$$\Phi_{\mathrm{tri}} = -\frac{A}{r_p} \ln\left(1 + \frac{r_p}{r_s}\right) \qquad A, r_s = \mathrm{const.},$$

$$r_p = \frac{(r_s + r)r_e}{r_s + r_e}, \qquad r_e = \sqrt{\left(\frac{x}{a}\right)^2 + \left(\frac{y}{b}\right)^2 + \left(\frac{z}{c}\right)^2}.$$

All parameters of this model were fitted using DM particles located within 6 to 12 kpc (Aquarius Project).

The potential changes from ellipsoidal to near spherical at r_s :

- $r \ll r_s$, $r_p \simeq r_e$;
- $r \gg r_s$, $r_p \simeq r$.

Up to the 10% level, this approximation can reproduce the true gravitational potential within $r \lesssim 100$ kpc.

On the relevance of chaos for halo stars in the solar neighborhood (Maffione et al. 2014–2016)

The galactic potential (DM Halo)

$$\Phi_{\rm tri} = -\frac{A}{r_p}\ln\left(1+\frac{r_p}{r_s}\right) \qquad A, r_s = \text{const.},$$

$$r_p = \frac{(r_s + r)r_e}{r_s + r_e}, \qquad r_e = \sqrt{\left(\frac{x}{a}\right)^2 + \left(\frac{y}{b}\right)^2 + \left(\frac{z}{c}\right)^2}.$$

All parameters of this model were fitted using DM particles located within 6 to 12 kpc (Aquarius Project).

The potential changes from ellipsoidal to near spherical at r_s :

- $r \ll r_s$, $r_p \simeq r_e$;
- $r \gg r_s$, $r_p \simeq r$.

Up to the 10% level, this approximation can reproduce the true gravitational potential within $r \lesssim 100$ kpc.

On the relevance of chaos for halo stars in the solar neighborhood (Maffione et al. 2014–2016)

The galactic potential (DM Halo)

$$\Phi_{\rm tri} = -\frac{A}{r_p} \ln\left(1 + \frac{r_p}{r_s}\right) \qquad A, r_s = \text{const.},$$

$$r_p = \frac{(r_s + r)r_e}{r_s + r_e}, \qquad r_e = \sqrt{\left(\frac{x}{a}\right)^2 + \left(\frac{y}{b}\right)^2 + \left(\frac{z}{c}\right)^2}.$$

All parameters of this model were fitted using DM particles located within 6 to 12 kpc (Aquarius Project).

The potential changes from ellipsoidal to near spherical at r_s :

- $r \ll r_s$, $r_p \simeq r_e$;
- $r \gg r_s$, $r_p \simeq r$.

Up to the 10% level, this approximation can reproduce the true gravitational potential within $r \lesssim 100$ kpc.

On the relevance of chaos for halo stars in the solar neighborhood (Maffione et al. 2014–2016)

The galactic potential (DM Halo)

$$\Phi_{\mathrm{tri}} = -\frac{A}{r_p} \ln\left(1 + \frac{r_p}{r_s}\right) \qquad A, r_s = \mathrm{const.},$$

$$r_p = \frac{(r_s + r) r_e}{r_s + r_e}, \qquad r_e = \sqrt{\left(\frac{x}{a}\right)^2 + \left(\frac{y}{b}\right)^2 + \left(\frac{z}{c}\right)^2}.$$

All parameters of this model were fitted using DM particles located within 6 to 12 kpc (Aquarius Project).

The potential changes from ellipsoidal to near spherical at r_s :

- $r \ll r_s$, $r_p \simeq r_e$;
- $r \gg r_s$, $r_p \simeq r$.

Up to the 10% level, this approximation can reproduce the true gravitational potential within $r \lesssim 100$ kpc.

On the relevance of chaos for halo stars in the solar neighborhood (Maffione et al. 2014–2016)

The galactic potential (DM Halo)

$$\Phi_{\mathrm{tri}} = -\frac{A}{r_p} \ln\left(1 + \frac{r_p}{r_s}\right) \qquad A, r_s = \mathrm{const.},$$

$$r_p = \frac{(r_s + r) r_e}{r_s + r_e}, \qquad r_e = \sqrt{\left(\frac{x}{a}\right)^2 + \left(\frac{y}{b}\right)^2 + \left(\frac{z}{c}\right)^2}.$$

All parameters of this model were fitted using DM particles located within 6 to 12 kpc (Aquarius Project).

The potential changes from ellipsoidal to near spherical at r_s :

- $r \ll r_s$, $r_p \backsimeq r_e$;
- $r \gg r_s$, $r_p \backsimeq r$.

Up to the 10% level, this approximation can reproduce the true gravitational potential within $r \lesssim 100$ kpc.

On the relevance of chaos for halo stars in the solar neighborhood (Maffione et al. 2014–2016)

The galactic potential (DM Halo)

$$\Phi_{\rm tri} = -\frac{A}{r_p}\ln\left(1+\frac{r_p}{r_s}\right) \qquad A, r_s = \text{const.},$$

$$r_p = \frac{(r_s+r)r_e}{r_s+r_e}, \qquad r_e = \sqrt{\left(\frac{x}{a}\right)^2+\left(\frac{y}{b}\right)^2+\left(\frac{z}{c}\right)^2}.$$

All parameters of this model were fitted using DM particles located within 6 to 12 kpc (Aquarius Project).

The potential changes from ellipsoidal to near spherical at r_s :

- $r \ll r_s$, $r_p \backsimeq r_e$;
- $r \gg r_s$, $r_p \backsimeq r$.

Up to the 10% level, this approximation can reproduce the true gravitational potential within $r \lesssim 100$ kpc.

Power expansion for $r_p < r_s (r < r_s)$

$$\Phi_{\rm tri} = -\frac{A}{r_s} \sum_{n=1}^{\infty} \frac{(-1)^{n+1}}{n} \left(\frac{r_p}{r_s}\right)^{n-1}$$

Up to fist order

$$\Phi_{\rm tri}(r,\vartheta,\varphi) \approx \Phi_0(r) + \Phi_1(r)\left\{(\varepsilon_2 - \varepsilon_1)\cos 2\vartheta - \right.$$
$$\left. -\varepsilon_1 \cos 2\varphi + \frac{\varepsilon_1}{2}\cos 2(\vartheta+\varphi) + \frac{\varepsilon_1}{2}\cos 2(\vartheta-\varphi)\right\},$$

$$\begin{aligned}
\Phi_0(r) &= \frac{Ar}{2ar_s^2}(1+r/r_s)(1-r/ar_s) + (\varepsilon_1+\varepsilon_2)\Phi_1(r), \\
\Phi_1(r) &= \frac{Ar^2}{2ar_s^2}(1+r/r_s)(1/r - 2/ar_s).
\end{aligned}$$

$$\varepsilon_1 = \frac{1}{8}(a^2/b^2 - 1), \quad \varepsilon_2 = \frac{1}{4}(a^2/c^2 - 1), \quad \text{assumed small.}$$

Power expansion for $r_p < r_s (r < r_s)$

$$\Phi_{\text{tri}} = -\frac{A}{r_s} \sum_{n=1}^{\infty} \frac{(-1)^{n+1}}{n} \left(\frac{r_p}{r_s}\right)^{n-1}$$

Up to fist order

$$\Phi_{\text{tri}}(r,\vartheta,\varphi) \approx \Phi_0(r) + \Phi_1(r)\left\{(\varepsilon_2 - \varepsilon_1)\cos 2\vartheta - \right.$$
$$\left. - \varepsilon_1 \cos 2\varphi + \frac{\varepsilon_1}{2}\cos 2(\vartheta+\varphi) + \frac{\varepsilon_1}{2}\cos 2(\vartheta - \varphi)\right\},$$

$$\Phi_0(r) = \frac{Ar}{2ar_s^2}(1 + r/r_s)(1 - r/ar_s) + (\varepsilon_1 + \varepsilon_2)\Phi_1(r),$$

$$\Phi_1(r) = \frac{Ar^2}{2ar_s^2}(1 + r/r_s)(1/r - 2/ar_s).$$

$$\varepsilon_1 = \frac{1}{8}(a^2/b^2 - 1), \quad \varepsilon_2 = \frac{1}{4}(a^2/c^2 - 1), \quad \text{assumed small.}$$

Power expansion for $r_p < r_s (r < r_s)$

$$\Phi_{\rm tri} = -\frac{A}{r_s} \sum_{n=1}^{\infty} \frac{(-1)^{n+1}}{n} \left(\frac{r_p}{r_s}\right)^{n-1}$$

Up to fist order

$$\Phi_{\rm tri}(r,\vartheta,\varphi) \approx \Phi_0(r) + \Phi_1(r) \{ (\varepsilon_2 - \varepsilon_1) \cos 2\vartheta - \\ - \varepsilon_1 \cos 2\varphi + \frac{\varepsilon_1}{2} \cos 2(\vartheta + \varphi) + \frac{\varepsilon_1}{2} \cos 2(\vartheta - \varphi) \},$$

$$\begin{aligned} \Phi_0(r) &= \frac{Ar}{2ar_s^2}(1 + r/r_s)(1 - r/ar_s) + (\varepsilon_1 + \varepsilon_2)\Phi_1(r), \\ \Phi_1(r) &= \frac{Ar^2}{2ar_s^2}(1 + r/r_s)(1/r - 2/ar_s). \end{aligned}$$

$$\varepsilon_1 = \frac{1}{8}(a^2/b^2 - 1), \quad \varepsilon_2 = \frac{1}{4}(a^2/c^2 - 1), \quad \text{assumed small.}$$

Power expansion for $r_p < r_s (r < r_s)$

$$\Phi_{\mathrm{tri}} = -\frac{A}{r_s} \sum_{n=1}^{\infty} \frac{(-1)^{n+1}}{n} \left(\frac{r_p}{r_s}\right)^{n-1}$$

Up to fist order

$$\Phi_{\mathrm{tri}}(r, \vartheta, \varphi) \approx \Phi_0(r) + \Phi_1(r) \{ (\varepsilon_2 - \varepsilon_1) \cos 2\vartheta - \\ - \varepsilon_1 \cos 2\varphi + \frac{\varepsilon_1}{2} \cos 2(\vartheta + \varphi) + \frac{\varepsilon_1}{2} \cos 2(\vartheta - \varphi) \},$$

$$\begin{aligned} \Phi_0(r) &= \frac{Ar}{2ar_s^2}(1 + r/r_s)(1 - r/ar_s) + (\varepsilon_1 + \varepsilon_2)\Phi_1(r), \\ \Phi_1(r) &= \frac{Ar^2}{2ar_s^2}(1 + r/r_s)(1/r - 2/ar_s). \end{aligned}$$

$$\varepsilon_1 = \frac{1}{8}(a^2/b^2 - 1), \quad \varepsilon_2 = \frac{1}{4}(a^2/c^2 - 1), \quad \text{assumed small.}$$

Perturvative approach:

$$\mathcal{H}(\mathbf{p},\mathbf{r}) = \mathcal{H}_0(\mathbf{p},r,\vartheta) + \hat{\Phi}_1(\mathbf{r}),$$

$$\mathcal{H}_0(\mathbf{p},r,\theta) = \frac{p_r^2}{2}+\frac{p_\vartheta^2}{2r^2}+\frac{p_\varphi^2}{2r^2\sin^2\vartheta}+\Phi_0(r), \quad \hat{\Phi}_1(\mathbf{r}) = \Phi_{\mathrm{tri}}(\mathbf{r})-\Phi_0(r).$$

Prime integrals:

$$\mathcal{H}_0(\mathbf{p},r,\vartheta) = h_0, \qquad L^2, \qquad L_z.$$

Variation of the unperturbed integrals:

$$\begin{aligned} \frac{dL_z}{dt} &= [\mathrm{L}_z,\mathcal{H}] = -\frac{\partial\hat{\Phi}_1}{\partial\varphi}, \\ \frac{d\mathrm{L}^2}{dt} &= [\mathrm{L}^2,\mathcal{H}] = -2p_\vartheta\frac{\partial\hat{\Phi}_1}{\partial\vartheta} - \frac{2p_\varphi}{\sin^2\vartheta}\frac{\partial\hat{\Phi}_1}{\partial\varphi}, \end{aligned}$$

Perturvative approach:

$$\mathcal{H}(\mathbf{p},\mathbf{r}) = \mathcal{H}_0(\mathbf{p},r,\vartheta) + \hat{\Phi}_1(\mathbf{r}),$$

$$\mathcal{H}_0(\mathbf{p},r,\theta) = \frac{p_r^2}{2}+\frac{p_\vartheta^2}{2r^2}+\frac{p_\varphi^2}{2r^2\sin^2\vartheta}+\Phi_0(r), \quad \hat{\Phi}_1(\mathbf{r}) = \Phi_{\rm tri}(\mathbf{r})-\Phi_0(r).$$

Prime integrals:

$$\mathcal{H}_0(\mathbf{p},r,\vartheta) = h_0, \qquad L^2, \qquad L_z.$$

Variation of the unperturbed integrals:

$$\begin{aligned} \frac{dL_z}{dt} &= [\mathrm{L}_z,\mathcal{H}] = -\frac{\partial\hat{\Phi}_1}{\partial\varphi}, \\ \frac{d\mathrm{L}^2}{dt} &= [\mathrm{L}^2,\mathcal{H}] = -2p_\vartheta\frac{\partial\hat{\Phi}_1}{\partial\vartheta} - \frac{2p_\varphi}{\sin^2\vartheta}\frac{\partial\hat{\Phi}_1}{\partial\varphi}, \end{aligned}$$

Perturvative approach:

$$\mathcal{H}(\mathbf{p},\mathbf{r}) = \mathcal{H}_0(\mathbf{p},r,\vartheta) + \hat{\Phi}_1(\mathbf{r}),$$

$$\mathcal{H}_0(\mathbf{p},r,\theta) = \frac{p_r^2}{2}+\frac{p_\vartheta^2}{2r^2}+\frac{p_\varphi^2}{2r^2\sin^2\vartheta}+\Phi_0(r), \quad \hat{\Phi}_1(\mathbf{r}) = \Phi_{\rm tri}(\mathbf{r})-\Phi_0(r).$$

Prime integrals:

$$\mathcal{H}_0(\mathbf{p},r,\vartheta) = h_0, \qquad L^2, \qquad L_z.$$

Variation of the unperturbed integrals:

$$\begin{aligned} \frac{dL_z}{dt} &= [\mathrm{L}_z,\mathcal{H}] = -\frac{\partial\hat{\Phi}_1}{\partial\varphi}, \\ \frac{d\mathrm{L}^2}{dt} &= [\mathrm{L}^2,\mathcal{H}] = -2p_\vartheta\frac{\partial\hat{\Phi}_1}{\partial\vartheta} - \frac{2p_\varphi}{\sin^2\vartheta}\frac{\partial\hat{\Phi}_1}{\partial\varphi}, \end{aligned}$$

Perturvative approach:

$$\mathcal{H}(\mathbf{p},\mathbf{r}) = \mathcal{H}_0(\mathbf{p},r,\vartheta) + \hat{\Phi}_1(\mathbf{r}),$$

$$\mathcal{H}_0(\mathbf{p},r,\theta) = \frac{p_r^2}{2} + \frac{p_\vartheta^2}{2r^2} + \frac{p_\varphi^2}{2r^2\sin^2\vartheta} + \Phi_0(r), \quad \hat{\Phi}_1(\mathbf{r}) = \Phi_{\text{tri}}(\mathbf{r}) - \Phi_0(r).$$

Prime integrals:

$$\mathcal{H}_0(\mathbf{p},r,\vartheta) = h_0, \qquad L^2, \qquad L_z.$$

Variation of the unperturbed integrals:

$$\begin{aligned} \frac{dL_z}{dt} &= [\mathrm{L}_z,\mathcal{H}] = -\frac{\partial\hat{\Phi}_1}{\partial\varphi}, \\ \frac{d\mathrm{L}^2}{dt} &= [\mathrm{L}^2,\mathcal{H}] = -2p_\vartheta\frac{\partial\hat{\Phi}_1}{\partial\vartheta} - \frac{2p_\varphi}{\sin^2\vartheta}\frac{\partial\hat{\Phi}_1}{\partial\varphi}, \end{aligned}$$

Perturvative approach:

$$\mathcal{H}(\mathbf{p},\mathbf{r}) = \mathcal{H}_0(\mathbf{p},r,\vartheta) + \hat{\Phi}_1(\mathbf{r}),$$

$$\mathcal{H}_0(\mathbf{p},r,\theta) = \frac{p_r^2}{2}+\frac{p_\vartheta^2}{2r^2}+\frac{p_\varphi^2}{2r^2\sin^2\vartheta}+\Phi_0(r), \quad \hat{\Phi}_1(\mathbf{r}) = \Phi_{\rm tri}(\mathbf{r})-\Phi_0(r).$$

Prime integrals:

$$\mathcal{H}_0(\mathbf{p},r,\vartheta) = h_0, \qquad L^2, \qquad L_z.$$

Variation of the unperturbed integrals:

$$\begin{aligned}
\frac{dL_z}{dt} &= [\mathrm{L}_z,\mathcal{H}] = -\frac{\partial\hat{\Phi}_1}{\partial\varphi},\\
\frac{d\mathrm{L}^2}{dt} &= [\mathrm{L}^2,\mathcal{H}] = -2p_\vartheta\frac{\partial\hat{\Phi}_1}{\partial\vartheta} - \frac{2p_\varphi}{\sin^2\vartheta}\frac{\partial\hat{\Phi}_1}{\partial\varphi},
\end{aligned}$$

Perturvative approach:

$$\mathcal{H}(\mathbf{p},\mathbf{r}) = \mathcal{H}_0(\mathbf{p},r,\vartheta) + \hat{\Phi}_1(\mathbf{r}),$$

$$\mathcal{H}_0(\mathbf{p},r,\theta) = \frac{p_r^2}{2} + \frac{p_\vartheta^2}{2r^2} + \frac{p_\varphi^2}{2r^2\sin^2\vartheta} + \Phi_0(r), \quad \hat{\Phi}_1(\mathbf{r}) = \Phi_{\rm tri}(\mathbf{r}) - \Phi_0(r).$$

Prime integrals:

$$\mathcal{H}_0(\mathbf{p},r,\vartheta) = h_0, \qquad L^2, \qquad L_z.$$

Variation of the unperturbed integrals:

$$\begin{aligned} \frac{dL_z}{dt} &= [\mathrm{L}_z,\mathcal{H}] = -\frac{\partial\hat{\Phi}_1}{\partial\varphi}, \\ \frac{d\mathrm{L}^2}{dt} &= [\mathrm{L}^2,\mathcal{H}] = -2p_\vartheta\frac{\partial\hat{\Phi}_1}{\partial\vartheta} - \frac{2p_\varphi}{\sin^2\vartheta}\frac{\partial\hat{\Phi}_1}{\partial\varphi}, \end{aligned}$$

Perturvative approach:

$$\mathcal{H}(\mathbf{p},\mathbf{r}) = \mathcal{H}_0(\mathbf{p},r,\vartheta) + \hat{\Phi}_1(\mathbf{r}),$$

$$\mathcal{H}_0(\mathbf{p},r,\theta) = \frac{p_r^2}{2}+\frac{p_\vartheta^2}{2r^2}+\frac{p_\varphi^2}{2r^2\sin^2\vartheta}+\Phi_0(r), \quad \hat{\Phi}_1(\mathbf{r}) = \Phi_{\rm tri}(\mathbf{r})-\Phi_0(r).$$

Prime integrals:

$$\mathcal{H}_0(\mathbf{p},r,\vartheta) = h_0, \qquad L^2, \qquad L_z.$$

Variation of the unperturbed integrals:

$$\begin{aligned}
\frac{dL_z}{dt} &= [\mathrm{L}_z,\mathcal{H}] = -\frac{\partial\hat{\Phi}_1}{\partial\varphi}, \\
\frac{d\mathrm{L}^2}{dt} &= [\mathrm{L}^2,\mathcal{H}] = -2p_\vartheta\frac{\partial\hat{\Phi}_1}{\partial\vartheta} - \frac{2p_\varphi}{\sin^2\vartheta}\frac{\partial\hat{\Phi}_1}{\partial\varphi},
\end{aligned}$$

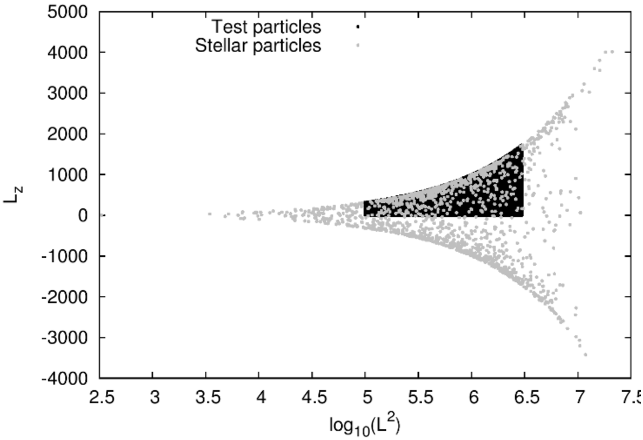

Figure: Ranges in L^2 and L_z for 1400 particles (grey) of the Aq–A2 DM halo. In black, the region of the plane to be considered in the experiments, $(x_0, y_0, z_0) = (8, 0, 0)$ kpc (i.e. the position of the *Sun*) and h_0 is taken as mean value of the energy distribution of the stellar particles located within a 2.5 kpc sphere around the Sun.

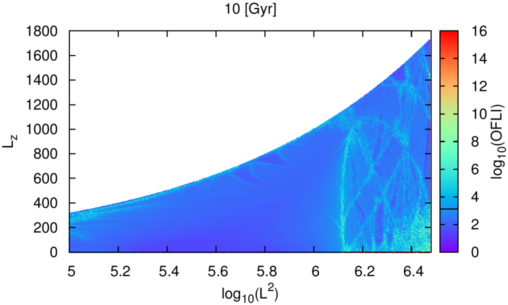
10 [Gyr]
1800
1600
1400
1200
1000
800
600
400
200
0
L_z
5
5.2
5.4
5.6
5.8
6
6.2
6.4
$\log_{10}(L^2)$
16
14
12
10
8
6
4
2
0
$\log_{10}$(OFLI)

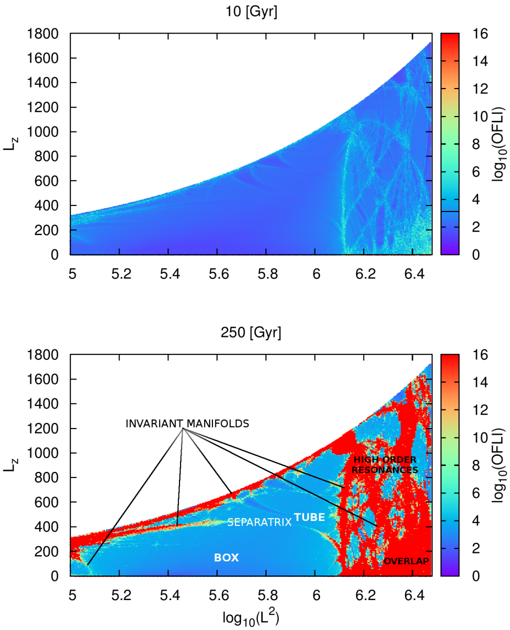
10 [Gyr]
1800
1600
1400
1200
1000
800
600
400
200
0
L_z
5
5.2
5.4
5.6
5.8
6
6.2
6.4
16
14
12
10
8
6
4
2
0
$\log_{10}(\mathrm{OFLI})$
250 [Gyr]
INVARIANT MANIFOLDS
HIGH ORDER RESONANCES
SEPARATRIX
TUBE
BOX
OVERLAP
$\log_{10}(L^2)$

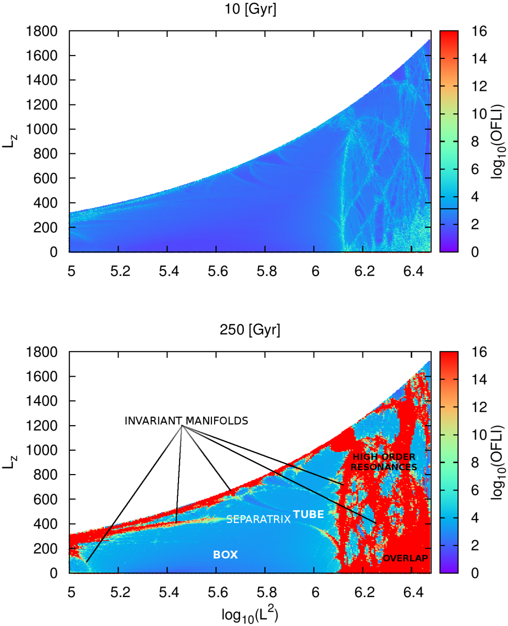

Figure: OFLI contour plots for 10 and 250 Gyr for the Aq–A2 halo model for $(x_0, y_0, z_0) = (8, 0, 0)$, $\mathrm{h}_0 \simeq -204449$ km^2 s^{-2}.

Diffusion experiments

- Ensembles of 90000 i.c. of size 10^{-6} on different chaotic regions
- Section: $|\mathbf{x}(t) - \mathbf{x}_{\odot}| \leq 0.1$ kpc,
- Different motion times $t > 10$ Gyrs.
- Numerical integrations using the full expression of $\Phi_{\rm tri}$ (not the first order approximation).
- Only a few results will be shown (full set of experiments: Maffione et al., MNRAS, 2015).

Diffusion experiments

- Ensembles of 90000 i.c. of size 10^{-6} on different chaotic regions
- Section: $|\mathbf{x}(t) - \mathbf{x}_{\odot}| \leq 0.1$ kpc,
- Different motion times $t > 10$ Gyrs.
- Numerical integrations using the full expression of Φ_{tri} (not the first order approximation).
- Only a few results will be shown (full set of experiments: Maffione et al., MNRAS, 2015).

Diffusion experiments

- Ensembles of 90000 i.c. of size 10^{-6} on different chaotic regions
- Section: $|\mathbf{x}(t) - \mathbf{x}_{\odot}| \leq 0.1$ kpc,
- Different motion times $t > 10$ Gyrs.
- Numerical integrations using the full expression of $\Phi_{\rm tri}$ (not the first order approximation).
- Only a few results will be shown (full set of experiments: Maffione et al., MNRAS, 2015).

Diffusion experiments

- Ensembles of 90000 i.c. of size 10^{-6} on different chaotic regions
- Section: $|\mathbf{x}(t) - \mathbf{x}_{\odot}| \leq 0.1$ kpc,
- Different motion times $t > 10$ Gyrs.
- Numerical integrations using the full expression of $\Phi_{\rm tri}$ (not the first order approximation).
- Only a few results will be shown (full set of experiments: Maffione et al., MNRAS, 2015).

Diffusion experiments

- Ensembles of 90000 i.c. of size 10^{-6} on different chaotic regions
- Section: $|\mathbf{x}(t) - \mathbf{x}_{\odot}| \leq 0.1$ kpc,
- Different motion times $t > 10$ Gyrs.
- Numerical integrations using the full expression of Φ_{tri} (not the first order approximation).
- Only a few results will be shown (full set of experiments: Maffione et al., MNRAS, 2015).

Diffusion experiments

- Ensembles of 90000 i.c. of size 10^{-6} on different chaotic regions
- Section: $|\mathbf{x}(t) - \mathbf{x}_{\odot}| \leq 0.1$ kpc,
- Different motion times $t > 10$ Gyrs.
- Numerical integrations using the full expression of $\Phi_{\rm tri}$ (not the first order approximation).
- Only a few results will be shown (full set of experiments: Maffione et al., MNRAS, 2015).

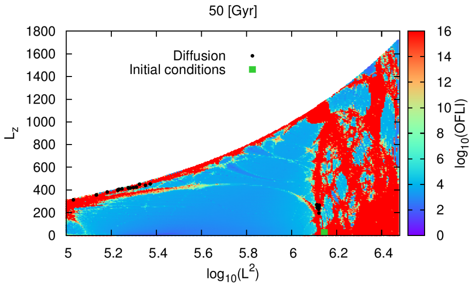

50 [Gyr]
Diffusion
Initial conditions
L_z
$\log_{10}(L^2)$
$\log_{10}(\mathrm{OFLI})$
1800
1600
1400
1200
1000
800
600
400
200
0
5
5.2
5.4
5.6
5.8
6
6.2
6.4
16
14
12
10
8
6
4
2
0

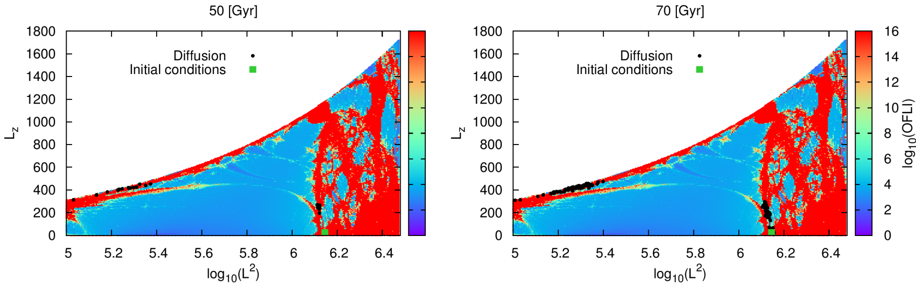

50 [Gyr]
70 [Gyr]
Diffusion
Initial conditions
L_z
$\log_{10}(L^2)$
$\log_{10}(\mathrm{OFLI})$

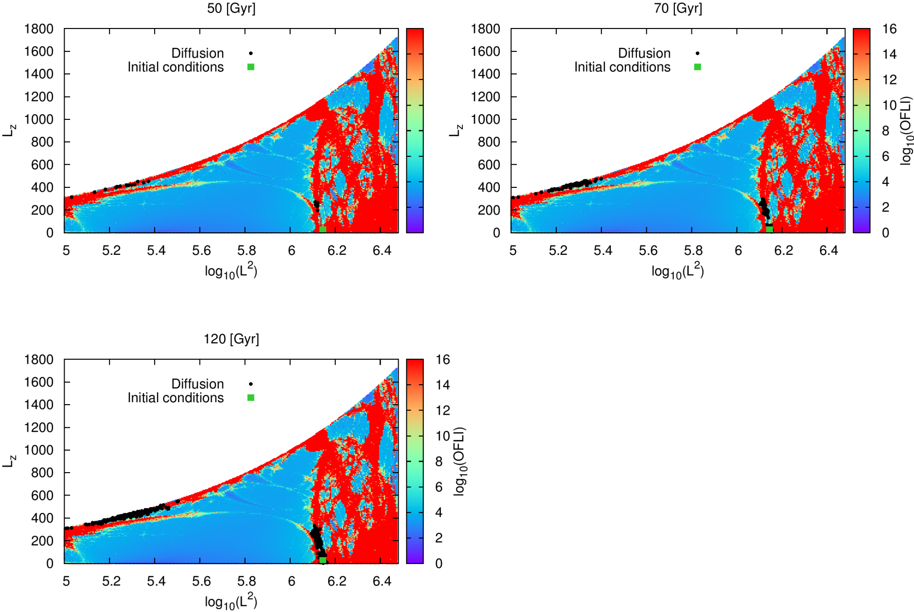

50 [Gyr]
70 [Gyr]
120 [Gyr]
Diffusion
Initial conditions
L_z
log_10(L^2)
log_10(OFLI)

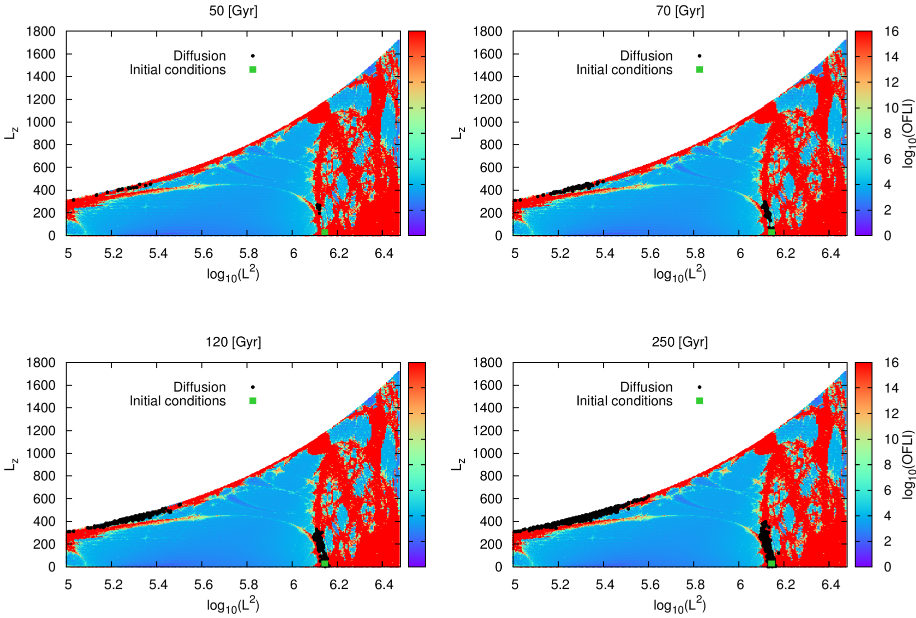

50 [Gyr]
70 [Gyr]
120 [Gyr]
250 [Gyr]
Diffusion
Initial conditions
L_z
$\log_{10}(L^2)$
$\log_{10}(\mathrm{OFLI})$

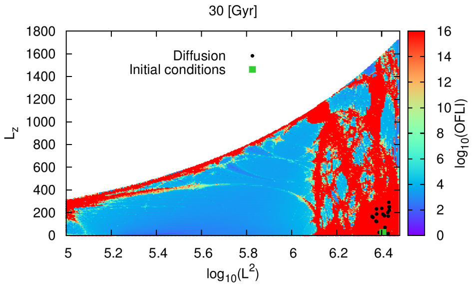
30 [Gyr]
Diffusion
Initial conditions
L_z
1800
1600
1400
1200
1000
800
600
400
200
0
5
5.2
5.4
5.6
5.8
6
6.2
6.4
$\log_{10}(L^2)$
16
14
12
10
8
6
4
2
0
$\log_{10}(\mathrm{OFLI})$

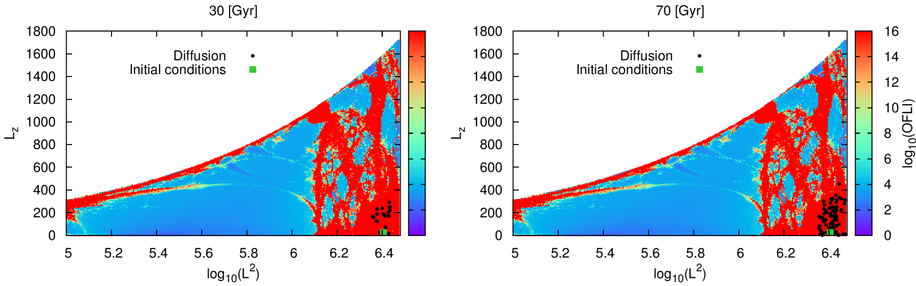
30 [Gyr]
70 [Gyr]
Diffusion
Initial conditions
L_z
$\log_{10}(L^2)$
$\log_{10}(\mathrm{OFLI})$
1800
1600
1400
1200
1000
800
600
400
200
0
5
5.2
5.4
5.6
5.8
6
6.2
6.4
16
14
12
10
8
6
4
2
0

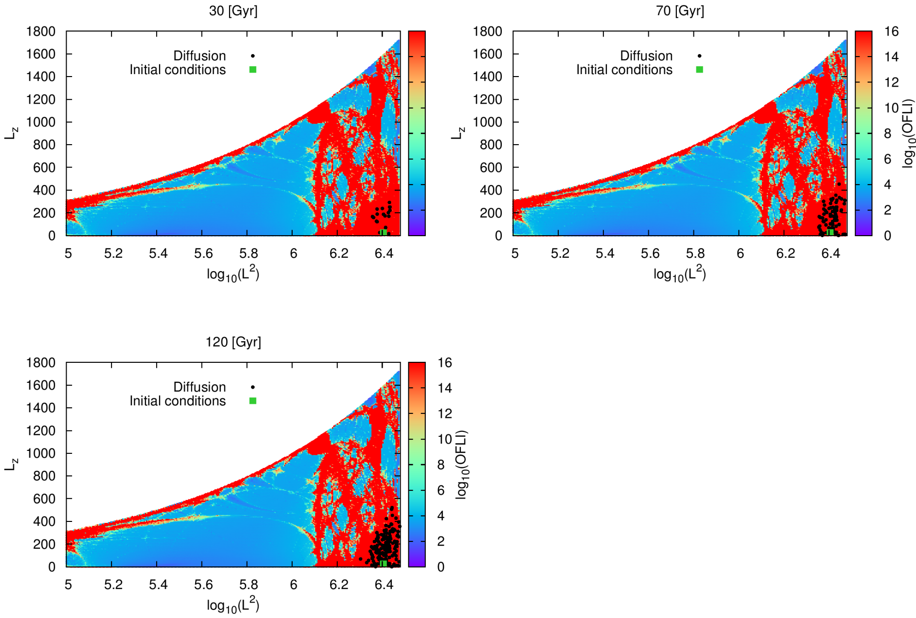
30 [Gyr]
70 [Gyr]
120 [Gyr]
Diffusion
Initial conditions
L_z
$\log_{10}(L^2)$
$\log_{10}(\mathrm{OFLI})$
1800
1600
1400
1200
1000
800
600
400
200
0
5
5.2
5.4
5.6
5.8
6
6.2
6.4
16
14
12
10
8
6
4
2

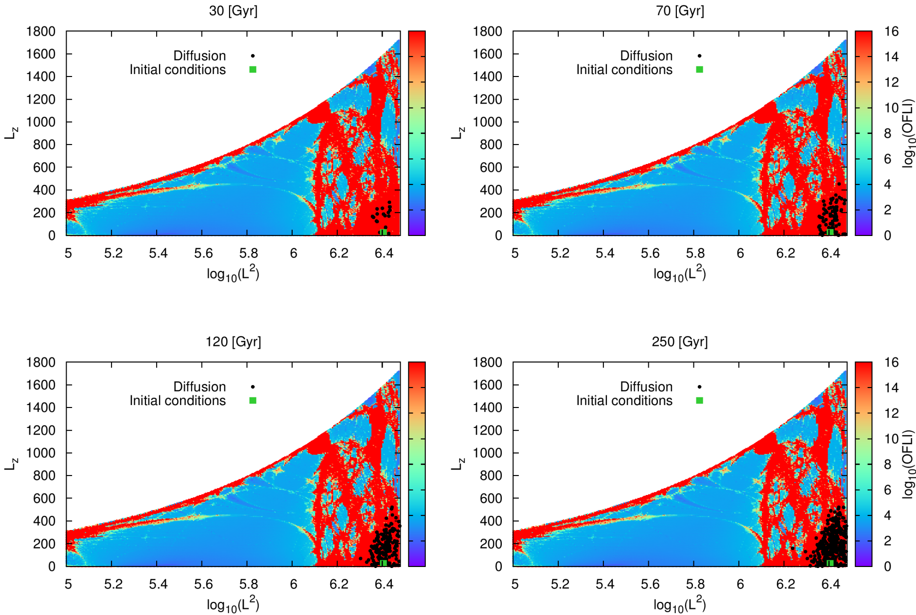

30 [Gyr]
70 [Gyr]
120 [Gyr]
250 [Gyr]
Diffusion
Initial conditions
L_z
$\log_{10}(L^2)$
$\log_{10}(\mathrm{OFLI})$

If we add to the DM halo potential, a central concentration, a bulge and a disc (work in progress, Maffione et al.)

$$\Phi = \Phi_{\rm tri} + \Phi_{\rm smbh} + \Phi_{\rm bulge} + \Phi_{\rm disk}$$

$$\Phi_{\rm smbh} = -\frac{GM_{\rm smbh}}{\sqrt{r^2 + \epsilon_{\rm smbh}^2}} \quad ({\rm Plummer})$$

$$\Phi_{\rm bulge} = -\frac{GM_{\rm bulge}}{r + \epsilon_{\rm bulge}} \quad ({\rm Hernquist})$$

$$\Phi_{\rm disk} = -\frac{GM_{\rm disk}}{\sqrt{r^2 - z^2 + \left(\epsilon_s + \sqrt{z^2 + \epsilon_h^2}\right)^2}} \quad ({\rm Miyamoto - Nagai})$$

$$M_{\rm smbh} \sim 10^7 M_\odot, \quad M_{\rm bulge} \sim 3 \times 10^{10} M_\odot,$$
$$M_{\rm disk} \sim 8 \times 10^{10} M_\odot, \quad M_{\rm dmh} \sim 150 \times 10^{10} M_\odot.$$

If we add to the DM halo potential, a central concentration, a bulge and a disc (work in progress, Maffione et al.)

$$\Phi = \Phi_{\mathrm{tri}} + \Phi_{\mathrm{smbh}} + \Phi_{\mathrm{bulge}} + \Phi_{\mathrm{disk}}$$

$$\Phi_{\mathrm{smbh}} = -\frac{GM_{\mathrm{smbh}}}{\sqrt{r^2 + \epsilon_{\mathrm{smbh}}^2}} \quad \text{(Plummer)}$$

$$\Phi_{\mathrm{bulge}} = -\frac{GM_{\mathrm{bulge}}}{r + \epsilon_{\mathrm{bulge}}} \quad \text{(Hernquist)}$$

$$\Phi_{\mathrm{disk}} = -\frac{GM_{\mathrm{disk}}}{\sqrt{r^2 - z^2 + \left(\epsilon_s + \sqrt{z^2 + \epsilon_h^2}\right)^2}} \quad \text{(Miyamoto} - \text{Nagai)}$$

$$M_{\mathrm{smbh}} \sim 10^7 M_\odot, \quad M_{\mathrm{bulge}} \sim 3 \times 10^{10} M_\odot,$$

$$M_{\mathrm{disk}} \sim 8 \times 10^{10} M_\odot, \quad M_{\mathrm{dmh}} \sim 150 \times 10^{10} M_\odot.$$

If we add to the DM halo potential, a central concentration, a bulge and a disc (work in progress, Maffione et al.)

$$\Phi = \Phi_{\rm tri} + \Phi_{\rm smbh} + \Phi_{\rm bulge} + \Phi_{\rm disk}$$

$$\Phi_{\rm smbh} = -\frac{GM_{\rm smbh}}{\sqrt{r^2 + \epsilon_{\rm smbh}^2}} \quad ({\rm Plummer})$$

$$\Phi_{\rm bulge} = -\frac{GM_{\rm bulge}}{r + \epsilon_{\rm bulge}} \quad ({\rm Hernquist})$$

$$\Phi_{\rm disk} = -\frac{GM_{\rm disk}}{\sqrt{r^2 - z^2 + \left(\epsilon_s + \sqrt{z^2 + \epsilon_h^2}\right)^2}} \quad ({\rm Miyamoto - Nagai})$$

$$M_{\rm smbh} \sim 10^7 M_\odot, \quad M_{\rm bulge} \sim 3 \times 10^{10} M_\odot,$$

$$M_{\rm disk} \sim 8 \times 10^{10} M_\odot, \quad M_{\rm dmh} \sim 150 \times 10^{10} M_\odot.$$

If we add to the DM halo potential, a central concentration, a bulge and a disc (work in progress, Maffione et al.)

$$\Phi = \Phi_{\rm tri} + \Phi_{\rm smbh} + \Phi_{\rm bulge} + \Phi_{\rm disk}$$

$$\Phi_{\rm smbh} = -\frac{GM_{\rm smbh}}{\sqrt{r^2 + \epsilon_{\rm smbh}^2}} \quad \text{(Plummer)}$$

$$\Phi_{\rm bulge} = -\frac{GM_{\rm bulge}}{r + \epsilon_{\rm bulge}} \quad \text{(Hernquist)}$$

$$\Phi_{\rm disk} = -\frac{GM_{\rm disk}}{\sqrt{r^2 - z^2 + \left(\epsilon_s + \sqrt{z^2 + \epsilon_h^2}\right)^2}} \quad \text{(Miyamoto – Nagai)}$$

$$M_{\rm smbh} \sim 10^7 M_\odot, \quad M_{\rm bulge} \sim 3 \times 10^{10} M_\odot,$$
$$M_{\rm disk} \sim 8 \times 10^{10} M_\odot, \quad M_{\rm dmh} \sim 150 \times 10^{10} M_\odot.$$

If we add to the DM halo potential, a central concentration, a bulge and a disc (work in progress, Maffione et al.)

$$\Phi = \Phi_{\mathrm{tri}} + \Phi_{\mathrm{smbh}} + \Phi_{\mathrm{bulge}} + \Phi_{\mathrm{disk}}$$

$$\Phi_{\mathrm{smbh}} = -\frac{GM_{\mathrm{smbh}}}{\sqrt{r^2 + \epsilon_{\mathrm{smbh}}^2}} \quad \text{(Plummer)}$$

$$\Phi_{\mathrm{bulge}} = -\frac{GM_{\mathrm{bulge}}}{r + \epsilon_{\mathrm{bulge}}} \quad \text{(Hernquist)}$$

$$\Phi_{\mathrm{disk}} = -\frac{GM_{\mathrm{disk}}}{\sqrt{r^2 - z^2 + \left(\epsilon_s + \sqrt{z^2 + \epsilon_h^2}\right)^2}} \quad \text{(Miyamoto – Nagai)}$$

$$M_{\mathrm{smbh}} \sim 10^7 M_\odot, \quad M_{\mathrm{bulge}} \sim 3 \times 10^{10} M_\odot,$$

$$M_{\mathrm{disk}} \sim 8 \times 10^{10} M_\odot, \quad M_{\mathrm{dmh}} \sim 150 \times 10^{10} M_\odot.$$

If we add to the DM halo potential, a central concentration, a bulge and a disc (work in progress, Maffione et al.)

$$\Phi = \Phi_{\rm tri} + \Phi_{\rm smbh} + \Phi_{\rm bulge} + \Phi_{\rm disk}$$

$$\Phi_{\rm smbh} = -\frac{GM_{\rm smbh}}{\sqrt{r^2 + \epsilon^2_{\rm smbh}}} \quad \text{(Plummer)}$$

$$\Phi_{\rm bulge} = -\frac{GM_{\rm bulge}}{r + \epsilon_{\rm bulge}} \quad \text{(Hernquist)}$$

$$\Phi_{\rm disk} = -\frac{GM_{\rm disk}}{\sqrt{r^2 - z^2 + \left(\epsilon_s + \sqrt{z^2 + \epsilon_h^2}\right)^2}} \quad \text{(Miyamoto – Nagai)}$$

$$M_{\rm smbh} \sim 10^7 M_\odot, \quad M_{\rm bulge} \sim 3 \times 10^{10} M_\odot,$$
$$M_{\rm disk} \sim 8 \times 10^{10} M_\odot, \quad M_{\rm dmh} \sim 150 \times 10^{10} M_\odot.$$

Grid: (L^2, L_z) and E = -164803. OFLI levels: 121224 c.i., 10Gyrs.

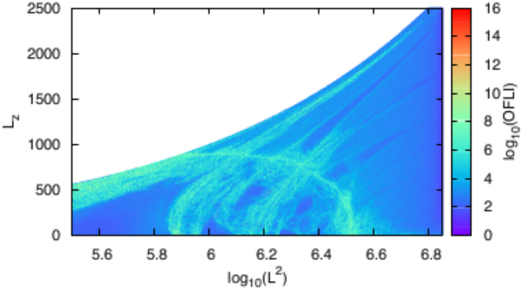

Grid: (L^2, L_z) and E = -164803. OFLI levels: 121224 c.i., 10Gyrs.

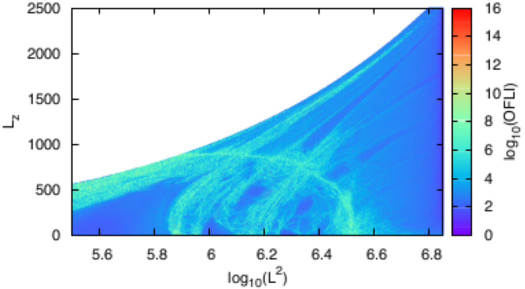

Grid: (L^2, L_z) and E = -164803. OFLI levels: 121224 c.i., 100Gyrs.

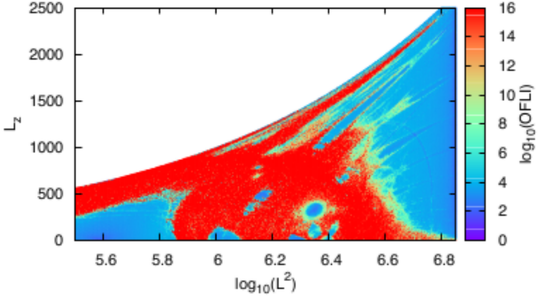

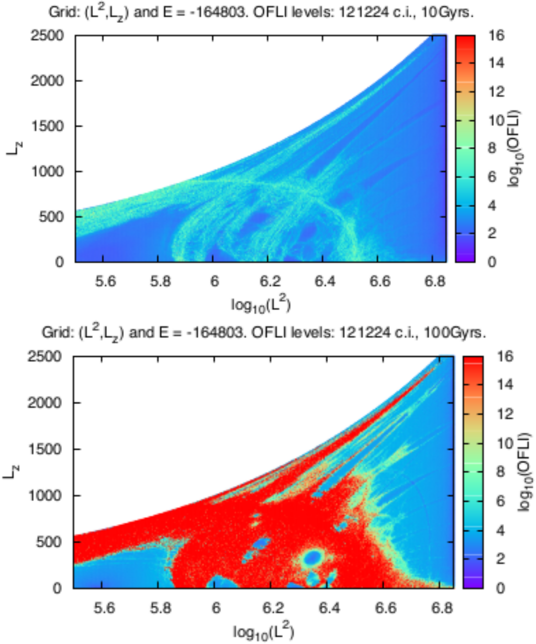

Figure: OFLI contour plots for 10 and 100 Gyrs. $(x_0, y_0, z_0) = (8, 0, 0)$.

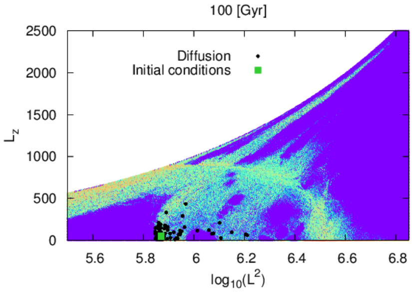
100 [Gyr]
Diffusion
Initial conditions
L_z
$\log_{10}(L^2)$
2500
2000
1500
1000
500
0
5.6
5.8
6
6.2
6.4
6.6
6.8

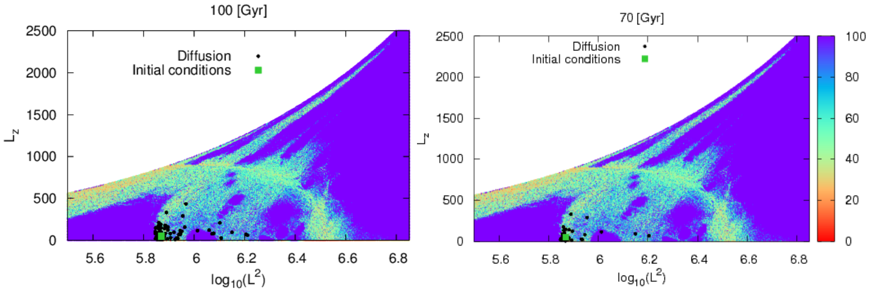

100 [Gyr]
Diffusion
Initial conditions
2500
2000
1500
1000
500
0
L_z
5.6
5.8
6
6.2
6.4
6.6
6.8
$\log_{10}(L^2)$
70 [Gyr]
Diffusion
Initial conditions
2500
2000
1500
1000
500
0
L_z
5.6
5.8
6
6.2
6.4
6.6
6.8
$\log_{10}(L^2)$
100
80
60
40
20
0

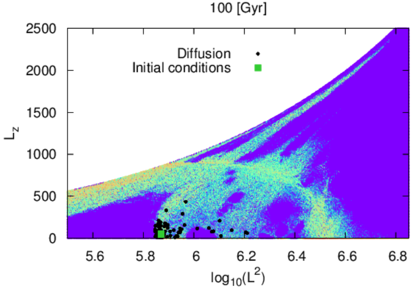
100 [Gyr]
Diffusion
Initial conditions
L_z
2500
2000
1500
1000
500
0
5.6
5.8
6
6.2
6.4
6.6
6.8
$\log_{10}(L^2)$

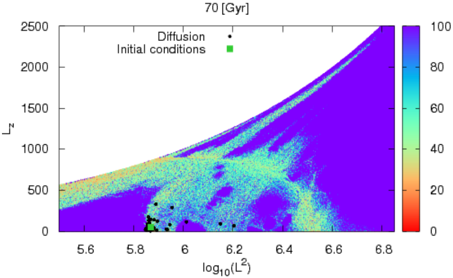
70 [Gyr]
Diffusion
Initial conditions
L_z
2500
2000
1500
1000
500
0
5.6
5.8
6
6.2
6.4
6.6
6.8
$\log_{10}(L^2)$
100
80
60
40
20
0

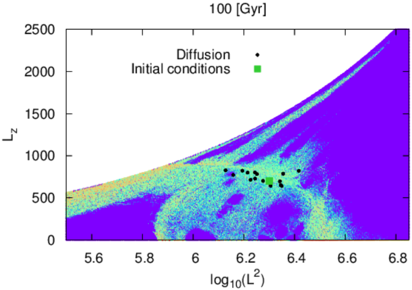
100 [Gyr]
Diffusion
Initial conditions
L_z
2500
2000
1500
1000
500
0
5.6
5.8
6
6.2
6.4
6.6
6.8
$\log_{10}(L^2)$

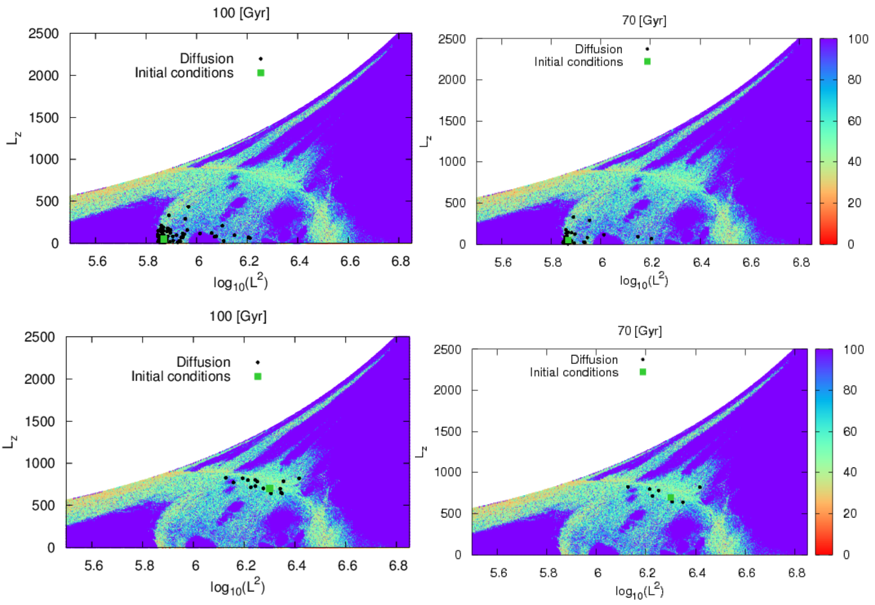
100 [Gyr]
Diffusion
Initial conditions
2500
2000
1500
1000
500
0
L_z
5.6
5.8
6
6.2
6.4
6.6
6.8
$\log_{10}(L^2)$
70 [Gyr]
Diffusion
Initial conditions
2500
2000
1500
1000
500
0
L_z
5.6
5.8
6
6.2
6.4
6.6
6.8
$\log_{10}(L^2)$
100
80
60
40
20
0
100 [Gyr]
Diffusion
Initial conditions
2500
2000
1500
1000
500
0
L_z
5.6
5.8
6
6.2
6.4
6.6
6.8
$\log_{10}(L^2)$
70 [Gyr]
Diffusion
Initial conditions
2500
2000
1500
1000
500
0
L_z
5.6
5.8
6
6.2
6.4
6.6
6.8
$\log_{10}(L^2)$
100
80
60
40
20
0

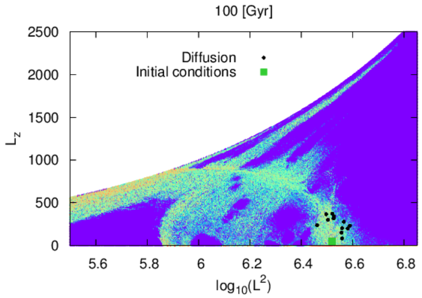
100 [Gyr]
Diffusion
Initial conditions
2500
2000
1500
1000
500
0
L_z
5.6
5.8
6
6.2
6.4
6.6
6.8
$\log_{10}(L^2)$

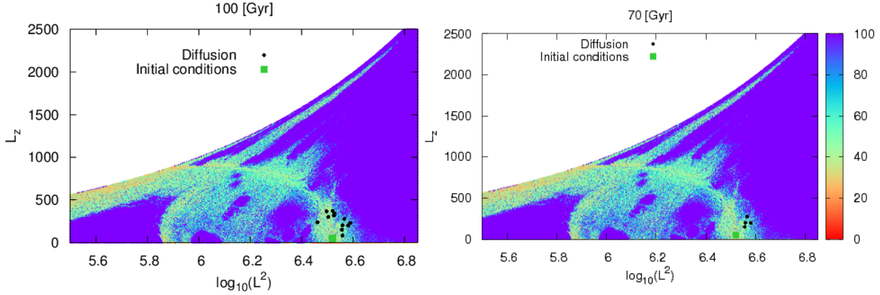
100 [Gyr]
Diffusion
Initial conditions
L_z
$\log_{10}(L^2)$
70 [Gyr]
Diffusion
Initial conditions
L_z
$\log_{10}(L^2)$

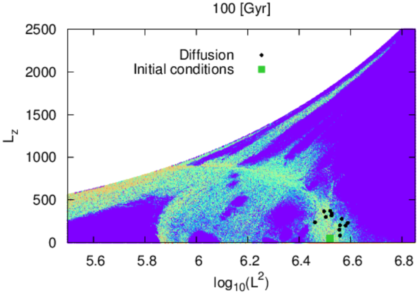
100 [Gyr]
Diffusion
Initial conditions
2500
2000
1500
1000
500
0
L_z
5.6
5.8
6
6.2
6.4
6.6
6.8
$\log_{10}(L^2)$

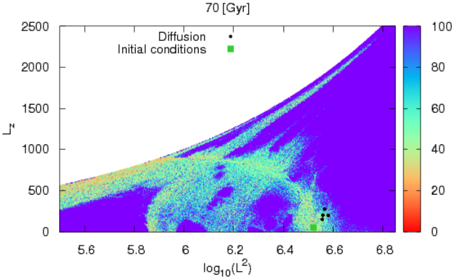
70 [Gyr]
Diffusion
Initial conditions
2500
2000
1500
1000
500
0
L_z
5.6
5.8
6
6.2
6.4
6.6
6.8
$\log_{10}(L^2)$
100
80
60
40
20
0

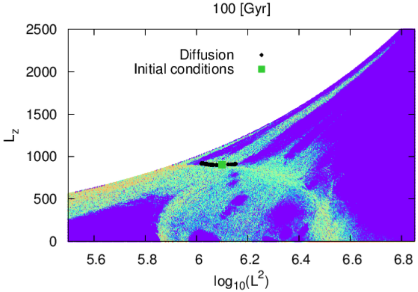
100 [Gyr]
Diffusion
Initial conditions
2500
2000
1500
1000
500
0
L_z
5.6
5.8
6
6.2
6.4
6.6
6.8
$\log_{10}(L^2)$

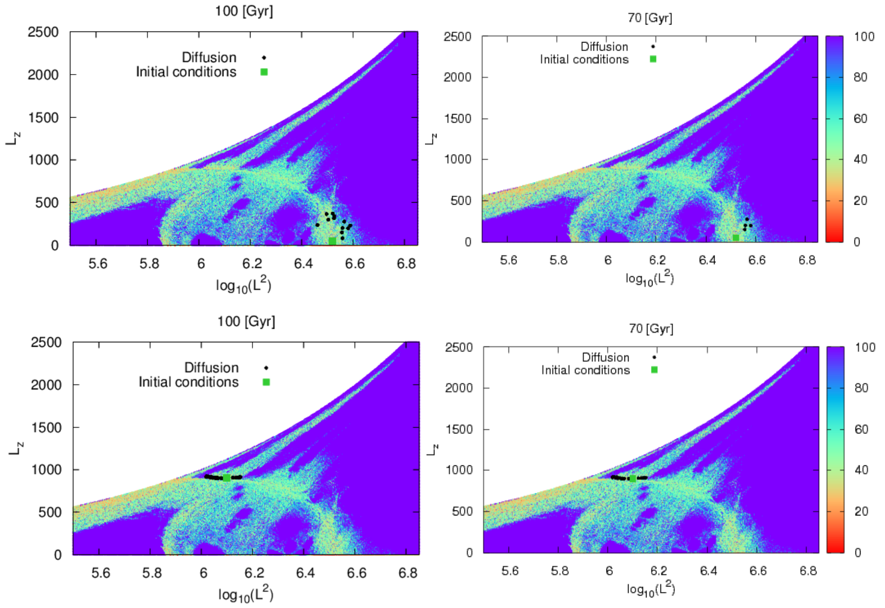

100 [Gyr]
Diffusion
Initial conditions
L_z
log10(L^2)
70 [Gyr]
Diffusion
Initial conditions
L_z
log10(L^2)
100 [Gyr]
Diffusion
Initial conditions
L_z
log10(L^2)
70 [Gyr]
Diffusion
Initial conditions
L_z
log10(L^2)

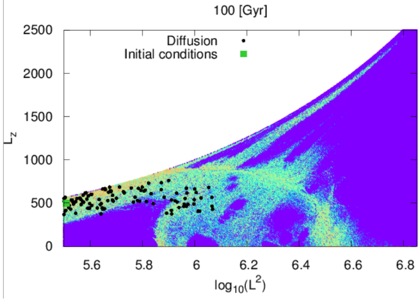
100 [Gyr]
Diffusion
Initial conditions
2500
2000
1500
1000
500
0
L_z
5.6
5.8
6
6.2
6.4
6.6
6.8
$\log_{10}(L^2)$

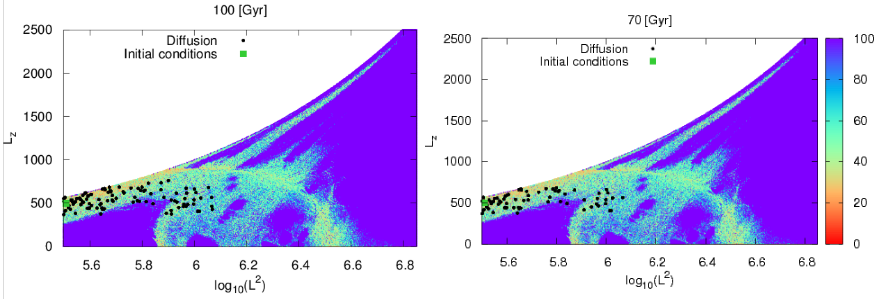

100 [Gyr]
Diffusion
Initial conditions
2500
2000
1500
1000
500
0
L_z
5.6
5.8
6
6.2
6.4
6.6
6.8
$\log_{10}(L^2)$
70 [Gyr]
Diffusion
Initial conditions
2500
2000
1500
1000
500
0
L_z
5.6
5.8
6
6.2
6.4
6.6
6.8
$\log_{10}(L^2)$
100
80
60
40
20
0

- The results indicate that while the amount of chaos is relevant (for large time-scales), chaotic mixing is not a significant factor in erasing for instance, local signatures of accretion events at least within a physically meaningful time-scale in the Solar Neighborhood.
- As long as the main sources of chaos are included (i.e., central cusp, triaxial shape, disk, etc.), slight variations of the galactic potential do not dramatically alter the global dynamics of the system.
- It seems plausible then the approximation that for time-scales ~ 10 Gys, halo orbits in the vicinity of the Sun respect 3 integrals of motion.

- The results indicate that while the amount of chaos is relevant (for large time-scales), chaotic mixing is not a significant factor in erasing for instance, local signatures of accretion events at least within a physically meaningful time-scale in the Solar Neighborhood.

- As long as the main sources of chaos are included (i.e., central cusp, triaxial shape, disk, etc.), slight variations of the galactic potential do not dramatically alter the global dynamics of the system.

- It seems plausible then the approximation that for time-scales ~ 10 Gys, halo orbits in the vicinity of the Sun respect 3 integrals of motion.

- The results indicate that while the amount of chaos is relevant (for large time-scales), chaotic mixing is not a significant factor in erasing for instance, local signatures of accretion events at least within a physically meaningful time-scale in the Solar Neighborhood.

- As long as the main sources of chaos are included (i.e., central cusp, triaxial shape, disk, etc.), slight variations of the galactic potential do not dramatically alter the global dynamics of the system.

- It seems plausible then the approximation that for time-scales ~ 10 Gys, halo orbits in the vicinity of the Sun respect 3 integrals of motion.